Report No. **159**

epaResearch
Climate - Water - Sustainability
Identifying pressures • Informing policy • Developing solutions

Ensemble of regional climate model projections for Ireland

Author: Paul Nolan, Irish Centre for High-End Computing and Meteorology and Climate Centre, School of Mathematical Sciences, University College Dublin

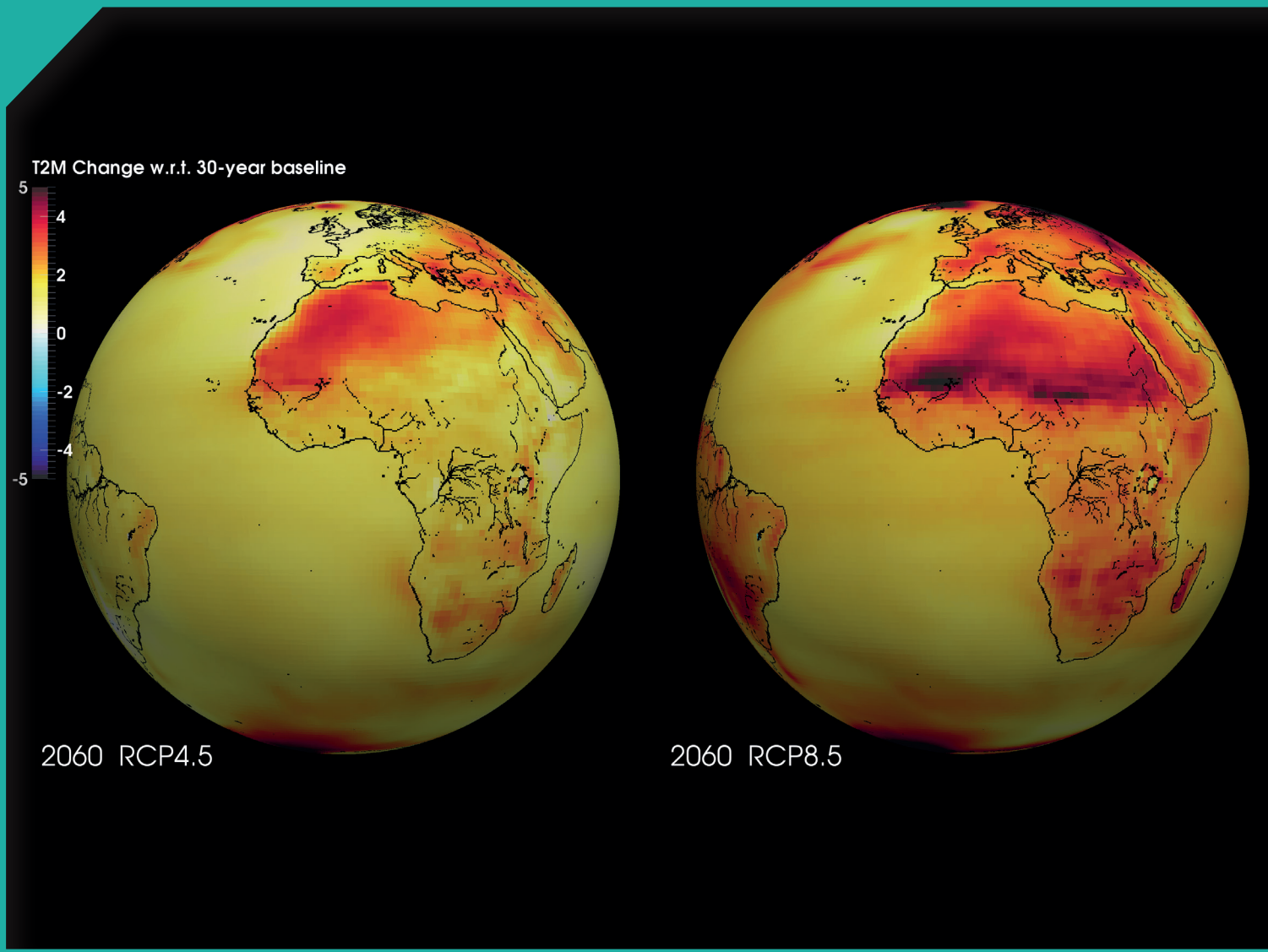

Comhshaol, Pobal agus Rialtas Áitiúil
Environment, Community and Local Government

www.epa.ie

ENVIRONMENTAL PROTECTION AGENCY

The Environmental Protection Agency (EPA) is responsible for protecting and improving the environment as a valuable asset for the people of Ireland. We are committed to protecting people and the environment from the harmful effects of radiation and pollution.

The work of the EPA can be divided into three main areas:

Regulation: *We implement effective regulation and environmental compliance systems to deliver good environmental outcomes and target those who don't comply.*

Knowledge: *We provide high quality, targeted and timely environmental data, information and assessment to inform decision making at all levels.*

Advocacy: *We work with others to advocate for a clean, productive and well protected environment and for sustainable environmental behaviour.*

Our Responsibilities

Licensing

We regulate the following activities so that they do not endanger human health or harm the environment:

- waste facilities *(e.g. landfills, incinerators, waste transfer stations)*;
- large scale industrial activities *(e.g. pharmaceutical, cement manufacturing, power plants)*;
- intensive agriculture *(e.g. pigs, poultry)*;
- the contained use and controlled release of Genetically Modified Organisms *(GMOs)*;
- sources of ionising radiation *(e.g. x-ray and radiotherapy equipment, industrial sources)*;
- large petrol storage facilities;
- waste water discharges;
- dumping at sea activities.

National Environmental Enforcement

- Conducting an annual programme of audits and inspections of EPA licensed facilities.
- Overseeing local authorities' environmental protection responsibilities.
- Supervising the supply of drinking water by public water suppliers.
- Working with local authorities and other agencies to tackle environmental crime by co-ordinating a national enforcement network, targeting offenders and overseeing remediation.
- Enforcing Regulations such as Waste Electrical and Electronic Equipment (WEEE), Restriction of Hazardous Substances (RoHS) and substances that deplete the ozone layer.
- Prosecuting those who flout environmental law and damage the environment.

Water Management

- Monitoring and reporting on the quality of rivers, lakes, transitional and coastal waters of Ireland and groundwaters; measuring water levels and river flows.
- National coordination and oversight of the Water Framework Directive.
- Monitoring and reporting on Bathing Water Quality.

Monitoring, Analysing and Reporting on the Environment

- Monitoring air quality and implementing the EU Clean Air for Europe (CAFÉ) Directive.
- Independent reporting to inform decision making by national and local government *(e.g. periodic reporting on the State of Ireland's Environment and Indicator Reports)*.

Regulating Ireland's Greenhouse Gas Emissions

- Preparing Ireland's greenhouse gas inventories and projections.
- Implementing the Emissions Trading Directive, for over 100 of the largest producers of carbon dioxide in Ireland.

Environmental Research and Development

- Funding environmental research to identify pressures, inform policy and provide solutions in the areas of climate, water and sustainability.

Strategic Environmental Assessment

- Assessing the impact of proposed plans and programmes on the Irish environment *(e.g. major development plans)*.

Radiological Protection

- Monitoring radiation levels, assessing exposure of people in Ireland to ionising radiation.
- Assisting in developing national plans for emergencies arising from nuclear accidents.
- Monitoring developments abroad relating to nuclear installations and radiological safety.
- Providing, or overseeing the provision of, specialist radiation protection services.

Guidance, Accessible Information and Education

- Providing advice and guidance to industry and the public on environmental and radiological protection topics.
- Providing timely and easily accessible environmental information to encourage public participation in environmental decision-making (*e.g. My Local Environment, Radon Maps)*.
- Advising Government on matters relating to radiological safety and emergency response.
- Developing a National Hazardous Waste Management Plan to prevent and manage hazardous waste.

Awareness Raising and Behavioural Change

- Generating greater environmental awareness and influencing positive behavioural change by supporting businesses, communities and householders to become more resource efficient.
- Promoting radon testing in homes and workplaces and encouraging remediation where necessary.

Management and structure of the EPA

The EPA is managed by a full time Board, consisting of a Director General and five Directors. The work is carried out across five Offices:

- Office of Climate, Licensing and Resource Use
- Office of Environmental Enforcement
- Office of Environmental Assessment
- Office of Radiological Protection
- Office of Communications and Corporate Services

The EPA is assisted by an Advisory Committee of twelve members who meet regularly to discuss issues of concern and provide advice to the Board.

EPA Research Programme 2014–2020

Ensemble of regional climate model projections for Ireland

(2008-FS-CC-m)

Prepared for the Environmental Protection Agency

by

Irish Centre for High-End Computing and Meteorology and Climate Centre, School of Mathematical Sciences, University College Dublin

Author:

Paul Nolan

ENVIRONMENTAL PROTECTION AGENCY
An Ghníomhaireacht um Chaomhnú Comhshaoil
PO Box 3000, Johnstown Castle, Co. Wexford, Ireland

Telephone: +353 53 916 0600 Fax: +353 53 916 0699
Email: info@epa.ie Website: www.epa.ie

ACKNOWLEDGEMENTS

The author wishes to acknowledge and thank the EPA for supporting and funding this research. In particular, Margaret Desmond, Philip O'Brien and Frank McGovern are thanked for their helpful input and support. The research was carried out at the Irish Centre for High-End Computing (ICHEC) and the Meteorology and Climate Centre, University College Dublin (UCD).

We are grateful for the input of Ray McGrath of the Research and Applications Division, Met Éireann, and Conor Sweeney and John O'Sullivan of the Meteorology and Climate Centre, UCD. Seamus Walsh of Met Éireann is acknowledged for supplying the observed climate data. We are thankful to Daniel Purdy of ICHEC/Trinity College Dublin for his assistance with the storm-tracking analysis. Emily Gleeson of Met Éireann is also acknowledged. Finally, Professor Peter Lynch of the Meteorology and Climate Centre, UCD, is thanked for his supervision and support while the author worked at UCD.

The author wishes to acknowledge ICHEC for the provision of computational facilities and support. All simulations of the study were carried out on the ICHEC supercomputing facilities (funded by Science Foundation Ireland).

EPA RESEARCH PROGRAMME 2014–2020
Published by the Environmental Protection Agency, Ireland

PRINTED ON RECYCLED PAPER

ISBN: 978-1-84095-609-2

Price: Free 10/15/150

Project partner

Dr Paul Nolan
Irish Centre for High-end Computing
Trinity Technology and Enterprise Campus
Grand Canal Quay
Dublin 2
and formerly of the Meteorology and Climate Centre
School of Mathematical Sciences
University College Dublin
Belfield
Dublin 4
Tel.: +353 1 5241608 (ext. 32)
E-mail: paul.nolan@ichec.ie

Contents

List of figures

List of tables

Executive summary

This report provides an analysis of the impacts of global climate change on the mid-21st-century climate of Ireland. The projections are based on the output of an ensemble of high-resolution regional climate models (RCMs).

The impact of rising greenhouse gas emissions and changing land use on climate can be simulated using global climate models (GCMs). However, since GCMs are computationally expensive to run, long climate simulations are currently feasible only with horizontal resolutions of 50 km or coarser. Since climate fields such as precipitation and wind speed are closely correlated with the local topography, this resolution is inadequate for the simulation of the detail and pattern of climate change on the scale of a region the size of Ireland. To overcome this limitation, the RCM method dynamically downscales the coarse information provided by the global models and provides high-resolution information on a subdomain covering Ireland. The computational cost of running the RCM, for a given resolution, is considerably less than that of a global model. The RCMs of the current study were run at high spatial resolution, up to 4 km, thus allowing a better evaluation of the local effects of climate change. Since RCMs have a better representation of coastlines and general topography, the resulting model output is more useful for focused climate impact studies. An additional advantage is that the physically based RCMs explicitly resolve more smaller scale atmospheric features than the coarser GCMs.

In this work, projections for the future Irish climate were generated by embedding or "nesting" two RCMs within a set of GCM simulations, and so providing high-resolution local detail over Ireland. The RCMs used in this work are the COnsortium for Small-scale MOdeling–Climate Limited-area Modelling (COSMO-CLM) model and the Weather Research and Forecasting (WRF) model. The GCMs used are the Max Planck Institute's ECHAM5, the UK Met Office's HadGEM2-ES (Hadley Centre Global Environment Model version 2 Earth System configuration), the CGCM (Coupled Global Climate Model) 3.1 from the Canadian Centre for Climate Modelling and the EC-Earth consortium GCM. Simulations were run for a reference period 1981–2000 and future period 2041–2060. Differences between the two periods give a measure of climate change. The future climate was simulated using the Intergovernmental Panel on Climate Change (IPCC) Special Report on Emissions Scenarios (SRES) A1B, A2 and B1 and the Representative Concentration Pathways (RCP) 4.5 and 8.5 (IPCC, Fifth Assessment Report) emission scenarios. The RCP4.5 and the B1 scenario simulations were used to create a "medium- to low-emission" ensemble while the RCP8.5, A1B and A2 simulations were used to create a "high-emission" ensemble. To address the issue of uncertainty, a multi-model ensemble (MME) approach was employed. Through the MME approach, the uncertainty in RCM projections can be partially quantified, thus providing a measure of confidence in the predictions.

The RCMs were validated using 20-year simulations of the past Irish climate (1981–2000), driven both by European Centre for Medium-Range Weather Forecasts (ECMWF) ERA-40 global re-analysis and the GCM datasets and by comparing the output against Met Éireann observational data. Extensive validations were carried out to test the ability of the RCMs to accurately model the climate of Ireland. Results confirm that the output of the RCMs exhibits reasonable and realistic features as documented in the historical data record.

Temperature projections

Projections for mid-century indicate an increase of 1–1.6°C in mean annual temperatures, with the largest increases seen in the east of the country. Warming is enhanced for the extremes (i.e. hot or cold days), with the warmest 5% of daily maximum summer temperatures projected to increase by 0.7–2.6°C compared with the baseline period. The coldest 5% of night-time temperatures in winter are projected to rise by 1.1–3.1°C. Averaged over the whole country, the number of frost days (days when the minimum temperature is less than 0°C) is projected to decrease by over 50%. The projections indicate an average increase in the length of the growing season by mid-century of over 35 days per year.

Rainfall projections

Significant decreases in average precipitation amounts are projected for the spring and summer months as

well as over the full year. These drier conditions are projected to be more pronounced in the summer, with "likely" reductions in rainfall ranging from 0% to 13% and from 3% to 20% for the medium- to low-emission and high-emission scenarios, respectively. Nevertheless, the frequencies of heavy precipitation events show notable increases (approximately 20%) over the year as a whole, and in the winter and autumn months. The number of extended dry periods (defined as at least 5 consecutive days for which the daily precipitation is less than 1 mm) is also projected to increase substantially by mid-century over the full year and during autumn and summer. The projected increases in dry periods are largest for summer, with "likely" values ranging from 12% to 40% for both emission scenarios. The precipitation projections, summarised above, were found to be robust, as over 66% of the ensemble members were in agreement.

Storm track and mean sea-level pressure projections

To assess the potential impact of climate change on extreme cyclonic activity in the North Atlantic, an algorithm was developed to identify and track cyclones as simulated by the RCMs. Results indicate that the tracks of intense storms are projected to extend further south over Ireland than those in the reference simulation. In contrast, the overall number of North Atlantic cyclones is projected to decrease by approximately 10%. The projected decrease in overall cyclone activity is consistent with a projected increase in average mean sea-level pressure (MSLP) of approximately 1.5 hPa for all seasons by mid-century.

Wind energy projections

Results show significant projected decreases in the energy content of the wind for the spring, summer and autumn months. Projected increases for winter were found to be statistically insignificant. The projected decreases were largest for summer, with "likely" values ranging from 3% to 10% for the medium- to low-emission scenario and from 7% to 15% for the high-emission scenario. Projections of wind direction show no substantial change. The projected increase in extreme storm activity over Ireland is expected to adversely affect the future wind energy supply.

Future work and recommendations

Future validation work will focus on downscaling and analysing the more up-to-date and accurate ERAInterim dataset from ECMWF, in place of ERA-40. Furthermore, the individual RCM–GCM past simulations will be validated in detail.

It should be noted that the climate projections presented in this report are derived from the currently available dataset of high-resolution climate simulations for Ireland and that additional simulations and future improvements in modelling will alter the projections, as uncertainty is gradually reduced. Currently, there is higher confidence in the temperature projections than in the wind and rainfall projections. This is reflected in a rather large spread, particularly at regional level, in the wind and rainfall projections between the individual RCM ensemble members. Future work will attempt to address this issue by increasing the RCM ensemble size and employing more up-to-date RCMs, GCMs and the RCP2.6 and RCP6.0 emission scenarios. Furthermore, the accuracy and usefulness of the predictions will be enhanced by running the RCMs at a higher spatial resolution.

As extreme storm events are rare, the storm-tracking research needs to be extended. Future work will focus on analysing a larger ensemble, thus allowing a robust statistical analysis of extreme storm track projections.

1 Introduction

The main objective of the research presented herein is to evaluate the effects of climate change on the future climate of Ireland using the method of high-resolution regional climate modelling. There is a lack of research in dynamically downscaled high-resolution (finer than 10-km spatial resolution) climate modelling over Ireland, for projections in the medium term. Existing studies have focused on analysing relatively small ensembles of regional climate model (RCM) simulations (McGrath and Lynch, 2008; Nolan et al., 2011, 2014; Gleeson et al., 2013), or have instead analysed a large ensemble of relatively low-resolution RCM simulations (van der Linden and Mitchell, 2009; Jacob et al., 2014). Other studies have used statistical downscaling, which is not based on physical principles, to provide projections of the future climate of Ireland (Fealy and Sweeney, 2008). The analysis presented in this report was undertaken to address this lack of research by analysing the output of three high-resolution RCMs over Ireland, driven by four global climate models (GCMs), under five possible future emission scenarios. Simulations were run for a reference period, 1981–2000, and a future period, 2041–2060. Differences between the two periods provide a measure of climate change. Specifically, we will focus on projections of temperature, precipitation, wind energy resource and extreme storm events.

The current research consolidates and expands on the RCM projections of previous studies (McGrath and Lynch, 2008; Nolan et al., 2011, 2014; Gleeson et al., 2013; O'Sullivan et al., 2015) by increasing the ensemble size. This allows likelihood levels to be assigned to the projections. In addition, the uncertainty of the projections is more accurately quantified. It is envisaged that the research will inform policy and further the understanding of the potential environmental impacts of climate change in Ireland at a local scale.

1.1 Regional climate models

The RCMs used in this work are the COnsortium for Small-scale MOdeling–Climate Limited-area Modelling (COSMO-CLM, versions 3.2 and 4.0) model (both Rockel et al., 2008) and the Weather Research and Forecasting (WRF) model (Skamarock et al., 2008). Projections for the future Irish climate were generated by downscaling four GCMs, under five different possible future scenarios (see sections 1.5 and 1.6 for a full description).

The COSMO-CLM regional climate model is the COSMO weather forecasting model in climate mode (Rockel et al., 2008). It is applied and further developed by members of the CLM Community (www.clm-community.eu). The COSMO model (www.cosmo-model.org) is the non-hydrostatic operational weather prediction model used by the German Weather Service (DWD). A detailed description of the COSMO model is given by Doms and Schattler (2002) and Steppeler et al. (2003). Henceforth, the COSMO-CLM model will be referred to as the CLM model, with versions 3.2 and 4.0 referred to as CLM3 and CLM4, respectively. The WRF model (www.wrf-model.org) is a numerical weather prediction system designed to serve atmospheric research, climate and operational forecasting needs. The model serves a wide range of meteorological applications across scales ranging from metres to thousands of kilometres. The WRF simulations of the present study adopted the Advanced Research WRF (ARW) dynamical core, developed by the US National Center for Atmospheric Research (NCAR) Mesoscale and Microscale Meteorology Division (Skamarock et al., 2008).

1.2 Downscaling to Ireland

The impact of greenhouse gases on climate change can be simulated using GCMs. However, long climate simulations using GCMs are currently feasible only with horizontal resolutions of 50 km or coarser. Since climate fields such as precipitation, wind speed and direction are closely correlated to the local topography, this is inadequate to simulate the detail and pattern of climate change and its effects on the future climate of Ireland. The RCM method dynamically downscales the coarse information provided by the global models and provides high-resolution information on a subdomain covering Ireland. The computational cost of running the RCM, for a given resolution, is considerably less than that of a global model. The RCMs of the current study were run

at high spatial resolution, up to 4 km, thus allowing a better evaluation of the local effects of climate change. The resulting model output is more useful for focused climate impact studies and allows a better representation of coastlines and general topography. An additional advantage is that the physically based RCMs explicitly resolve more smaller scale atmospheric features than the coarser GCMs. In particular, numerous studies have demonstrated the added value of RCMs in the simulation of topography-influenced phenomena and extremes with relatively small spatial or short temporal character (Feser et al., 2011; Feser and Barcikowska, 2012; Shkol'nik et al., 2012; Flato et al., 2013). Other examples of the added value of RCMs include improved simulation of convective precipitation (Rauscher et al., 2010) and near-surface temperature (Feser, 2006). The IPCC have concluded that there is "high confidence that downscaling adds value to the simulation of spatial climate detail in regions with highly variable topography (e.g., distinct orography, coastlines) and for mesoscale phenomena and extremes" (Flato et al. 2013).

The RCMs of the current study were initially driven by GCM boundary conditions (achieving a ~50-km grid size), and were then nested twice in succession, to achieve the finest resolution (ranging from 4-km to 7-km grid size). A brief overview of the GCMs used in the current study is given in section 1.6. The CLM simulations were run at 50-km, 18-km, 7-km and 4-km resolutions. The WRF simulations were run at 54-km, 18-km and 6-km resolutions. The WRF model domains are shown in Figure 1.1. The CLM domains are similar (not shown). The advantage of high-resolution RCM simulations is highlighted by Figure 1.2, which shows how the surface topography is better resolved by the high-resolution data.

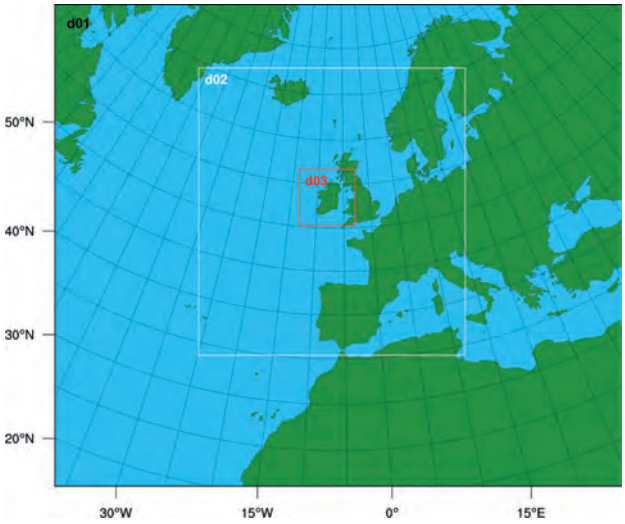

Figure 1.1. The WRF model domains. The d01, d02 and d03 domains have 54-km, 18-km and 6-km horizontal resolution, respectively.

The climate fields of the RCM simulations were output at 3-hour intervals. In addition, extra climate statistics were calculated and archived for WRF data on a daily temporal resolution. Table 1.1 presents the data as archived by the WRF simulations. The CLM climate data were output at 3-hour intervals and are similar to the WRF 3-hour output (Table 1.1, column 1).

The RCM simulations were run on the Irish Centre for High-End Computing (ICHEC) supercomputers. Running such a large ensemble of high-resolution RCMs was a substantial computational task and required extensive use of the ICHEC supercomputer systems over 3 to 4 years. This archive of data will be made available to the wider research community and general public through the EPA.

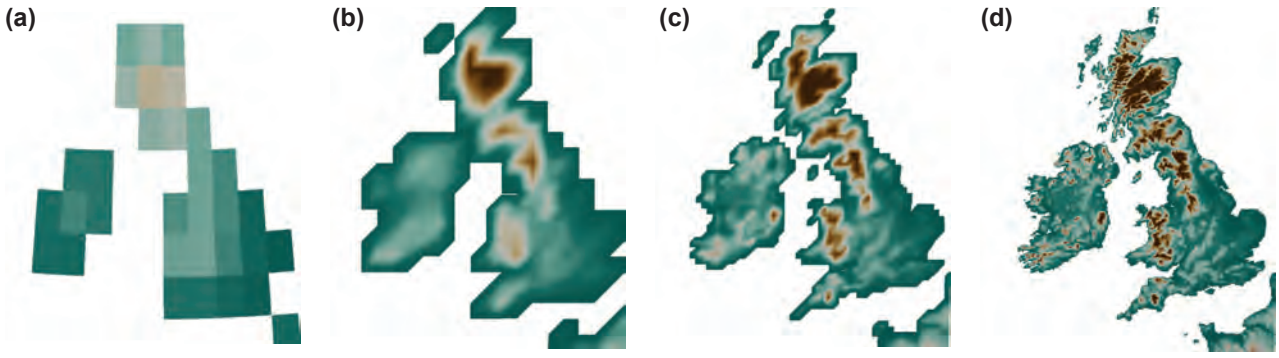

Figure 1.2. The topography of Ireland and the UK as resolved by the EC-Earth GCM and the CLM RCM for different spatial resolutions. (a) EC-Earth 125-km resolution; (b) CLM 50-km resolution; (c) CLM 18-km resolution; (d) CLM 4-km resolution.

Table 1.1. Output fields of the WRF simulations

3-hour WRF output	Unit	Daily WRF output	Unit
Terrain height	m	Daily mean 2-m temperature	K
Land–sea mask	0/1	Daily min. 2-m temperature	K
Sea surface temperature	K	Daily max. 2-m temperature	K
Surface temperature	K	Daily mean skin temperature	K
2-m temperature	K	Daily min. skin temperature	K
Surface air pressure	hPa	Daily max. skin temperature	K
Mean sea-level pressure	hPa	Standard deviation of 2-m temperature	K
Specific humidity	kg/kg	Standard deviation of skin temperature	K
Humidity mixing ratio at 2 m	kg/kg	Daily time of min. 2-m temperature	minute
Eastward wind at 10 m, U	m/s	Daily time of max. 2-m temperature	minute
Northward wind at 10 m, V	m/s	Daily time of min. skin temperature	minute
Wind speed at 10 m	m/s	Daily time of max. skin temperature	minute
Wind speed at 60 m	m/s	Mean 10-m U	m/s
Wind speed at 100 m	m/s	Max. 10-m U	m/s
Friction velocity	m/s	Standard deviation of 10-m U	m/s
3-hour grid scale precipitation	mm	Mean 10-m V	m/s
3-hour convective precipitation	mm	Max. 10-m V	m/s
Snowfall	mm	Standard deviation of 10-m V	m/s
Snow height	m	Mean 10-m wind speed	m/s
Surface snow amount	kg/m^2	Max. 10-m wind speed	m/s
Soil temperature (6 layers)	K	Standard deviation of 10-m wind speed	m/s
Soil moisture (6 layers)	m^3/m^3	Time of max. 10-m wind speed	minute
Surface runoff	mm	Mean 2-m specific humidity	kg/kg
Subsurface runoff	mm	Min. 2-m specific humidity	kg/kg
Surface downwelling SW flux	W/m^2	Max. 2-m specific humidity	kg/kg
Surface upwelling SW flux	W/m^2	Standard deviation of 2-m specific humidity	kg/kg
Surface downwelling LW flux	W/m^2	Time of min. 2-m specific humidity	minute
Surface upwelling LW flux	W/m^2	Time of max. 2-m specific humidity	minute
LW flux – outgoing at top of atmosphere	W/m^2	Mean cumulus precipitation	$kg/m^2/s$
Surface upward sensible heat flux	W/m^2	Max. cumulus precipitation	$kg/m^2/s$
Surface upward latent heat flux	W/m^2	Standard deviation of cumulus precipitation	$kg/m^2/s$
Ground heat flux	W/m^2	Time of max. cumulus precipitation	minute
Upward surface moisture heat flux	$kg/m^2/s$	Mean grid scale precipitation	$kg/m^2/s$
Surface albedo	0–1	Max. grid scale precipitation	$kg/m^2/s$
Surface emissivity	0–1	Standard deviation grid scale precipitation	$kg/m^2/s$
Sea ice (domain 1)	0–1	Time of max. grid scale precipitation	minute

LW, longwave; SW, shortwave; U is the zonal velocity, i.e. the component of the horizontal wind towards east; V is the meridional velocity, i.e. the component of the horizontal wind towards north.

1.3 Regional climate model evaluation

The RCMs were validated by running 20-year simulations of the past Irish climate (1981–2000), driven by both European Centre for Medium-Range Weather Forecasts (ECMWF) ERA-40 global re-analysis and the GCM datasets, and comparing the output against Met Éireann observational data (Walsh, 2012). Extensive validations were carried out to test the ability of the RCMs to accurately model the climate of Ireland. Results confirm that the output of the RCMs exhibits reasonable and realistic features as documented in the historical data record.

1.4 Greenhouse gas emission scenarios

To estimate future changes in the climate we need to have some indication of how global emissions of greenhouse gases (and other pollutants) will change in the future. In previous Intergovernmental Panel on Climate Change (IPCC) reports this was handled using Special Report on Emissions Scenarios (SRES) (Nakićenović et al., 2000), e.g. A1B scenario, that were based on projected emissions, changes in land use and other relevant factors. The more recent Representative Concentration Pathways (RCPs) scenarios are focused on radiative forcing – the change in the balance between incoming and outgoing radiation via the atmosphere caused primarily by changes in atmospheric composition – rather than being linked to any specific combination of socioeconomic and technological development scenarios. Unlike SRES, they explicitly include scenarios allowing for climate mitigation. There are four such scenarios (RCP2.6, RCP4.5, RCP6.0 and RCP8.5), named with reference to a range of radiative forcing values for the year 2100 or after, i.e. 2.6, 4.5, 6.0 and 8.5 W/m^2, respectively (Moss et al., 2010; van Vuuren et al., 2011).

The future climate simulations of the current study used the A1B, A2 and B1 (SRES) and the RCP4.5 and RCP8.5 emission scenarios. The RCP4.5 and the B1 scenario simulations were used to create a "medium- to low-emission" ensemble while the RCP8.5, A1B and A2 simulations were used to create a "high-emission" ensemble.

1.5 Regional climate model projections

Projections for the future Irish climate were generated by downscaling the Max Planck Institute's ECHAM5 GCM (Roeckner et al., 2003), the UK Met Office's Hadley Centre Global Environment Model version 2 Earth System configuration (HadGEM2-ES) GCM (Collins et al., 2011), the Coupled Global Climate Model (CGCM) 3.1 from the Canadian Centre for Climate Modelling (Scinocca et al., 2008) and the EC-Earth consortium GCM (Hazeleger et al., 2011). The future climate was simulated using the A1B, A2 and B1 [SRES, Fourth Assessment Report (AR4)] and RCP4.5 and RCP8.5 (AR5) emission scenarios (see section 1.5).

Table 1.2. Details of the ensemble of RCM simulations

RCM	GCM	Scenario/GCM realisation	Number of runs	Number of ensemble comparisons	Period	Resolution
Group 1						
CLM3	ECHAM5	C20_1, C20_2	2	–	1961–2000	7 km
CLM3	ECHAM5	A1B_1, A1B_2, B1	3	6	2021–2060	7 km
Group 2						
CLM4	ECHAM5	C20_1, C20_2	2	–	1961–2000	7 km*
CLM4	ECHAM5	A1B_1, A1B_2	2	4	2021–2060	7 km*
Group 3						
CLM4	CGCM3.1	C20	1	–	1961–2000	4 km
CLM4	CGCM3.1	A1B, A2	2	2	2021–2060	4 km
Group 4						
CLM4	HadGEM2-ES	C20	1	–	1961–2000	4 km
CLM4	HadGEM2-ES	RCP4.5, RCP8.5	2	2	2021–2060	4 km
Group 5						
CLM4	EC-Earth	mei1, mei2, mei3	3	–	1981–2009	4 km
CLM4	EC-Earth	me41, me42, me43 me81, me82, me83	6	18	2021–2060	4 km
Group 6						
WRF	EC-Earth	mei1, mei2, mei3	3	–	1981–2009	6 km
WRF	EC-Earth	me41, me42, me43 me81, me82, me83	6	18	2021–2060	6 km

me41 refers to RCP4.5 run 1; me82 refers to RCP8.5 run 2; etc. *No precipitation data available.

An overview of the simulations is presented in Table 1.2; the rows include information on the RCM used, the corresponding downscaled GCM, the GCM realisations and SRES/RCP used for future simulations, the number of runs, the number of ensemble comparisons, the time-slice simulated and the finest grid size achieved. The GCM realisations result from running the same GCM with slightly different conditions, i.e. the starting date of historical simulations (Gleeson et al., 2013, see chapter 1, "The path to climate information: global to local scale"; O'Sullivan et al., 2015). Data from two time-slices, 1981–2000 (the control) and 2041–2060, were used for analysis of projected changes in the mid-21st-century Irish climate. These periods were chosen because these are the longest decadal time periods common to all simulations. The historical period was compared with the corresponding future period for all simulations *within the same group*. This results in *future anomalies* for each model run; that is, the difference between future and past. In this way, biases of particular models will not skew results, and each anomaly can be meaningfully compared with the other groups. In addition, the method of cross-comparing simulations within the same group helps identify the more robust climate change signals. In total, there are 50 ensemble comparisons available for analysis.

To create the large ensemble, the RCMs were regridded to a common 7-km grid over Ireland. The simulations carried out using RCP4.5 and the B1 scenario were used to create a medium- to low-emission ensemble while the RCP8.5, A1B and A2 simulations were used to create a high-emission ensemble. This results in 29 high-emission ensemble comparisons and 21 medium- to low-emission comparisons. The relatively large ensemble size allows likelihood levels to be assigned to the projections (see section 1.7). In addition, the uncertainty of the projections can be more accurately quantified.

1.6 Overview of uncertainty

Climate change projections are subject to uncertainty, which limits their utility. Fronzek et al. (2012) suggest that there are four main sources of uncertainty: (1) the natural variability of the climate system, (2) uncertainties due to the formulation of the models themselves, (3) uncertainties in future regional climate due to the coarse resolution of GCMs and (4) uncertainties in the future atmospheric composition, which affects the radiative balance of the Earth. The uncertainties arising from (1) and (2) can be addressed, in part, by employing a multi-model ensemble (MME) approach (Déqué et al., 2007; van der Linden and Mitchell, 2009; Jacob et al., 2014). The ensemble approach of the current project uses three different RCMs, driven by several GCMs, to simulate climate change. Through the MME approach, the uncertainty in the projections can be quantified, proving a measure of confidence in the predictions. The uncertainty arising from (3) can be addressed by running the RCM simulations at high spatial resolution. To account for the uncertainty arising from (4), the current study uses a number of SRES (B1, A1B, A2) and RCP (4.5, 8.5) emission scenarios to simulate the future climate of Ireland. Future studies will include additional scenarios, such as RCP2.6 and RCP6, to better quantify the uncertainty of the emission scenarios.

The current study analyses 29 high-emission and 21 medium- to low-emission RCM ensemble comparisons. This relatively large ensemble size allows the construction of a probability distribution function (pdf) of climate projections. Likelihood values can then be assigned to the projected changes. Figure 1.3 presents a schematic example of the pdf of projected temperature *increases*. The figure shows the projected temperature increase (red line) such that 66% of the RCM ensemble members project greater increases. It follows that it is likely that increases in temperature will be greater than or equal to this value. In a similar manner, a likely projected decrease in a climate field is defined as a projection such that over 66% of RCM ensemble members project

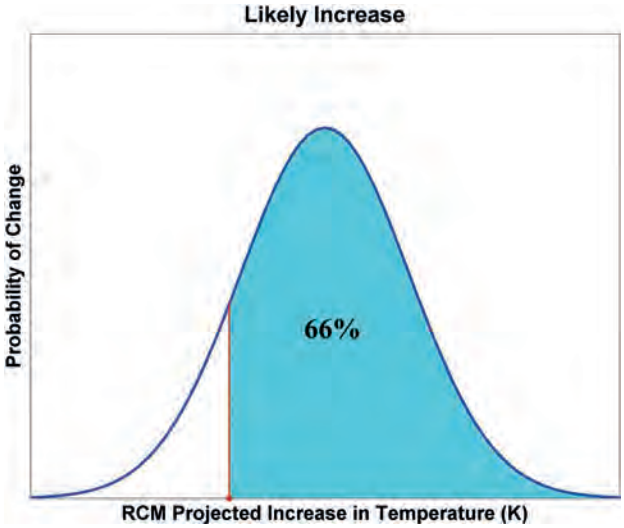

Figure 1.3. A schematic diagram of the probability density function of the ensemble of projected changes in temperature. The red vertical line shows the likely increase in temperature.

Table 1.3. Likelihood terms and their associated probabilities

Term	Likelihood of a climate projection (percentage of RCM ensemble members in agreement)
Very likely	> 90
Likely	> 66

larger decreases. Table 1.3 presents an overview of the likelihood values used throughout this report. Note that the accuracy of these statistical descriptions is based on the assumption that the ensemble members represent an unbiased sampling of the (unknown) future climate. It should also be noted that the likelihood values presented in this report are derived from the currently available dataset of high-resolution projections for Ireland and that additional simulations and future improvements in modelling will alter the projections, as uncertainty is gradually reduced. Future work will focus on reducing this uncertainty by increasing the ensemble size and employing more up-to-date RCMs and GCMs.

In addition to the likelihood values, the large ensemble size allows the uncertainty of the projections to be more accurately quantified. For example, if all ensemble members agree on a particular climate projection, it follows that this projection can be assigned a high level of confidence. Conversely, if a large spread exists between the RCM ensemble members, the projection is assigned low confidence.

1.7 Statistical significance analysis

A key purpose of this study is to establish the significance level of any changes in the future temperature, precipitation and wind speed climate fields. Considering that wind speeds and precipitation are generally not normally distributed, the non-parametric Kolmogorov–Smirnov and Wilcoxon rank-sum tests were employed to test for statistical significance of projected changes. The Wilcoxon rank-sum tests the null hypothesis that the past and future data are from continuous distributions with equal medians, against the alternative that they are not. The Kolmogorov–Smirnov null hypothesis states that the past and future data are from the same continuous distribution. The alternative hypothesis is that they are from different continuous distributions. Small values of the confidence level p cast doubt on the validity of the null hypothesis. Let φ be the level of significance at which the null hypothesis is rejected. If $p < \varphi$, for small φ, this indicates that the null hypothesis is rejected, the alternative hypothesis is accepted and the difference between the future and past climate fields is statistically significant at the $100 \times (1-\varphi)\%$ confidence level. Three different alternative hypotheses (Ha) are chosen depending on the sign of the future projections. The alternative hypotheses are as follows:

- Ha_o: $F \neq P$
  - Wilcoxon rank-sum: the past (P) and future (F) medians are not equal.
  - Kolmogorov–Smirnov: the future and past cumulative distribution functions (cdfs) are not equal.

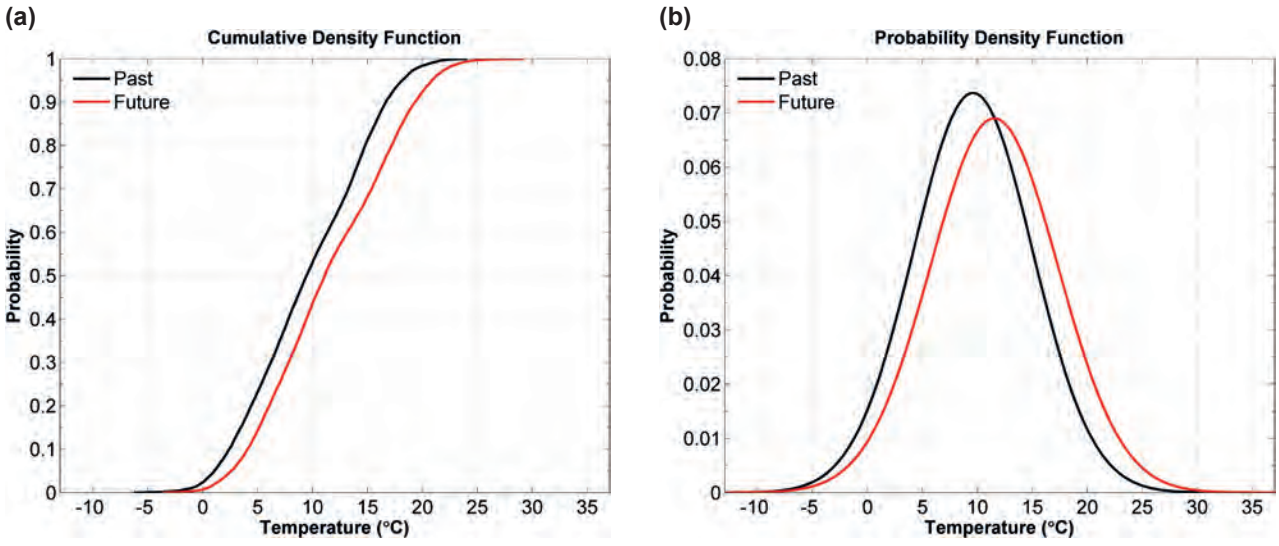

Figure 1.4. Distributions of past and future temperature data. (a) Cumulative density function; (b) probability density function.

- Ha_1: $F < P$
  - Wilcoxon rank-sum: the future median is less than the past median.
  - Kolmogorov–Smirnov: the future cdf is greater than the past cdf, implying a decrease in the future climate variable under analysis.
- Ha_2: $F > P$
  - Wilcoxon rank-sum: the future median is greater than the past median.
  - Kolmogorov–Smirnov: the future cdf is less than the past cdf, implying an increase in the future climate variable under analysis.

Figure 1.4 presents the past and future cdfs and pdfs of a sample of RCM temperature data at a location in Ireland.[1] The figures illustrate that, if the future cdf is less than the past cdf (i.e. if the curve shifts to the right), this implies an increase in the future climate variable under analysis (i.e. the future pdf of Figure 1.4b has shifted to the right, clearly indicating a projection of warmer conditions). The converse can also be shown. It is also interesting to note, in this example, that the shape of the pdf has widened, indicating greater variability in the projected future temperature regime. This approach of examining the distribution in detail allows a more complete understanding of the projections of climate change.

References

Collins, W.J., Bellouin, N., Doutriaux-Boucher, M., Gedney, N., Halloran, P., Hinton, T., Hughes, J., Jones, C.D., Joshi, M., Liddicoat, S., Martin, G., O'Connor, F., Rae, J., Senior, C., Sitch, S., Totterdell, I., Wiltshire, A. and Woodward, S., 2011. Development and evaluation of an Earth-System model: HadGEM2. Geoscientific Model Development, 4, 1051–1075.

Déqué, M., Rowell, D.P., Lüthi, D., Giorgi, F., Christensen, J.H., Rockel, B., Jacob, D., Kjellström, E., de Castro, M. and van den Hurk, B., 2007. An intercomparison of regional climate simulations for Europe: assessing uncertainties in model projections. Climatic Change, 81, 53–70.

Doms, G. and Schättler, U., 2002. A Description of the Nonhydrostatic Regional Model LM. Part I: Dynamics and Numerics. Deutscher Wetterdienst, Offenbach.

1 Note: these sample data have not been chosen to be representative of Ireland as a whole. The purpose of Figure 1.4 is simply to illustrate the concept of pdfs.

Fealy, R. and Sweeney, J., 2008. Statistical downscaling of temperature, radiation and potential evapotranspiration to produce a multiple GCM ensemble mean for a selection of sites in Ireland. Irish Geography, 41, 1–27.

Feser, F., 2006. Enhanced detectability of added value in limited-area model results separated into different spatial scales. Monthly Weather Review, 134, 2180–2190.

Feser, F. and Barcikowska, M., 2012. The influence of spectral nudging on typhoon formation in regional climate models. Environmental Research Letters, 7, 014024.

Feser, F., Rockel, B., von Storch, H., Winterfeldt, J. and Zahn, M., 2011. Regional climate models add value to global model data: a review and selected examples. Bulletin of the American Meteorological Society, 92, 1181–1192.

Flato, G., Marotzke, J., Abiodun, B., Braconnot, P., Chou, S.C., Collins, W., Cox, P., Driouech, F., Emori, S., Eyring, V., Forest, C., Gleckler, P., Guilyardi, E., Jakob, C., Kattsov, V., Reason, C. and Rummukainen, M., 2013. Evaluation of climate models. In Stocker, T.F., Qin, D., Plattner, G.-K., Tignor, M., Allen, S.K., Boschung, J., Nauels, A., Xia, Y., Bex, V. and Midgley, P.M. (eds), Climate Change 2013: The Physical Science Basis. Contribution of Working Group I to the Fifth Assessment Report of the Intergovernmental Panel on Climate Change. Cambridge University Press, Cambridge.

Fronzek, S., Carter, T.R. and Jylhä, K., 2012. Representing two centuries of past and future climate for assessing risks to biodiversity in Europe. Global Ecology and Biogeography, 21, 19–35.

Gleeson, E., McGrath, R. and Treanor, M. (eds), 2013. Ireland's Climate: The Road Ahead. Met Éireann, Dublin. Available online: www.met.ie/publications/IrelandsWeather-13092013.pdf (accessed 13 July 2015).

Hazeleger, W., Wang, X., Severijns, C., Ştefănescu, S., Bintanja, R., Sterl, A., Wyser, K., Semmler, T., Yang, S., van den Hurk, B., van Noije, T., van der Linden, E. and van der Wiel, K., 2011. EC-Earth V2.2: description and validation of a new seamless earth system prediction model. Climate Dynamics, 39, 2611–2629.

Jacob, D., Petersen, J., Eggert, B., Alias, A., Christensen, O.B., Bouwer, L.M., Braun, A., Colette, A., Déqué, M., Georgievski, G., Georgopoulou, E., Gobiet, A., Menut, L., Nikulin, G., Haensler, A., Hempelmann, N., Jones, C., Keuler, K., Kovats, S., Kröner, N., Kotlarski, S., Kriegsmann, A., Martin, E., van Meijgaard, E., Moseley, C., Pfeifer, S., Preuschmann, S., Radermacher, C., Radtke, K., Rechid, D., Rounsevell, M., Samuelsson, P., Somot, S., Soussana, J.-F., Teichmann, C., Valentini, R., Vautard, R., Weber, B. and Yiou, P., 2014. EURO-CORDEX: new high resolution climate change

projections for European impact research. Regional Environmental Change, 14, 563–578.

McGrath, R. and Lynch, P. (eds), 2008. Ireland in a Warmer World: Scientific Predictions of the Irish Climate in the Twenty-First Century. Community Climate Change Consortium for Ireland (C4I). Available online: www.met.ie/publications/warmerworld.asp (accessed 21 August 2015).

Moss, R.H., Edmonds, J.A., Hibbard, K.A., Manning, M.R., Rose, S.K., van Vuuren, D.P., Carter, T.R., Emori, S., Kainuma, M., Kram, T., Meehl, G.A., Mitchell, J.F.B., Nakićenović, N., Riahi, K., Smith, S.J., Stouffer, R.J., Thomson, A.M., Weyant, J.P. and Wilbanks, T.J., 2010. The next generation of scenarios for climate change research and assessment. Nature, 463(7282), 747–756.

Nakićenović, N., Alcamo, J., Davis, G., de Vries, B., Fenhann, J., Gaffin, S., Gregory, K., Grbler, A., Jung, T.Y., Kram, T., La Rovere, E.L., Michaelis, L., Mori, S., Morita, T., Pepper, W., Pitcher, H., Price, L., Raihi, K., Roehrl, A., Rogner, H.-H., Sankovski, A., Schlesinger, M., Shukla, P., Smith, S., Swart, R., van Rooijen, S., Victor, N. and Dadi, Z., 2000. IPCC Special Report on Emissions Scenarios. Cambridge University Press, Cambridge.

Nolan, P., Lynch, P., McGrath, R., Semmler, T. and Wang, S., 2011. Simulating climate change and its effects on the wind energy resource of Ireland. Wind Energy, 15, 593–608.

Nolan, P., Lynch, P. and Sweeney, C., 2014. Simulating the future wind energy resource of Ireland using the COSMO-CLM model. Wind Energy, 17, 19–37.

O'Sullivan, J., Sweeney, C., Nolan, P. and Gleeson, E., 2015. A high-resolution, multi-model analysis of Irish temperatures for the mid-21st century. International Journal of Climatology. doi: 10.1002/joc.4419 (Early Online View).

Rauscher, S.A., Coppola, E., Piani, C. and Giorgi, F., 2010. Resolution effects on regional climate model simulations of seasonal precipitation over Europe. Climate Dynamics, 35, 685–711.

Rockel, B., Will, A. and Hense, A., 2008. Special issue regional climate modelling with COSMO-CLM (CCLM). Meteorologische Zeitschrift, 17, 347–348.

Roeckner, E., Bäuml, G., Bonaventura, L., Brokopf, R., Esch, M., Giorgetta, M., Hagemann, S., Kirchner, I., Kornblueh, L., Manzini, E., Rhodin, A., Schlese, U., Schulzweida, U. and Tompkins, A., 2003. The Atmospheric General Circulation Model ECHAM5. Report No. 349. Max Planck Institute for Meteorology, Hamburg. Available online: www.mpimet.mpg.de/fileadmin/publikationen/Reports/max_scirep_349.pdf (accessed 13 July 2015).

Scinocca, J.F., McFarlane, N.A., Lazare, M., Li, J. and Plummer, D., 2008. The CCCma third generation AGCM and its extension into the middle atmosphere. Atmospheric Chemistry and Physics, 8, 7055–7074.

Skamarock, W.C., Klemp, J.B., Dudhia, J., Gill, D.O., Barker, D.M., Duda, M.G., Huang, X.Y., Wang, W. and Powers, J.G., 2008. A Description of the Advanced Research WRF Version 3 NCAR Tech. Note TN-475_STR. Available online: /www2.mmm.ucar.edu/wrf/users/docs/user_guide_V3.3/ARWUsersGuideV3.pdf (accessed 10 July 2015).

Shkol'nik, I., Meleshko V., Efimov, S. and Stafeeva, E., 2012. Changes in climate extremes on the territory of Siberia by the middle of the 21st century: An ensemble forecast based on the MGO regional climate model. Russian Meteorology and Hydrology, 37, 71–84.

Steppeler, J., Doms, G., Schättler, U., Bitzer, H.W., Gassmann, A., Damrath, U. and Gregoric, G., 2003. Meso-gamma scale forecasts using the nonhydrostatic model LM. Meteorology and Atmospheric Physics, 82, 75–96.

van der Linden, P. and Mitchell, J.F.B., 2009. ENSEMBLES: Climate Change and Its Impacts: Summary of research and Results from the ENSEMBLES Project. Met Office Hadley Centre, Exeter, UK.

van Vuuren, D.P., Edmonds, J., Kainuma, M.L.T., Riahi, K., Thomson, A., Matsui, T., Hurtt, G.C., Lamarque, J.-F., Toshihiko, M., Meinshausen, M., Smith, S.J., Rose, S., Hibbard, K.A., Nakicenovic, N., Krey, V. and Kram, T., 2011. The representative concentration pathways: an overview. Climatic Change 109(11), 5–31.

Walsh, S., 2012. A Summary of Climate Averages for Ireland 1981–2010. Climatological Note No. 14. Met Éireann, Dublin. Available online: www.met.ie/climate-ireland/SummaryClimAvgs.pdf (accessed 13 July 2015).

2 Impacts of climate change on Irish temperature

The impacts of climate change on air temperatures over Ireland are assessed for mid-century using an ensemble of downscaled climate simulations based on medium- to low-emission and high-emission scenarios. Projections indicate an increase of 1–1.6°C in mean annual temperatures, with the largest increases seen in the east of the country. The annual and seasonal projected increases were found to be statistically significant for both emission scenarios. Warming is enhanced for the extremes (i.e. hot or cold days), with highest daytime temperatures projected to rise by 0.7–2.6°C in summer and lowest night-time temperatures to rise by 1.1–3°C in winter.

Averaged over the whole country, the number of frost days (days when the minimum temperature is less than 0°C) is projected to decrease by 50% for the medium- to low-emission scenario and 62% for the high-emission scenario. Similarly, the number of ice days (days when the maximum temperature is less than 0°C) is projected to decrease by 73% for the medium- to low-emission scenario and 82% for the high-emission scenario. The projections indicate an average increase in the length of the growing season by mid-century of 35 and 40 days per year for the medium- to low-emission and high-emission scenarios, respectively.

2.1 Introduction

The full impact of rising greenhouse gas concentrations on the global climate is difficult to evaluate because of the interactions and dependencies between the numerous physical processes that make up the system. However, basic physics provides a direct link between temperatures and greenhouse gas concentrations. With rising concentrations the atmosphere becomes more opaque at infrared wavelengths, reducing the heat lost to space; the net result is that the Earth is absorbing more energy than it radiates and this imbalance ($0.59 \pm 0.15\,W/m^2$ during the 6-year period 2005–2010) warms the planet (Hansen et al., 2011). The warming is evident in the Irish observational records; a recent study shows a 0.5°C increase in observed mean annual air temperature over Ireland during the period 1981–2010 compared with the 1961–1990 period (Walsh et al., 2013; Met Éireann, n.d.).

2.1.1 Global and European climate projections

The heating effect is well marked in the global model simulations when the radiative forcing associated with greenhouse gases is increased. The IPCC estimates a rise in global mean surface temperatures by the late 21st century of between 0.3°C and 4.8°C (Collins et al., 2013). The warming is not regionally uniform and is amplified at the Arctic latitudes, for example. Changes in European mean temperatures are projected to exceed the global mean. The authors project the median temperature over Ireland for the period 2046–2065 to increase by 1–1.5°C in summer, and by 0.5–1.5°C in winter under the RCP4.5 scenario.

Heinrich and Gobiet (2012) used eight RCMs (all approximately 25-km resolution) from the ENSEMBLES project to analyse projected changes in mean temperature over Europe between 1961–1990 and 2021–2050. Examining the multi-model mean change seasonally, they found that warming is projected across all seasons and all areas; these are most pronounced in the north-east of Europe in winter and in southern Europe in summer. Temperatures over Britain and Ireland are projected to increase uniformly across all areas and all seasons in that period by approximately 1–1.5°C, which is consistent with the findings to be presented in this report. Jacob et al. (2014) compared regional climate change patterns for Europe projected by the regional climate change ensemble of EURO-CORDEX (COordinated Regional climate Downscaling Experiment) (RCP4.5 and RCP8.5 scenarios) with the A1B projections of the ENSEMBLES project. They found that the large-scale patterns of changes in mean temperature are similar in all three scenarios, but they differ in regional details, which can partly be related to the higher resolution (~12.5 km) of the EURO-CORDEX simulations. The results “strengthen the previous findings obtained from the ENSEMBLES data set” (Jacob et al., 2014).

2.1.2 Projections for Ireland

The Community Climate Change Consortium for Ireland (C4I) downscaled data from five GCMs over Ireland and Britain, using all SRES scenarios, achieving a finest horizontal resolution of 14 km. They found that mean seasonal temperatures for 2021–2060 are projected to increase by 1.1–1.4°C, with the greatest increases occurring during summer and autumn (1.2–1.4°C). The warming was found to be greatest in the south and east of the country (McGrath and Lynch, 2008). In 2013, the Research Division at Met Éireann led a major study on the future of Ireland's climate. A subset of the ensemble of RCM simulations used in the current study was analysed and projected an increase of ~1.5°C in mean temperatures by mid-century over Ireland (Nolan et al., 2013). O'Sullivan et al. (2015) expanded upon this research and concluded that "annual mean temperatures are projected to rise between 0.4°C and 1.8°C above control levels by mid-century".

2.1.3 Projections of extreme temperature

In addition to changes in mean temperatures, climate change will also have an impact on the extremes. This is reflected in the Irish observational record in recent decades (Met Éireann, n.d.) and is expected to continue in the future with possible consequences for human health and mortality (Seneviratne et al., 2012). The IPCC has found that it is now "very likely" that human-induced climate change has contributed "to the observed changes in the frequency and intensity of daily temperature extremes on the global scale" (Stocker et al., 2013). This confirms what was already suggested in both IPCC AR4 (Solomon et al., 2007) and an IPCC special report: *Managing the Risks of Extreme Events and Disasters to Advance Climate Change Adaptation* (Field et al., 2012). The authors warn that short-term projections suggest that increases in temperature extremes are likely. In Europe, high-percentile summer temperatures are projected to rise faster than mean temperatures (Field et al., 2012).

Beniston et al. (2007) used the RCM output from the Prediction of Regional scenarios and Uncertainties for Defining EuropeaN Climate change risks and Effects (PRUDENCE) project to examine how extreme temperature events in Europe are projected to change by the end of the 21st century (Beniston et al., 2007). They found that "the intensity of extreme temperatures increases more rapidly than the intensity of more moderate temperatures over the continental interior due to increases in temperature variability".

In their study of Northern Ireland, Mullan et al. (2012) examined the projected changes in extremes of temperature. They used the threshold approach to define percentile values for the control period that depend on each particular location; the 90th percentile of maximum temperature to examine changes in hot days and the 10th percentile of minimum temperature to examine changes in cold nights. The projected changes in these thresholds at each site were then calculated. Both the hot-day threshold and the cold-night threshold are projected to increase by similar amounts, and show an increasing trend through the 2020s, 2050s and 2080s. There is a large uncertainty range for both changes, though all ranges are non-negative (Mullan et al., 2012).

Results from the Met Éireann climate change report of 2013 (Nolan et al., 2013) show that the expected warming over Ireland was found to be enhanced for the extremes, with the highest daytime temperatures projected to rise by up to 2°C in summer and the lowest night-time temperatures to rise by up to 3°C in winter. These findings were confirmed by O'Sullivan et al. (2015).

2.1.4 Current study

The current study aims to assess the impacts of climate change on near-surface air temperatures over Ireland. To address the issue of model uncertainty, a large ensemble of simulations were run. The models were run at high spatial resolution, up to 4 km, thus allowing a sharper assessment of the regional variations in projected temperature increases. The current research consolidates and expands on the RCM temperature projections of a 2013 Met Éireann report (Nolan et al., 2013) by increasing the ensemble size. This allows likelihood levels to be assigned to the projections. In addition, the uncertainty of the projections can be more accurately quantified. Details of the different global climate datasets, the greenhouse gas emission scenarios and the downscaling models used to produce the ensemble of climate projections for Ireland are summarised in Chapter 1.

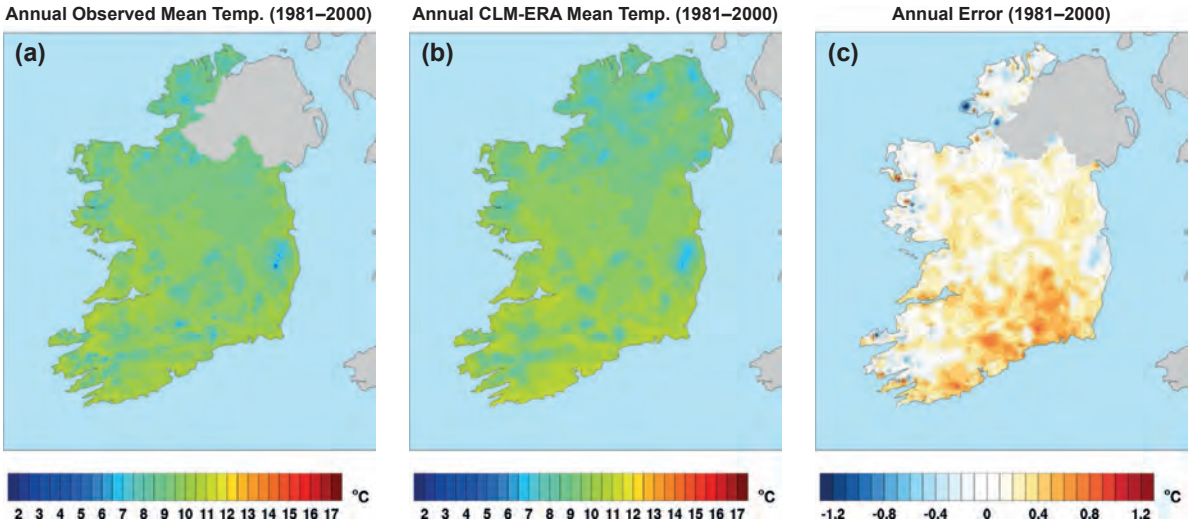

Figure 2.1. Annual 2-m temperature for the period 1981–2000. (a) Observations; (b) CLM-ERA 4 km data; (c) CLM-ERA minus observations (bias).

2.2 Regional climate model temperature validations

The RCMs were validated by performing 20-year simulations of the Irish climate (1981–2000), driven by ECMWF ERA-40 global re-analysis data and comparing the output against observational data. Figure 2.1a presents the observed 2-m temperature[2] averaged over the 20-year period 1981–2000 (data from Walsh, 2012). Figure 2.1b presents the downscaled ERA-40 data as simulated by the CLM4 model at 4-km resolution (denoted CLM-ERA). It is noted that the CLM-ERA data accurately capture the magnitude and spatial characteristics of the observed temperature climate. This is confirmed by Figure 2.1c, which shows a small positive bias, of mean value 0.21°C, over Ireland. Previous studies have shown that the ERA-40 data exhibit a positive bias of approximately 1°C over Ireland (McGrath et al., 2005).

The seasonal validations are presented in the rows of Figure 2.2. The first, second and third columns present the observed temperature, the CLM-ERA temperature and the bias, respectively. The CLM-ERA simulation data exhibit a positive bias for winter, spring and autumn and a small negative bias for summer. The largest bias, of approximately ~0.6°C, is noted for winter.

The validations were repeated for the different RCMs of the ensemble. In general, it was found that, while the accuracy decreased with lower model resolution, the output of the RCMs exhibited reasonable and realistic features as documented in the historical data record. Future validation work will focus on downscaling and analysing the more up-to-date and accurate ERAInterim dataset from ECMWF, in place of ERA-40.

2.3 Temperature projections for Ireland

2.3.1 Mean temperature projections

Figure 2.3a presents the time series of annual mean temperature anomalies, relative to the 1981–2000 mean, for the five greenhouse gas scenarios for 2041–2060. These are calculated using values averaged over all grid points covering Ireland. The dashed lines are lines of regression, calculated by the least-squares algorithm to show the linear trend over the two decades. There is a broad range of values for temperature changes projected across the five emission groups. Group B1 shows the least warming (its mean anomaly is 0.66°C) and the greatest interannual variability. Its large spread, seen through its annual mean anomalies ranging from −0.4°C to greater than 1.4°C, is most likely from its being composed of a single-member ensemble. The remaining four emission scenarios show greater warming than B1, with A2, A1B and RCP45 having large areas of overlap, and similar 20-year means (1.1°C, 1.2°C and 1.24°C, respectively). RCP85 shows the greatest warming, with a trend line always exceeding the other groups (its mean anomaly is 1.56°C). As expected, there is a general upward trend in temperature, which is more pronounced for the high-emission scenarios.

2 The observed gridded dataset has an estimated mean absolute error of 0.19°C and a root mean square error of 0.41°C.

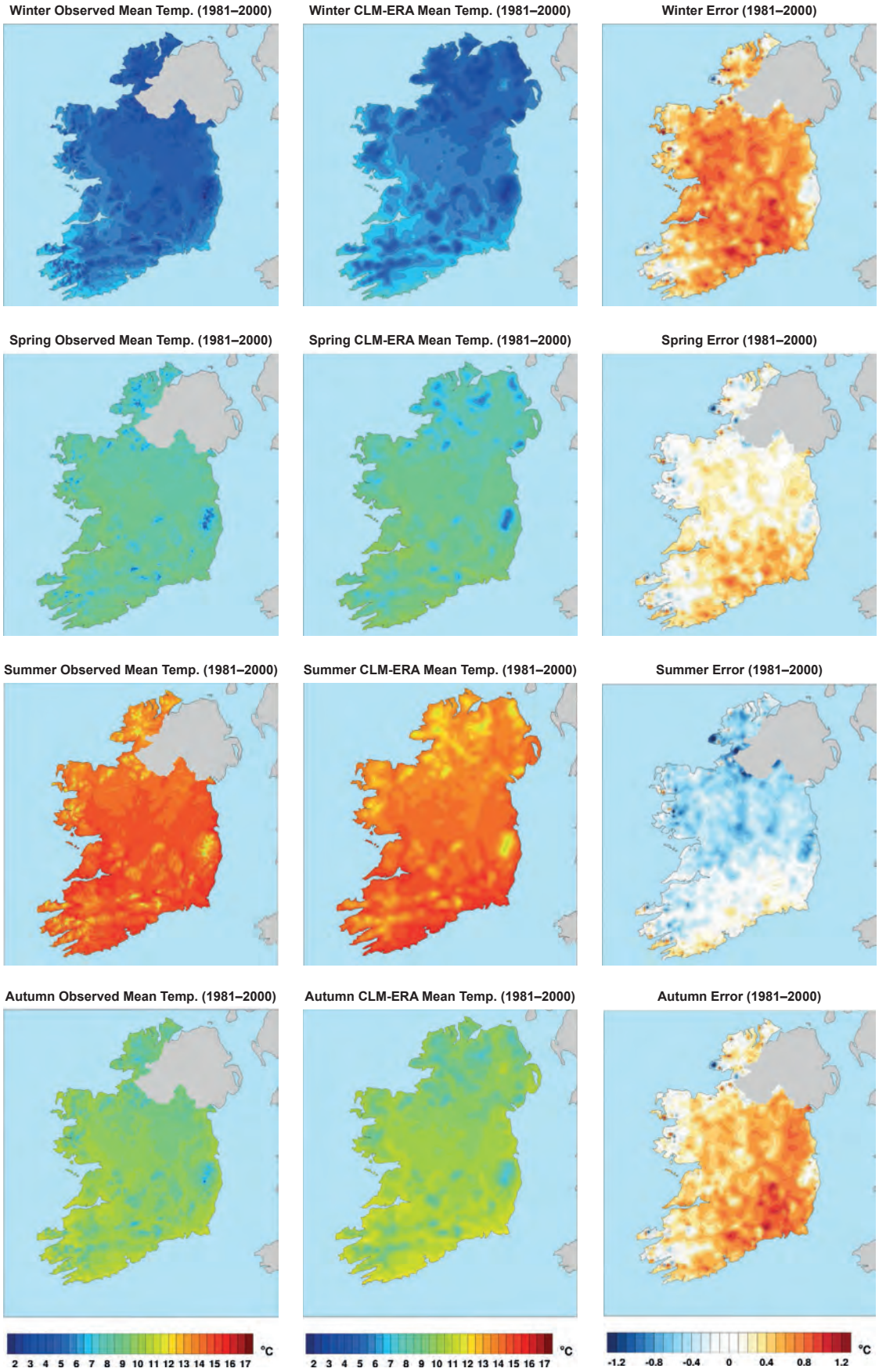

Figure 2.2. Seasonal 2-m temperature for 1981–2000. The first, second and third columns contain observations, CLM-ERA data and the bias, respectively. The colour scale is kept fixed for each column and is included in the last row.

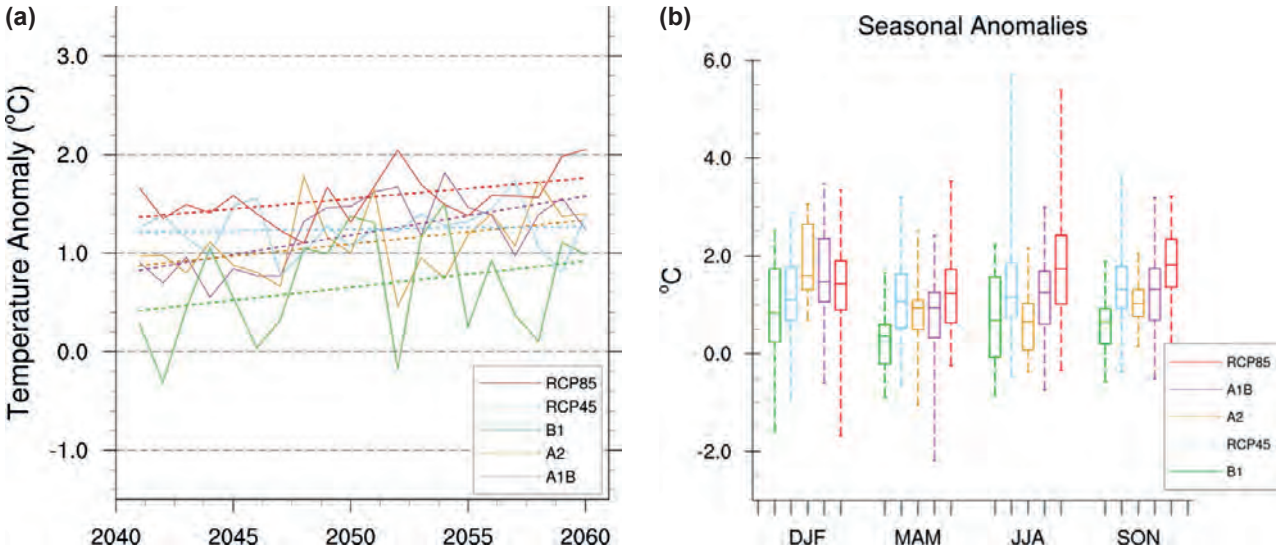

Figure 2.3. Annual mean temperature anomalies for each of the five emission scenarios, averaged across every grid point over Ireland. (a) Time series of the annual mean temperature anomalies. The dashed coloured lines are lines of regression fitted using the least-squares method. (b) Seasonal mean temperature anomalies for winter (December–February), spring (March–May), summer (June–August) and autumn (September–November). The boxplots represent the spread of each group; the bottom and top whiskers represent the minimum and maximum group values, respectively, the bottom and top of the box represent the group's first and third quartiles, respectively, and the middle line represents the group's median. For both figures, the future period 2041–2060 is compared with the past period 1981–2000.

Note, however, the large variability over short periods; the warming trend is essentially superimposed on the background, or natural variability, of the climate, which is expected to continue in the presence of rising greenhouse gas concentrations.

Since annual trends can hide or smooth larger seasonal trends, seasonal temperature anomalies were also examined. It was found that (1) the RCMs simulate interannual and seasonal variability in a manner consistent with the observed climate, including cold events, and (2) warming is evident for all scenarios across all seasons. The box and whisker plots for each emission scenario group are presented in Figure 2.3b for winter (December–February), spring (March–May), summer (June–August) and autumn (September–November). The whisker ends mark the maximum and minimum values, while the box marks the median value (central line) and the first and third quartile values (lower and upper sides, respectively). The seasonal anomalies in Figure 2.3b again illustrate that uncertainty exists in the future projections, both within each season and within each emission scenario group. Within summer, for example, temperature anomalies range from ~–1°C in one particular year (group B1) to almost 6°C in another (RCP45). The anomalies below 0°C are indicative of the natural variability inherent in the climate system. A particularly cold spring projected in group A1B, for example, has a seasonal temperature anomaly below −2°C. However, the overall trend of an increase in temperature is evident across all seasons. With the exception of group B1 in spring and summer, all first quartiles across all seasons exceed 0°C, suggesting a definitive upward shift in temperature, relative to the period 1981–2000, across all groups and all seasons. There are also clear differences between results across the different emission scenario groups. The largest summer increases are noted for group RCP85, whereas the largest winter increases are noted for groups A1B and A2. It should be noted that, for the above analysis (Figure 2.3), the individual RCMs within the same group were not cross-compared as described in section 1.6 and Table 1.2. While this results in a smaller ensemble, it allows for comparison with similar studies. It was found that the magnitude of the results for group RCP45 (shown in Figure 2.3b) broadly agrees with a study on a larger ensemble analysed in IPCC AR5 (Collins et al., 2013), which projected the median temperature over Ireland to increase by 1–1.5°C in future summers, and by 0.5–1.5°C in future winters under RCP4.5, for the period 2046–2065.

Figure 2.4 presents the spatial distribution of annual temperature changes for 2041–2060 relative to 1981–2000. As explained in Chapter 1, the RCM projections are regridded onto a common 7-km grid and grouped into a medium- to low-emission scenario and a high-emission scenario. The mean annual temperature is projected to increase by 1–1.3°C and 1.2–1.6°C for the medium- to low-emission scenario and the high-emission scenario, respectively. The warming is greatest in the east.

The seasonal temperature projections for the medium- to low-emission and high-emission ensembles are presented in Figure 2.5. Winter temperatures show increases ranging from 1°C in the south-west to 1.3°C in the north for the medium- to low-emission scenario (1.2°C in the south-west and 1.7°C in the north for the high-emission scenario). Summer temperatures, on the other hand, show increases from 0.9°C in the north-west to 1.3°C in the south-east for the medium- to

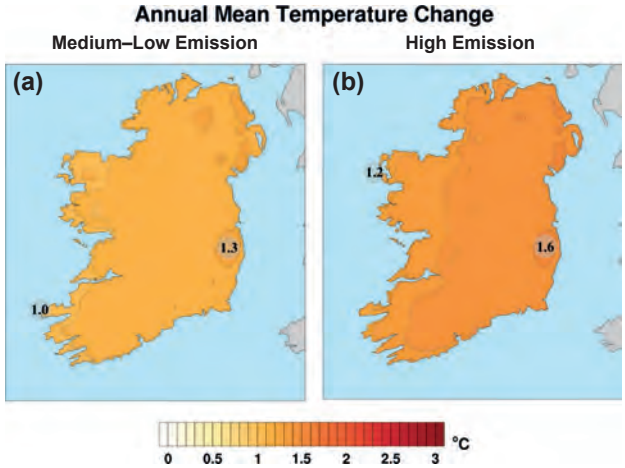

Figure 2.4. Projected changes in annual mean temperature for the (a) medium- to low-emission and (b) high-emission scenarios. In each case, the future period 2041–2060 is compared with the past period 1981–2000. The numbers included on each plot are the minimum and maximum projected changes, displayed at their locations.

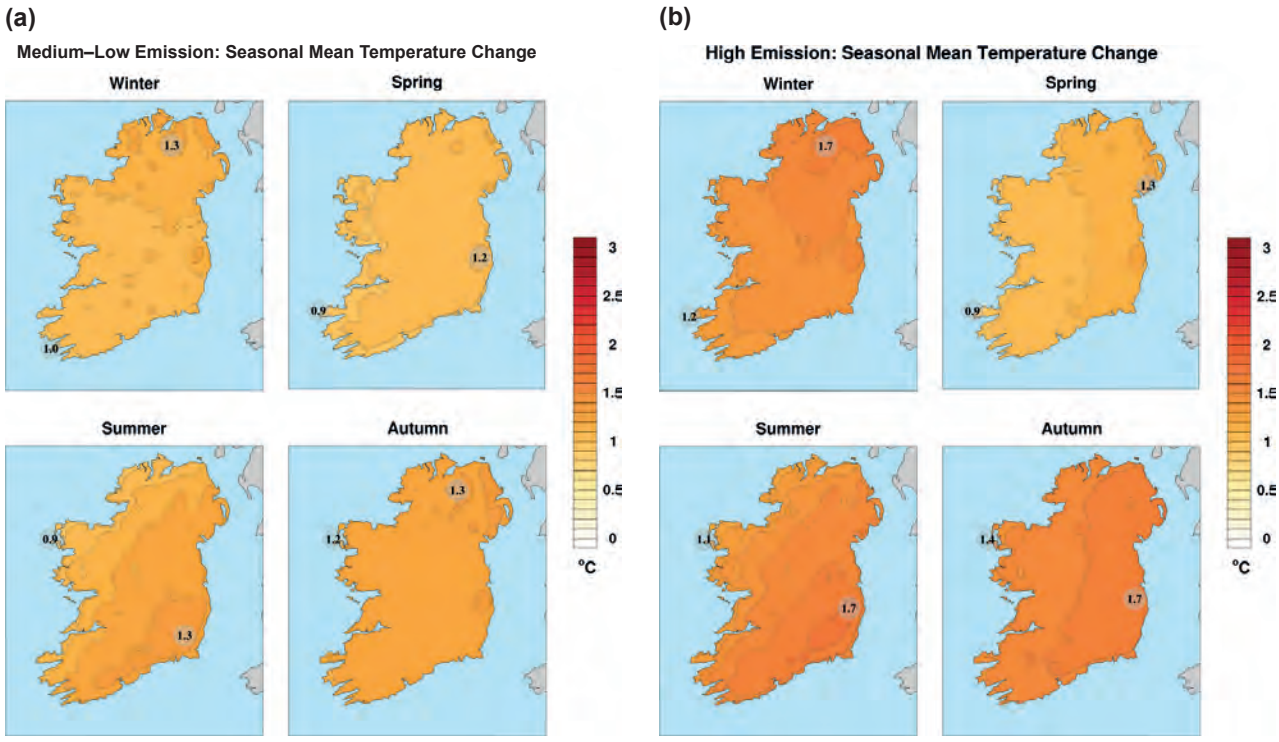

Figure 2.5. Projected changes in seasonal mean temperature for the (a) medium- to low-emission and (b) high-emission scenarios. In each case, the future period 2041–2060 is compared with the past period 1981–2000.

low-emission scenario (1.1°C in the north-west and 1.7°C in the south-east for the high-emission scenario). The temperature increment gradient is therefore from north-west to south-east in summer but from south-west to north-east in winter.

The patterns are different for spring and autumn. Spring shows a projected increase in temperature of approximately 1°C for both the medium- to low-emission and high-emission scenarios, with more warming projected in the east than in the west. Autumn shows a similar east–west pattern, but with greater warming: up to 1.3°C and 1.7°C for the medium- to low-emission and high-emission scenarios, respectively.

Figure 2.6 shows the spatial distribution of the projected "very likely" annual increases in temperature. As outlined in Chapter 1, a "very likely" projection is defined as one in which over 90% of the ensemble members agree. From Figure 2.6, it can be seen that over 90% of the ensemble members project an annual increase in temperature of 0.7°C to 1°C for the medium- to low-emission scenario and 0.8°C to 1.2°C for the high-emission scenario. That is to say, it is "very likely" that increases in annual temperature will be greater than or equal to these values. The "very likely" seasonal increases, presented in Figure 2.7, range from a minimum of 0.4°C for spring to a maximum of 1.3°C for winter.

Similarly, the "likely" (over 66% of the ensemble members agree) annual and seasonal increases in temperature are presented in Figures 2.8 and 2.9, respectively.

The warming gradients of Figures 2.4 and 2.5 are also evident in the "likely" projections of Figures 2.8 and 2.9 and, to a lesser extent, the "very likely" projections of Figures 2.6 and 2.7. For example, the annual west–east warming gradient is clearly evident in both the mean and "very likely" projections. Furthermore, the annual and seasonal warming gradients are similar for both emission scenarios. This agreement increases the confidence in the regional projections of temperature. There are many possible factors which could have influenced the contrasting seasonal warming gradients, such as a change in storm tracks or the North Atlantic Oscillation (NAO) relative to the control period, 1981–2000. However, further investigation of these factors is necessary to attribute causation, and is beyond the scope of this study.

2.3.2 *Projections of extreme temperature and frost/ice days*

Changes in the daily maximum and daily minimum temperatures are arguably of more immediate importance, since extreme events have an abrupt and much larger impact on lives and livelihoods than a gradual change in mean values (Easterling et al., 2000). A sustained increase in the daily maximum temperature is associated with heatwaves whereas an increase in the daily minimum temperature will typically imply warmer nights. Figure 2.10 shows how the warmest 5% of daily maximum summer temperatures are projected to change (TMAX 95%). A stronger warming is evident, which is greater than the projected mean summer

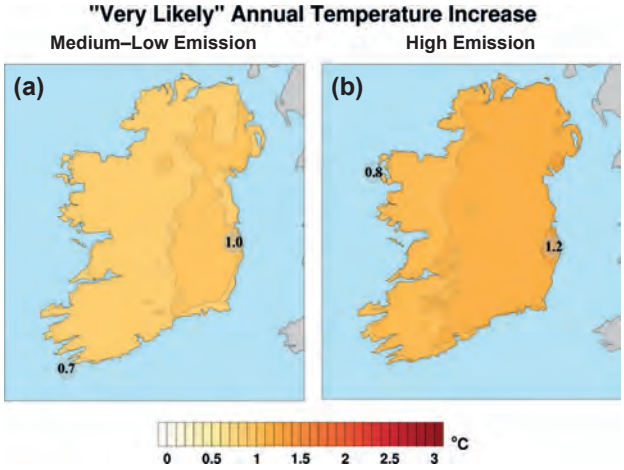

Figure 2.6. The "very likely" annual increase in temperature for the (a) medium- to low-emission and (b) high-emission scenarios. In each case, the future period 2041–2060 is compared with the past period 1981–2000. The numbers included on each plot are the minimum and maximum "very likely" increases, displayed at their locations.

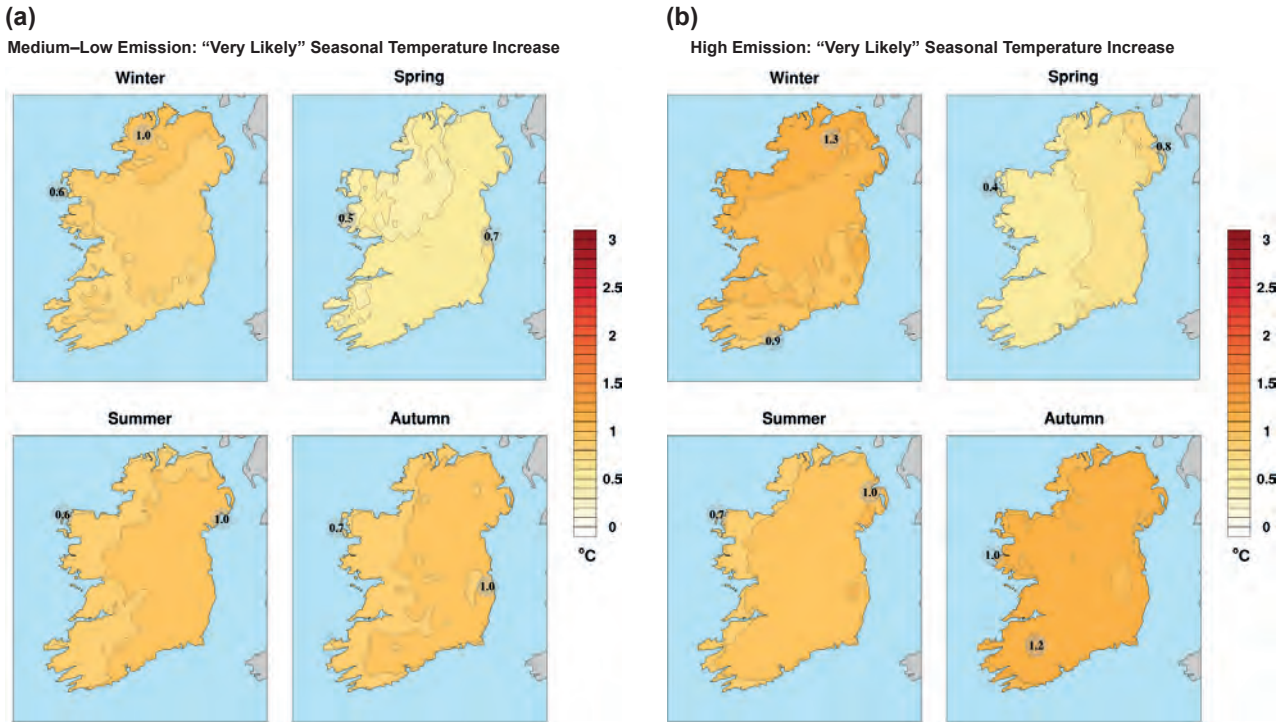

Figure 2.7. The "very likely" seasonal increase in temperature for the (a) medium- to low-emission and (b) high-emission scenarios. In each case, the future period 2041–2060 is compared with the past period 1981–2000.

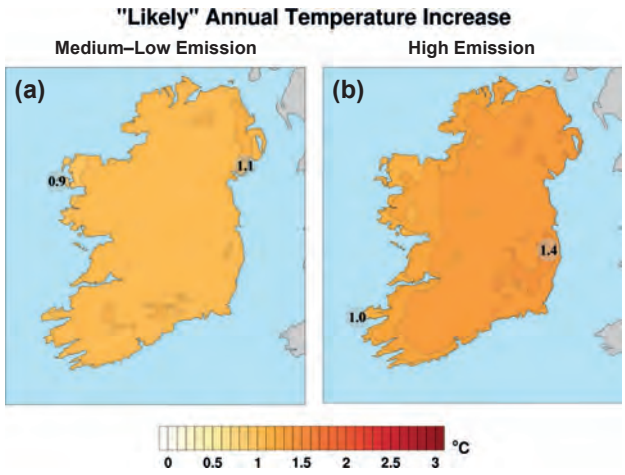

Figure 2.8. The "likely" annual increase in temperature for the (a) medium- to low-emission and (b) high-emission scenarios. In each case, the future period 2041–2060 is compared with the past period 1981–2000. The numbers included on each plot are the minimum and maximum "likely" increases, displayed at their locations.

increase (Figure 2.5), and ranges from 0.7°C to 2°C for the medium- to low-emission scenario and from 1.3°C to 2.6°C for the high-emission scenario. Warming is greater in the south than in the north.

Figure 2.11 shows how the coldest 5% of night-time temperatures in winter are projected to change (TMIN 5%). Both the medium- to low-emission and high-emission scenarios lead to greater warming in the north than in the south, with minimum temperatures projected to increase by 1.1°C in the south-west and by 2.5°C in the north for the medium- to low-emission scenario (1.4°C in the south-west and 3.1°C in the north for the high-emission scenario). The TMAX and TMIN temperature gradients of Figures 2.10 and 2.11 are

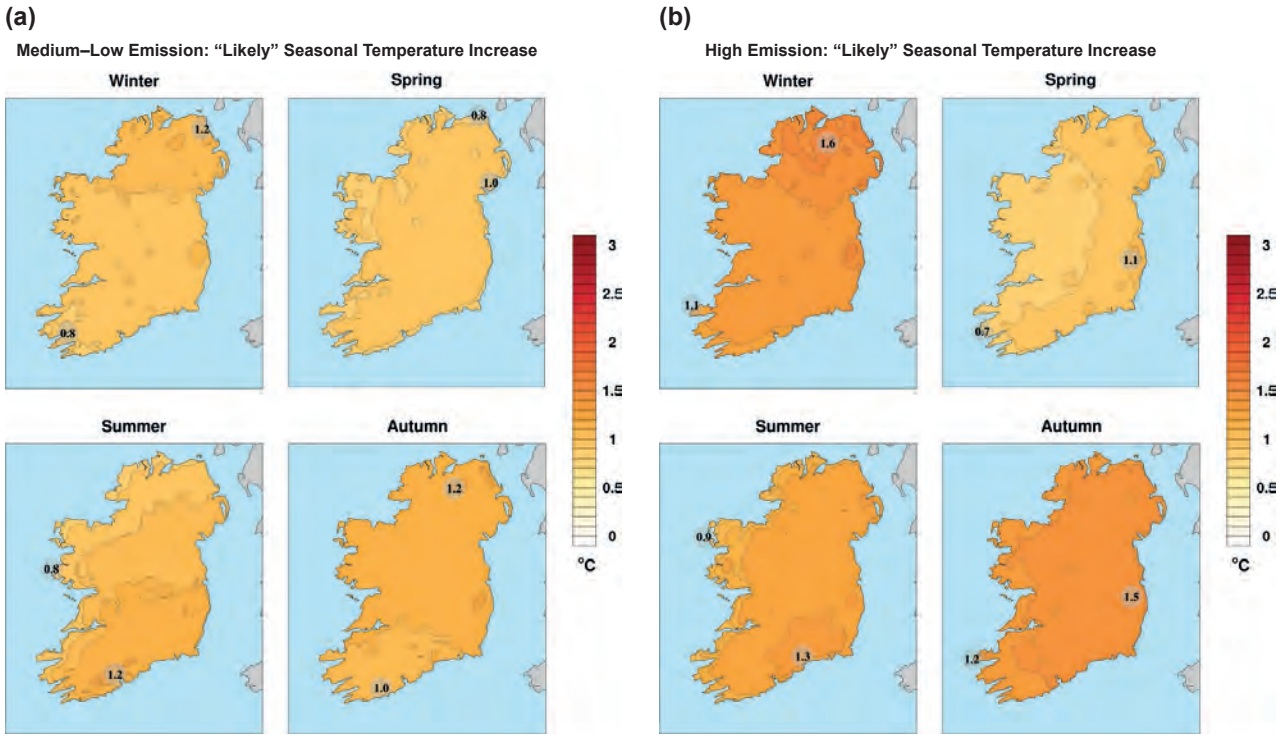

Figure 2.9. The "likely" seasonal increase in temperature for the (a) medium- to low-emission and (b) high-emission scenarios. In each case, the future period 2041–2060 is compared with the past period 1981–2000.

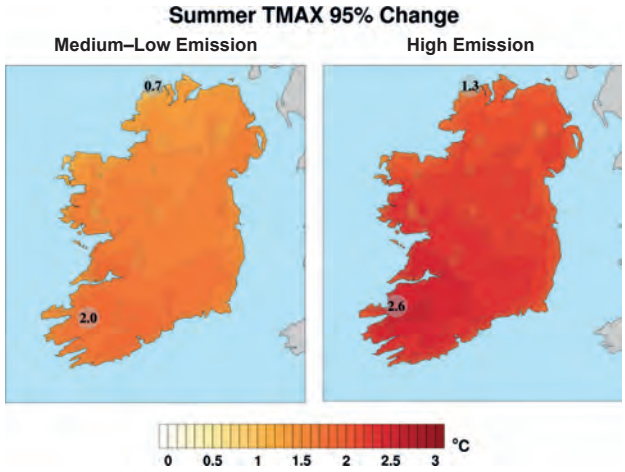

Figure 2.10. Projected changes in the top 5% of maximum daytime summer temperatures for the medium- to low-emission and high-emission scenarios. In each case, the future period 2041–2060 is compared with the past period 1981–2000. The numbers included on each plot are the minimum and maximum increases, displayed at their locations.

also evident in the "very likely" projections (not shown), thus increasing confidence in the regional variations of extreme temperature projections.

With mean night-time temperatures expected to rise faster than mean daytime temperatures, there is likely to be a reduction in winter mortality in Ireland but this may be offset by an increase in the frequency and severity of heatwaves (Nolan et al., 2013).

The large projected decrease in cold nights (TMIN 5%) implies a decrease in the number of frost and ice days

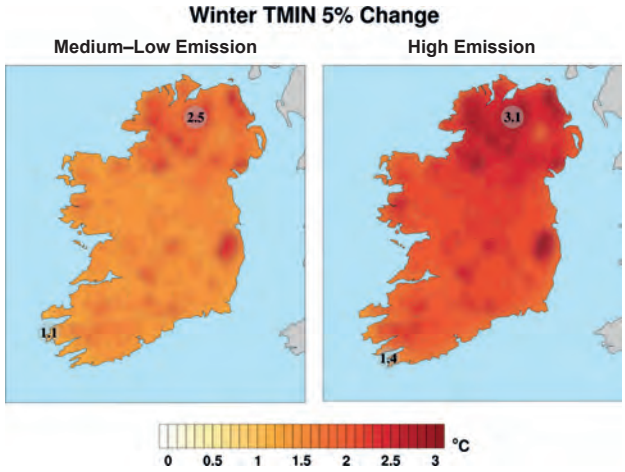

Figure 2.11. Projected changes in the lowest 5% of night-time winter temperatures for the medium- to low-emission and high-emission scenarios. In each case, the future period 2041–2060 is compared with the past period 1981–2000. The numbers included on each plot are the minimum and maximum increases, displayed at their locations.

by mid-century. This is confirmed by Figures 2.12a and 2.13a, which present the projected annual change in frost and ice days, respectively. Averaged over the whole country, the number of frost days (days when the minimum temperature is less than 0°C) is projected to decrease by 50% for the medium- to low-emission scenario and 62% for the high-emission scenario. Similarly, the number of ice days (days when the maximum temperature is less than 0°C) is projected to decrease by 73% for the medium- to low-emission scenario and 82% for the high-emission scenario. For comparison, the observed annual mean numbers of frost and ice days for 1981–2000 are presented in Figures 2.12b and 2.13b, respectively (data from Walsh, 2012). Note that the observed number of ice days is small. It is worth noting that periods of frost and ice are important environmental drivers which trigger phenological phases in many plant and animal species. Changes in the occurrence of these weather types may disrupt the life cycles of these species.

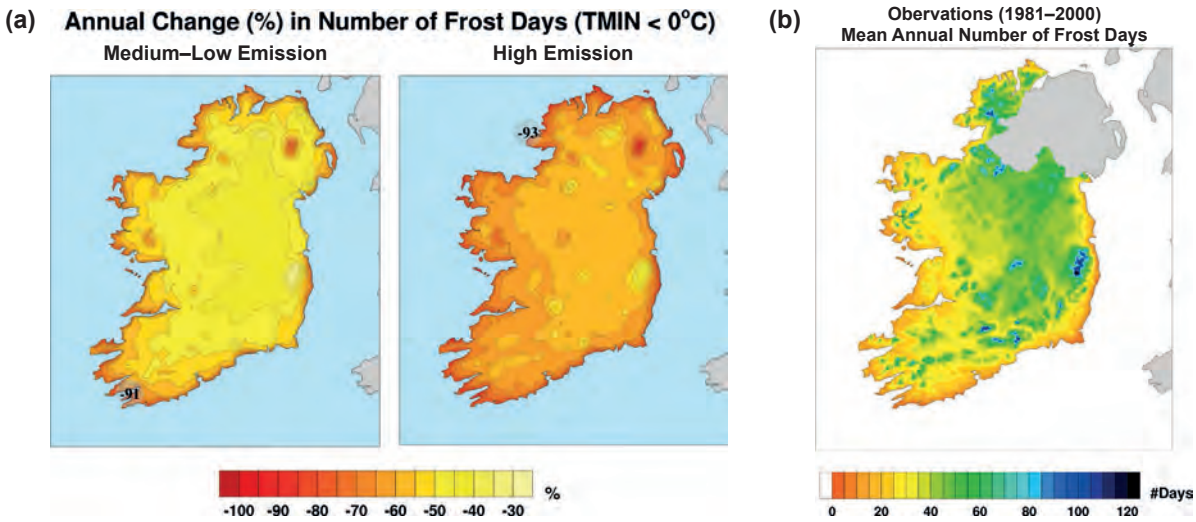

Figure 2.12. Annual frost day statistics. (a) Projected percentage change in annual number of frost days for the medium- to low-emission and high-emission scenarios. In each case, the future period 2041–2060 is compared with the past period 1981–2000. (b) The observed mean annual number of frost days, over land, for 1981–2000.

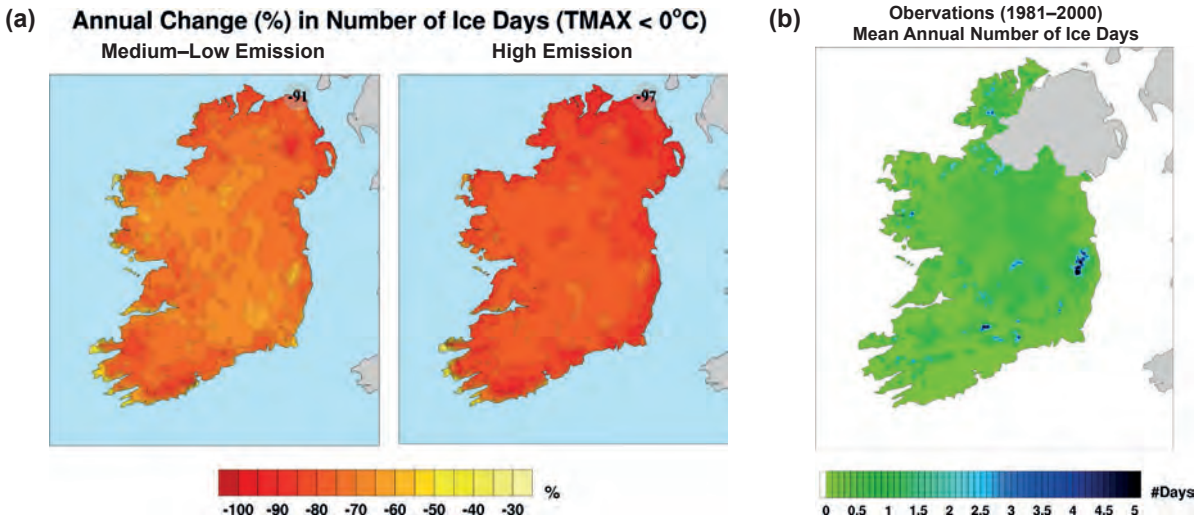

Figure 2.13. Annual ice day statistics. (a) Projected percentage change in annual number of ice days for the medium- to low-emission and high-emission scenarios. In each case, the future period 2041–2060 is compared with the past period 1981–2000. (b) The observed mean annual number of ice days, over land, for 1981–2000.

2.3.3 Changes in the shape of the future temperature distribution

A more comprehensive step in moving from analysing mean values to the examination of extreme events is to consider the distribution function of a quantity. The distribution of a quantity involving discrete data (as here) can be represented by its empirical density function. Figure 2.14 presents the seasonal density functions (hereafter, density) of mean daily temperature anomalies at every grid point over Ireland. For each past simulation, the anomalies are calculated by subtracting the mean temperature over the 20-year period 1981–2000 from the daily mean temperature.[3] Similarly, the future daily anomalies (2041–2060) are calculated by subtracting the historical mean temperature (1981–2000) from each future ensemble member within the same group (see Table 1.2).

The density of the past period is shown in black, with the densities of the medium- to low-emission and high-emission scenarios in blue and red, respectively. An *overlap score* was calculated, which assesses the similarity between the group's past and future (adapted from a methodology described by Perkins et al., 2007). The *overlap score* is given by:

$$0_{score} = 100 \times \sum_{1}^{n} \min\left(Z_{past}, Z_{future}\right) \qquad (2.1)$$

where n is the number of bins used to calculate the pdf, Z_{past} is the frequency of values in a given bin from the past data and Z_{future} is the frequency of values in a given bin from the future data. This score is between 0% and 100%, with 100% indicating perfect agreement (climate completely unchanged) and 0% indicating no agreement (past and future climates have no values in common).

Figure 2.14 shows temperature increases across all seasons, with each future density mean (blue and red vertical lines) shifted to the right of the historical distribution mean (black vertical line). In addition to this mean increase, the future density values across the entire range are shifted to the right, strengthening the evidence from all previous analysis of increases in both the mean values and the tails of the temperature distribution. The overlap scores range from 73% in summer (showing the largest increase across the distribution) to 88% in spring (showing the least change between historical and future densities). This result confirms the projected mean increases shown in Figure 2.5, where large increases are projected for summer and the smallest increases are projected for spring.

2.3.4 Statistical significance of temperature changes

Since all projections show a definite increase in temperature over Ireland for all seasons, the Ha_2 alternative hypothesis is tested for the future temperature distributions of Figure 2.14. Here, the

3 This results in two slightly different past densities (corresponding to the two future emission scenario groups). As the differences were found to be very small, the medium- to low-emission past densities are excluded from Figure 2.14.

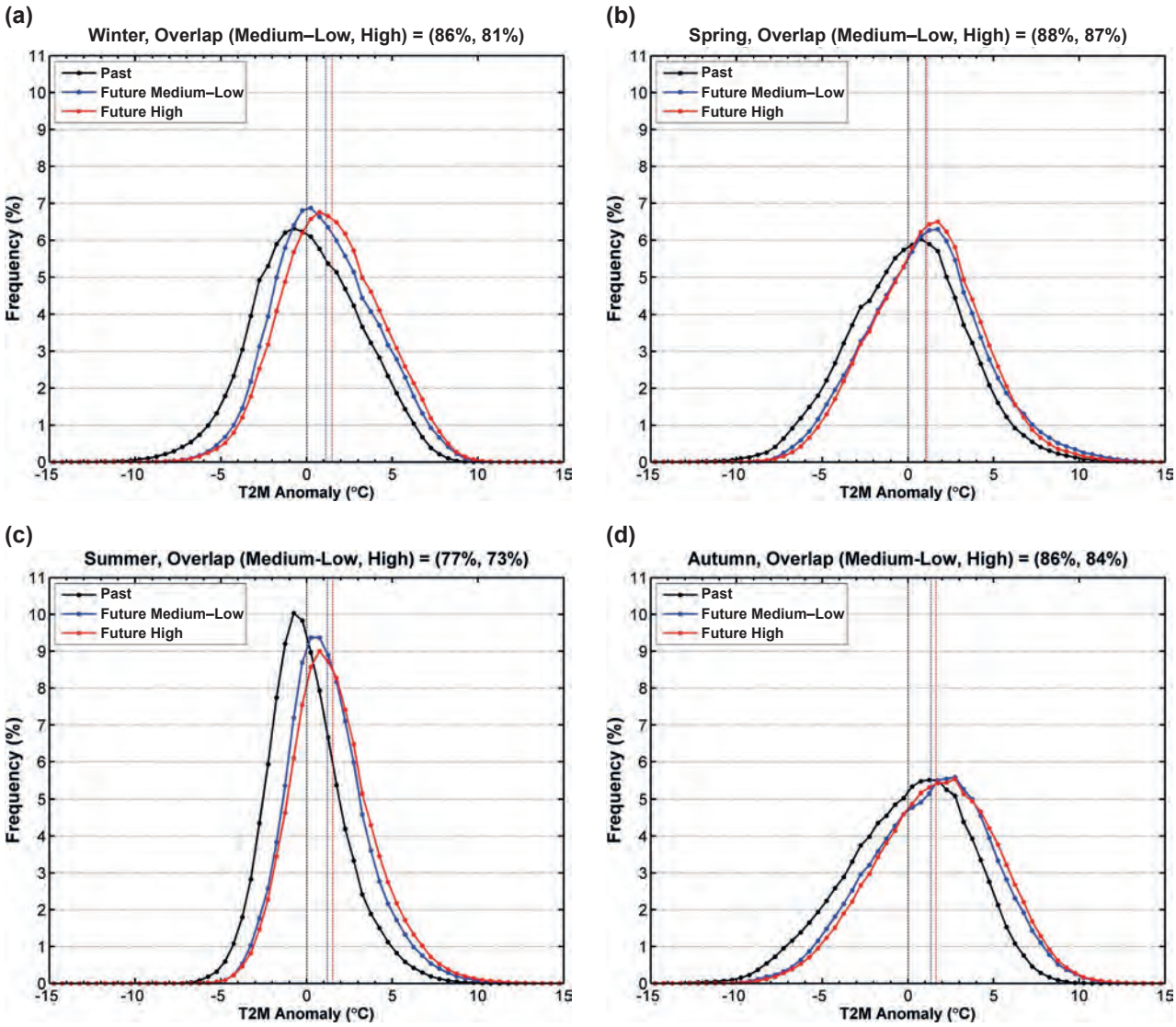

Figure 2.14. Empirical density functions illustrating the distribution of past (black), medium- to low-emission (blue) and high-emission (red) mean daily temperatures over Ireland. (a) Winter; (b) spring; (c) summer; (d) autumn. Each dataset has a size greater than 80 million. The distributions are created using histogram bins of size 0.5°C. A measure of overlap indicates how much the future distributions have changed relative to the past (0% indicating no common area, 100% indicating complete agreement). Means are shown for historical (black vertical line), medium- to low-emission (blue vertical line) and high-emission (red vertical line) densities.

alternative hypothesis states that the future temperatures (Kolmogorov–Smirnov) and the future median values (Wilcoxon rank-sum) are greater than the past. Both the Kolmogorov–Smirnov and Wilcoxon rank-sum tests show high levels of significance ($p \approx 0$) for the medium- to low-emission and high-emission scenarios across all seasons. We therefore conclude that the increase in future temperatures over Ireland is statistically significant.

2.3.5 Projected changes in the shape of temperature distribution

The temperature distributions of Figure 2.14 suggest that, while the future mean daily temperatures will increase significantly for all seasons, the changes in the shape of the spring and autumn distributions are small. This is consistent with Figure 2.15, which shows relatively small seasonal changes in the standard deviation of spring and autumn mean daily temperature for

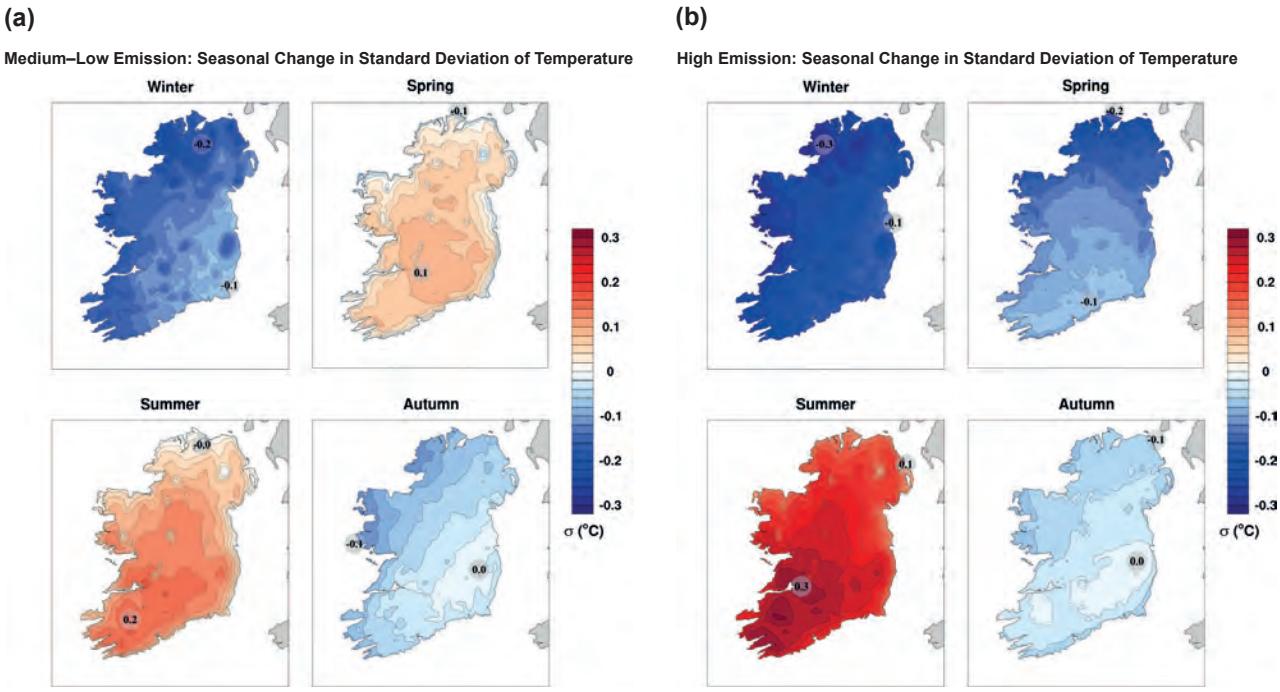

Figure 2.15. Seasonal projected changes in the standard deviation of mean daily temperature. (a) Medium- to low-emission ensemble; (b) high-emission ensemble. In each case, the future period 2041–2060 is compared with the past period 1981–2000. The numbers included on each plot are the minimum and maximum projected changes, displayed at their locations.

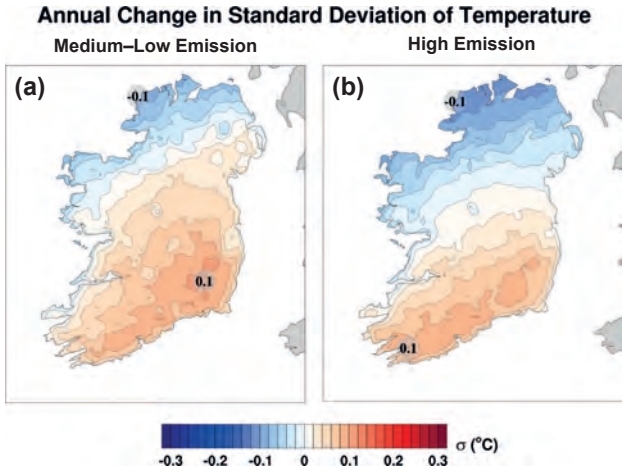

Figure 2.16. Annual projected changes in the standard deviation of mean daily temperature. (a) Medium- to low-emission scenario; (b) high-emission scenario. In each case, the future period 2041–2060 is compared with the past period 1981–2000.

both the medium- to low-emission and high-emission scenarios. The largest changes are noted for winter and summer. This is consistent with the distributions and low overlap scores of Figure 2.14a and c. The annual change in the standard deviation (Figure 2.16) shows small changes of between −0.1°C and 0.1°C for both the medium- to low-emission and high-emission scenarios.

To accurately interpret the projected changes of standard deviation, the annual and seasonal standard deviation of mean daily temperature for the control period are presented in Figure 2.17. The figures were generated using the entire RCM dataset for 1981–2000. As expected, the largest spread in temperature is noted over the entire year. Large variations in temperature are also noted during the spring and autumn months.

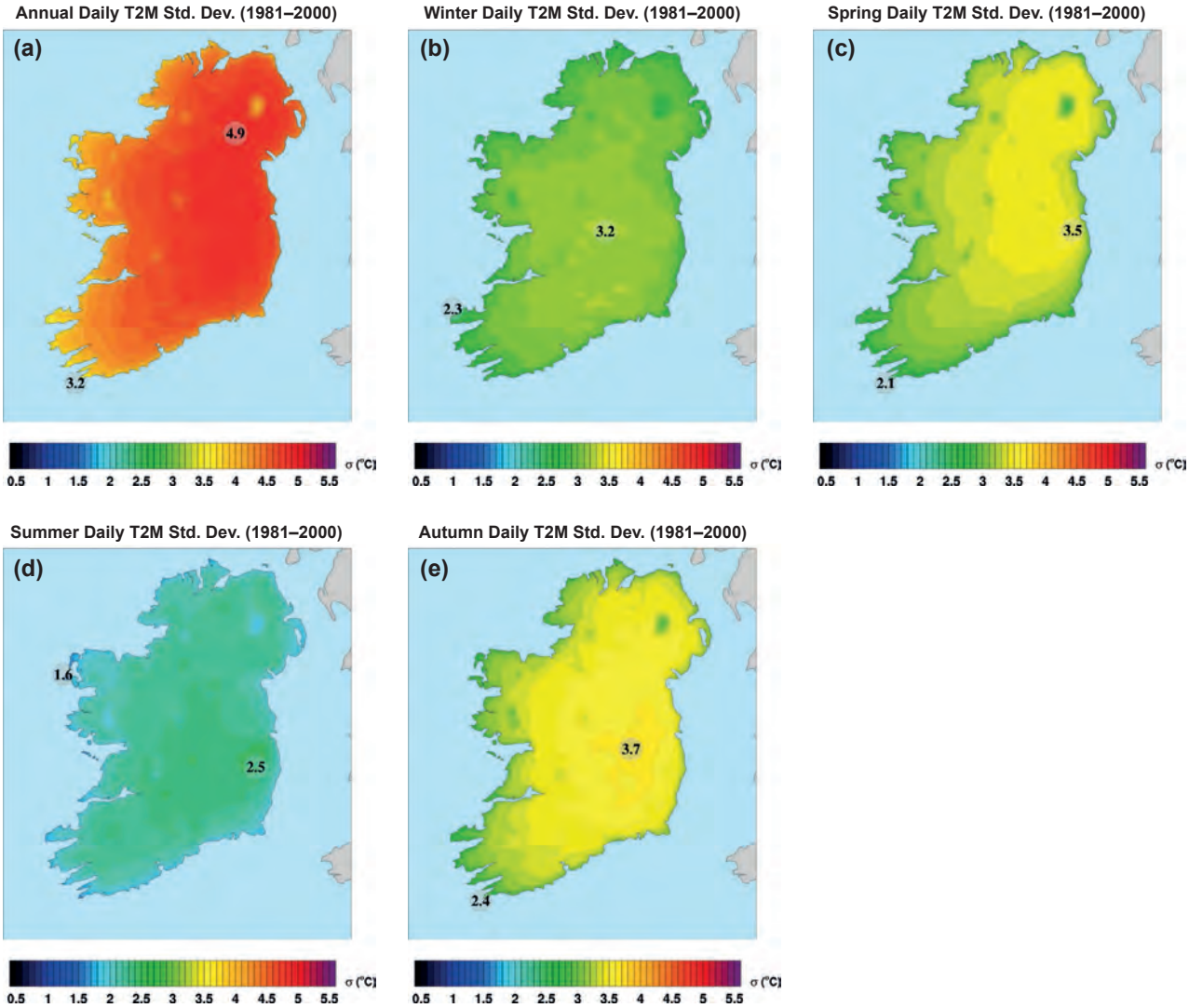

Figure 2.17. The standard deviation of mean daily temperature for the past period 1981–2000. (a) Annual; (b) winter; (c) spring; (d) summer; (e) autumn. The figures were generated using all RCM ensemble member data for the control period. The numbers included on each plot are the minimum and maximum values, displayed at their locations.

2.3.6 Growing season projections

A recent report (Flood, 2013) projects that the total economic costs of climate change to Ireland's agriculture sector will be in the region of €1–2 billion per annum by mid-century. This figure represents 8.2% of the current contribution of the agricultural sector to the national economy annually, and at the upper level is greater than the Harvest 2020 targeted increase of €1.5 billion in primary output. The report states that "the most significant climate change impacts on Irish agriculture relate to pests and diseases, crop yields, flooding, plant and animal stress factors, drought effects and the ability to provide sufficient resources for animals during extreme events". These adverse effects of climate change on the agriculture sector may be somewhat offset by a projected increase in the length of the Irish growing season. Within a period of 12 months, the thermal growing season length is officially defined as the number of days between the first occurrence of at least 6 consecutive days with daily mean temperature > 5°C and the first occurrence of at least 6 consecutive days with daily mean temperature < 5°C.

Figure 2.18 shows a large projected increase in the average length of the growing season over Ireland by mid-century. Averaged over the whole country, the medium- to low-emission and high-emission scenarios

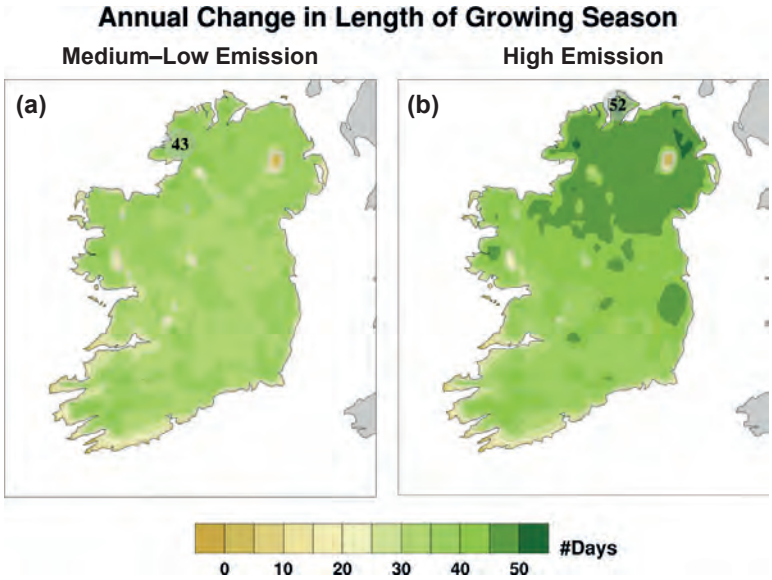

Figure 2.18. Projected changes the length of the growing season (days per year). (a) Medium- to low-emission scenario; (b) high-emission scenario. In each case, the future period 2041–2060 is compared with the past period 1981–2000.

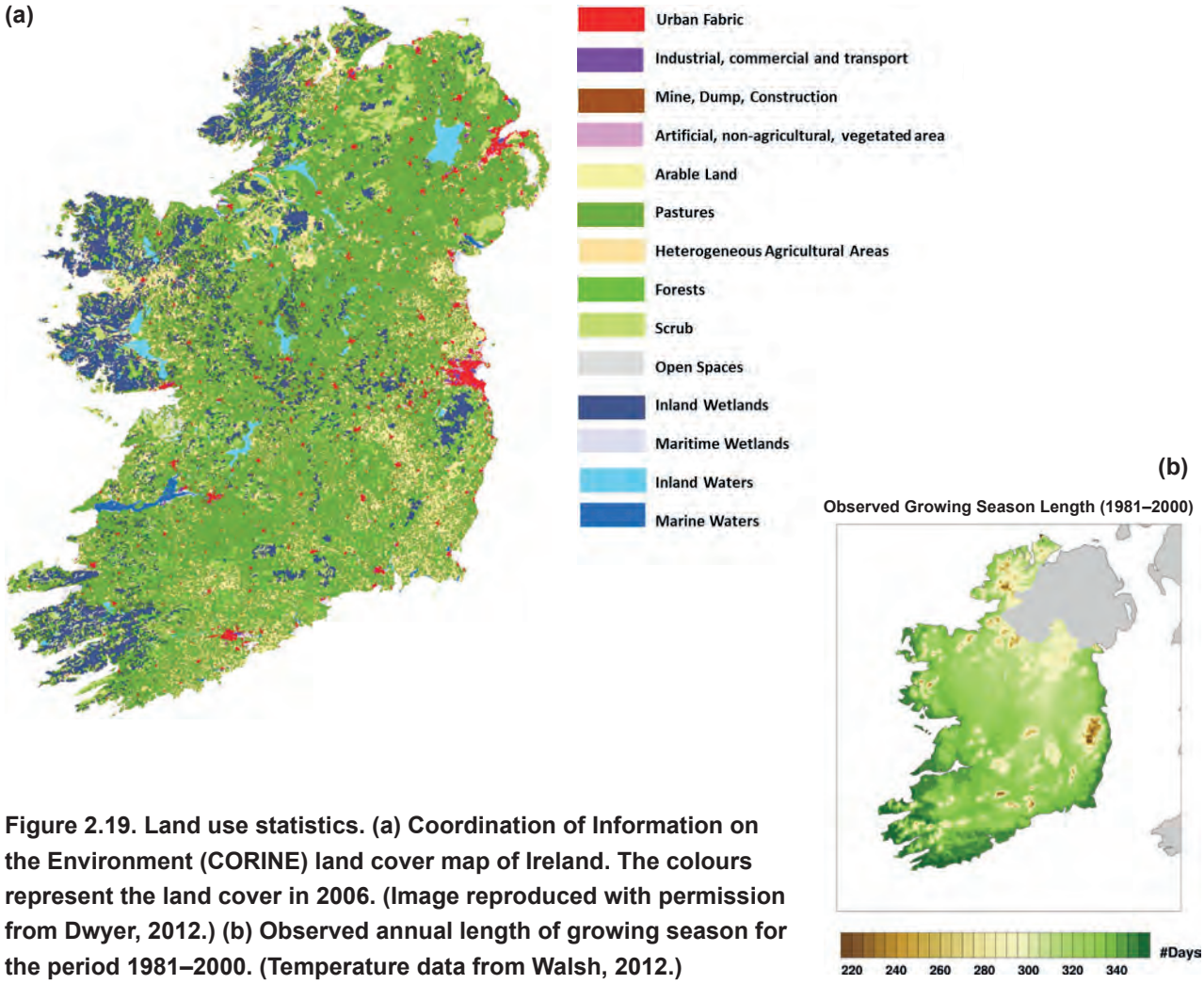

Figure 2.19. Land use statistics. (a) Coordination of Information on the Environment (CORINE) land cover map of Ireland. The colours represent the land cover in 2006. (Image reproduced with permission from Dwyer, 2012.) (b) Observed annual length of growing season for the period 1981–2000. (Temperature data from Walsh, 2012.)

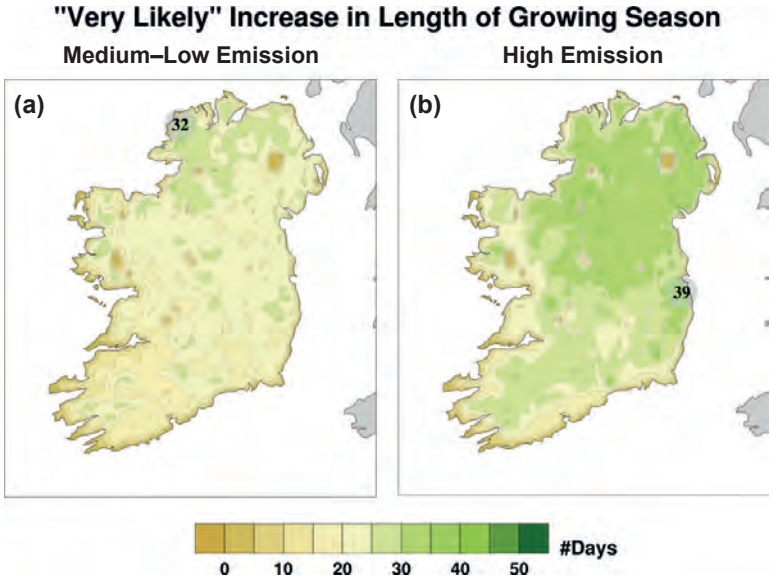

Figure 2.20. "Very likely" increase in the length of the growing season (days per year). (a) Medium- to low-emission scenario; (b) high-emission scenario. In each case, the future period 2041–2060 is compared with the past period 1981–2000.

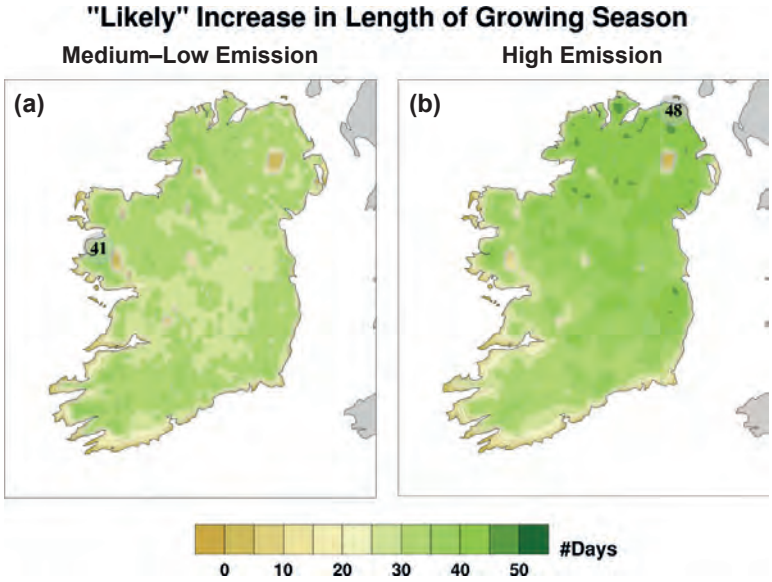

Figure 2.21. "Likely" increase in the length of the growing season (days per year). (a) Medium- to low-emission scenario; (b) high-emission scenario. In each case, the future period 2041–2060 is compared with the past period 1981–2000.

project increases of 35 and 40 days per year, respectively. It should be noted that not all areas presented in Figure 2.18 are suitable for agriculture and/or forestry. The projections should therefore be considered in the context of an observed soil/grass map as presented in Figure 2.19a. In addition, the observed mean length of the growing season for 1981–2000 is presented in Figure 2.19b. The "very likely" and "likely" increases in the mean length of the growing season are presented in Figures 2.20 and 2.21, respectively. It is worth noting that, in some parts of the country, the limitation to the increase in the number of growing days is because the conditions in these areas approach a potential all-year growth.

2.4 Conclusions

An ensemble of downscaled high-resolution climate simulations, based on medium- to low-emission and high-emission scenarios, was employed to assess the impacts of climate change on mid-century air temperatures over Ireland.

The RCMs were validated by performing 20-year simulations of the past Irish climate (1981–2000), driven by ECMWF ERA-40 data and comparing the output against observational data. Results confirm that the RCMs are able to capture the essential features of the temperature climate of Ireland. Although there is evidence of systematic errors in the simulation of temperature, they are not regarded as serious enough to compromise the ability of the RCMs to simulate the future climate of Ireland. The biases may be partly attributed to deficiencies in the ERA-40 re-analysis data used to drive the RCMs; the observation-based ERA-40 driving data, although generally regarded as providing a very accurate description of the atmosphere, are not free from error. Future validation work will focus on downscaling and analysing the more up-to-date and accurate ERAInterim dataset from ECMWF, in place of ERA-40. Furthermore, the individual RCM-GCM past simulations will be validated in detail.

The future climate was simulated using both medium- to low-emission and high-emission scenarios. The future period 2041–2060 was compared to the past period 1981–2000. Projections indicate a rise of 1–1.6°C in mean annual temperatures, with the largest changes seen in the east of the country. The annual and seasonal projected increases were found to be statistically significant for both emission scenarios. Warming is greater for the extremes (i.e. hot or cold days): the warmest 5% of daily maximum summer temperatures are projected to increase by 0.7–2.6°C from the baseline period; the coldest 5% of night-time temperatures in winter are projected to rise by 1.1–3.1°C. While mean temperatures are expected to rise across all seasons, the changes in the shape of the temperature distribution are projected to be small, particularly for the spring and autumn months.

The projected changes in temperatures are consistent with the findings from previous studies (e.g. McGrath and Lynch, 2008; Nolan et al., 2013; O'Sullivan at al., 2015). The current research consolidates and expands on the RCM projections of previous studies by increasing the ensemble size. This allows likelihood levels to be assigned to the projections. In addition, the uncertainties of the projections are more accurately quantified.

The number of frost days (days when the minimum temperature is less than 0°C) is projected to decrease, on average, by 50% for the medium- to low-emission scenario and 62% for the high-emission scenario. Similarly, the number of ice days (days when the maximum temperature is less than 0°C) is projected to decrease by 73% for the medium- to low-emission scenario and 82% for the high-emission scenario. The projections indicate an average increase in the length of the growing season by mid-century of 35 and 40 days per year for the medium- to low-emission and high-emission scenarios, respectively.

References

Beniston, M., Stephenson, D.B., Christensen, O.B., Ferro, C.A.T., Frei, C., Goyette, S., Halsnaes, K., Holt, T., Jylhä, K., Koffi, B., Palutikof, J., Schöll, R., Semmler, T. and Woth, K., 2007. Future extreme events in European climate: an exploration of regional climate model projections. Climatic Change, 81(Suppl. 1), 71–95.

Collins, M., Knutti, R., Arblaster, J., Dufresne, J.-L., Fichefet, T., Friedlingstein, P., Gao, X., Gutowski, W.J., Johns, T., Krinner, G., Shongwe, M., Tebaldi, C., Weaver, A.J. and Wehner, M., 2013. Long-term climate change: projections, commitments and irreversibility. In Stocker, T.F., Qin, D., Plattner, G.-K., Tignor, M., Allen, S.K., Boschung, J., Nauels, A., Xia, Y., Bex, V. and Midgley, P.M. (eds), Climate Change 2013: The Physical Science Basis. Contribution of Working Group I to the Fifth Assessment Report of the Intergovernmental Panel on Climate Change. Cambridge University Press, Cambridge.

Dwyer, N., 2012. Land cover. In Dwyer, N. (ed.), The Status of Ireland's Climate. CCRP Report No 26. EPA, Wexford.

Easterling, D.R., Meehl, G.A., Parmesan, C., Changnon, S.A., Karl, T.R. and Mearns, L.O., 2000. Climate extremes: observations, modeling, and impacts. Science, 289, 2068–2074.

Field, C.B., Barros, V., Stocker, T.F., Qin, D., Dokken, D.J., Ebi, K.L., Mastrandrea, M.D., Mach, K.J., Plattner G.-K., Allen, S.K., Tignor, M. and Midgley, P.M. (eds), 2012. Managing the Risks of Extreme Events and Disasters to Advance Climate Change Adaptation: A Special Report of Working Groups I and II of the Intergovernmental Panel on Climate Change. Cambridge University Press, Cambridge.

Flood, S., 2013. Projected Economic Impacts of Climate Change on Irish Agriculture. Available online: www.stopclimatechaos.ie/download/pdf/projected_economic_impacts_of_climate_change_on_irish_agriculture_oct_2013.pdf (accessed 13 July 2015).

Hansen, J., Sato, M., Kharecha, P. and von Schuckmann, K., 2011. Earth's energy imbalance and implications. Atmospheric Chemistry and Physics Discussions, 11, 13421–13449.

Heinrich, G. and Gobiet, A., 2012. The future of dry and wet spells in Europe: a comprehensive study based on the ENSEMBLES regional climate models. International Journal of Climatology, 32, 1951–1970.

Jacob, D., Petersen, J., Eggert, B., Alias, A., Christensen, O.B., Bouwer, L.M., Braun, A., Colette, A., Déqué, M., Georgievski, G., Georgopoulou, E., Gobiet, A., Menut, L., Nikulin, G., Haensler, A., Hempelmann, N., Jones, C., Keuler, K., Kovats, S., Kröner, N., Kotlarski, S., Kriegsmann, A., Martin, E., van Meijgaard, E., Moseley, C., Pfeifer, S., Preuschmann, S., Radermacher, C., Radtke, K., Rechid, D., Rounsevell, M., Samuelsson, P., Somot, S., Soussana, J.-F., Teichmann, C., Valentini, R., Vautard, R., Weber, B. and Yiou, P., 2014. EURO-CORDEX: new high resolution climate change projections for European impact research. Regional Environmental Change, 14, 563–578.

McGrath, R. and Lynch, P. (eds), 2008. Ireland in a Warmer World: Scientific Predictions of the Irish Climate in the Twenty-First Century. Community Climate Change Consortium for Ireland (C4I). Available online: www.met.ie/publications/warmerworld.asp (accessed 13 July 2015).

McGrath, R., Nishimura, E., Nolan, P., Ratnam, J.V., Semmler, T., Sweeney, C. and Wang, S., 2005. Climate Change: Regional Climate Model Predictions for Ireland. Environmental Protection Agency, Dublin.

Met Éireann, n.d. Air Temperature. Available online: www.met.ie/climate-ireland/surface-temperature.asp (accessed 13 July 2015).

Mullan, D., Fealy, R. and Favis-Mortlock, D., 2012. Developing site-specific future temperature scenarios for Northern Ireland: addressing key issues employing a statistical downscaling approach. International Journal of Climatology, 32, 2007–2019.

Nolan, P., Goodman, P., O'Sullivan, J., Sweeney, C., Gleeson, E. and McGrath, R., 2013. Climate change: impacts on Irish temperatures. In Gleeson, E., McGrath, R. and Treanor, M. (eds), Ireland's Climate: The Road Ahead. Met Éireann, Dublin, pp. 33–39. Available online: www.met.ie/publications/IrelandsWeather-13092013.pdf (accessed 13 July 2015).

O'Sullivan, J., Sweeney, C., Nolan, P. and Gleeson, E., 2015. A high-resolution, multi-model analysis of Irish temperatures for the mid-21st century. International Journal of Climatology. doi: 10.1002/joc.4419 (Early Online View).

Perkins, S.E., Pitman, A.J., Holbrook, N.J. and McAneney, J., 2007. Evaluation of the AR4 climate models' simulated daily maximum temperature, minimum temperature, and precipitation over Australia using probability density functions. Journal of Climate, 20, 4356–4376.

Seneviratne, S.I., Nicholls, N., Easterling, D., Goodess, C.M., Kanae, S., Kossin, J., Luo, Y., Marengo, J., McInnes, K., Rahimi, M., Reichstein, M., Sorteberg, A., Vera, C. and Zhang, X., 2012. Changes in climate extremes and their impacts on the natural physical environment. In Field, C.B., Barros, V., Stocker, T.F., Qin, D., Dokken, D.J., Ebi, K.L., Mastrandrea, M.D., Mach, K.J., Plattner G.-K., Allen, S.K., Tignor, M. and Midgley, P.M. (eds), Managing the Risks of Extreme Events and Disasters to Advance Climate Change Adaptation: A Special Report of Working Groups I and II of the Intergovernmental Panel on Climate Change. Cambridge University Press, Cambridge.

Solomon, S., Qin, D., Manning, M., Chen, Z., Marquis, M., Averyt, K.B., Tignor, M. and Miller, H.L. (eds), 2007. Climate Change 2007: The Physical Science Basis. Contribution of Working Group I to the Fourth Assessment Report of the Intergovernmental Panel on Climate Change. Cambridge University Press, Cambridge.

Stocker, T.F., Qin, D., Plattner, G.-K., Tignor, M., Allen, S.K., Boschung, J., Nauels, A., Xia, Y., Bex, V. and Midgley, P.M. (eds), 2013. Climate Change 2013: The Physical Science Basis. Contribution of Working Group I to the Fifth Assessment Report of the Intergovernmental Panel on Climate Change. Cambridge University Press, Cambridge.

Walsh, S., 2012. A Summary of Climate Averages for Ireland 1981–2010. Climatological Note No.14, Met Éireann, Dublin. Available online: www.met.ie/climate-ireland/SummaryClimAvgs.pdf (accessed 13 July 2015).

Walsh, S., 2013. Setting the scene: the climate of Ireland 1900-2012. In Gleeson, E., McGrath, R. and Treanor, M. (eds), Ireland's Climate: The Road Ahead. Met Éireann, Dublin, pp. 17–19. Available online: www.met.ie/publications/IrelandsWeather-13092013.pdf (accessed 13 July 2015).

3 Impacts of climate change on Irish precipitation

The impacts of climate change on precipitation over Ireland are assessed for mid-century using an ensemble of downscaled climate simulations based on medium- to low-emission and high-emission scenarios.

Results show significant projected decreases in mean annual, spring and summer precipitation amounts by mid-century. The projected decreases are largest for summer, with "likely" reductions ranging from 0% to 13% and from 3% to 20% for the medium- to low-emission and high-emission scenarios, respectively. The frequencies of heavy precipitation events show notable increases (approximately 20%) during the winter and autumn months. The number of extended dry periods is projected to increase substantially by mid-century during autumn and summer. The projected increases in dry periods are largest for summer, with "likely" values ranging from 12% to 40% for both emission scenarios. Regional variations of projected precipitation change remain statistically elusive.

3.1 Introduction

3.1.1 Observed precipitation

Precipitation amounts in Ireland exhibit a large degree of spatial and temporal heterogeneity. On average, most of the eastern half of the country experiences between 750 mm and 1000 mm of rainfall per year. Rainfall in the west generally averages between 1000 mm and 1250 mm per year. In many mountainous districts, rainfall exceeds 2000 mm per year. The wettest months, in almost all areas, are December and January. April is the driest month generally across the country. However, in many southern parts, June is the driest. Hail and snow contribute relatively little to the precipitation measured (Met Éireann, n.d.). The 1981–2000 mean annual precipitation is presented in Figure 3.1a (data from Walsh, 2012).

An analysis of annual rainfall totals, carried out by Met Éireann, shows there was a small increase in average annual national rainfall of approximately 60 mm (or 5%) in 1981–2010, compared with the 30-year period 1961–1990 (Walsh and Dwyer, 2012). The same study shows an increase in the frequency of wet (> 10 mm) and very wet (> 20 mm) days over 1961–2010. However, the trends for rainfall do not show the same level of confidence as those for temperature; there is large regional variation and occasionally conflicting trends from stations that are relatively close geographically. In addition, the observed change in precipitation may be because of natural variability as opposed to climate change.

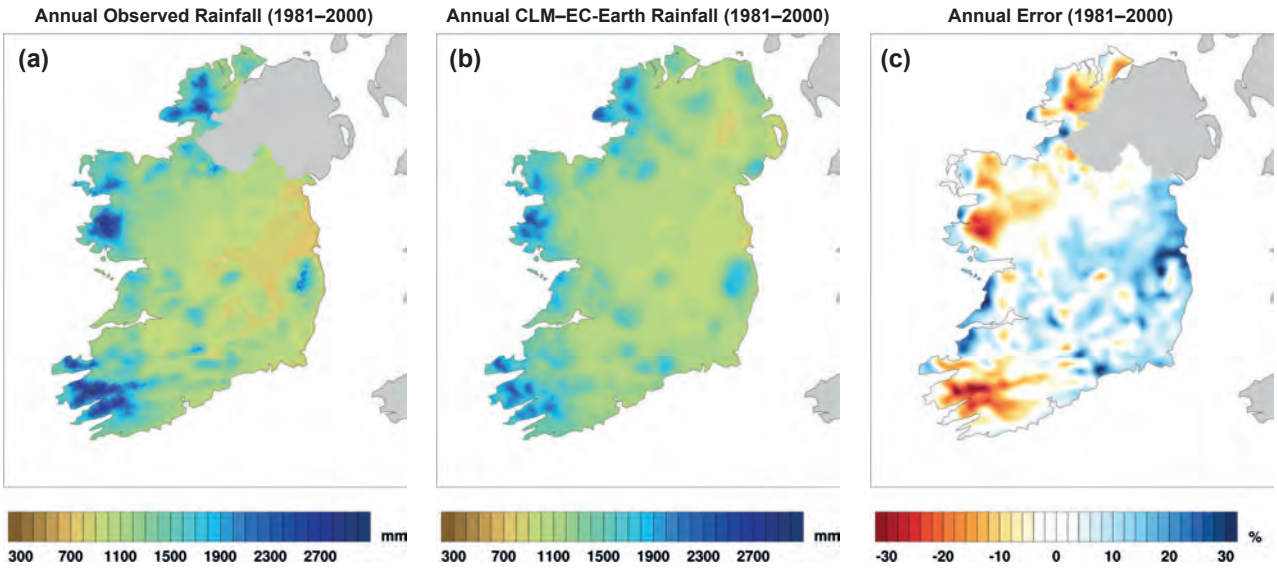

Figure 3.1. Mean annual precipitation for 1981–2000. (a) Observations; (b) CLM–EC-Earth 4-km data; (c) CLM–EC-Earth error (%).

3.1.2 Global projections

The IPCC Fifth Annual Assessment Report (AR5) states that the output of global models shows "it is *virtually certain* that, in the long term, global precipitation will increase with increased global mean surface temperature". Precipitation amounts are "*likely* [to] increase by 1 to 3%°C^{-1} for scenarios other than RCP2.6." Furthermore, "in many mid-latitude and subtropical dry regions, mean precipitation will likely decrease, while in many mid-latitude wet regions, mean precipitation will likely increase by the end of this century under the RCP8.5 scenario." Over most of the mid-latitude land masses, extreme precipitation events are *very likely* to be more intense and more frequent in a warmer world (Collins et al., 2013).

There are different physical mechanisms behind the changes; at the high latitudes the effects are linked to the ability of a warmer atmosphere to hold more moisture. Basic physical arguments (Trenberth et al., 2003) indicate that water vapour content should increase by ~7% for every 1°C rise in temperature but not all of the extra moisture goes into precipitation; other constraints suggest an increase in precipitation of 1–3%/1°C warming (Wild and Leipert, 2010; O'Gorman et al., 2012). For short-period extreme precipitation events, there is some evidence that the increase is much larger, perhaps double the 7% projection (Lenderink and Van Meijgaard, 2008). At a local scale, and over relatively small geographical regions, there is likely to be considerable variation in the climate change pattern.

3.1.3 Simulating precipitation

The simulation of precipitation, and the effects of a warming climate, is a major challenge for GCMs because of the nature of the interacting physical processes that lead to precipitation, and the lack of sufficient resolution in the models (Ma et al., 2013). The latter leads to a sacrificing of the fine details by introducing simplified "parameterisation" physical schemes; it also smooths the influence of surface features in forcing precipitation. In addition, cloud processes (which are linked to convection) and interactions with the boundary layer are a major source of uncertainty for the models.

3.1.4 Downscaling

Dynamical downscaling attempts to remedy some of these problems by employing a regional, and usually quite different, climate model with a higher spatial resolution that processes input from the global model. The approach has its flaws: all models have errors, which are cascaded in this technique, and new errors are introduced via the flow of data through the boundaries of the regional model. Nevertheless, high-resolution RCMs demonstrate improved ability to simulate precipitation (Lucas-Picher et al., 2012; Kendon et al., 2012, 2014). The higher resolution RCMs have been shown to improve the simulation of topography-influenced phenomena and extremes with relatively small spatial or short temporal character (Feser et al., 2011; Feser and Barcikowska, 2012; Shkol'nik et al., 2012; Flato et al., 2013). An additional advantage is that the physically based RCMs explicitly resolve more smaller scale atmospheric features and provide a better representation of convective precipitation (Rauscher et al., 2010) and extreme precipitation (Kanada et al., 2008).

To correctly resolve small-scale weather extremes such as extreme downpours, it is necessary to run the RCMs at a higher spatial resolution than is commonly employed. For example, the CORDEX simulations have a maximum horizontal resolution of 0.11° (~12.5 km), while extreme precipitation events often have a scale of 1 km or less. Furthermore, low-resolution RCMs use the hydrostatic approximation with parameterised cloud schemes, implying that the heaviest precipitation events (convective systems on hot summer days) are not adequately represented in the simulations (Prein et al., 2013; Kendon et al., 2014). Comparing results from an 11-km RCM and a 1.5-km weather model, Kendon et al. (2014) showed that the latter projects significantly larger changes of heavy precipitation than the former over the south of England. This work has been expanded upon by Chan et al. (2014), who concluded that the summer "uncertainty estimates have become narrower with the use of the 1.5 km RCM".

3.1.5 Downscaled projections for Europe and Ireland

The average forecast from the ENSEMBLES project (van der Linden and Mitchell, 2009), based on 12 climate simulations, is for an increase in the late autumn (November) rainfall over Ireland of about 8% in 2021–2050, rising to about 15% in 2071–2100 (both figures relative to the reference climate period of 1961–1990). However, compared with the expected temperature changes, there is less confidence in future projections of rainfall. This is reflected in a rather large spread,

particularly at regional level, between the individual simulation forecasts.

Heinrich and Gobiet (2012) used eight RCMs from the ENSEMBLES project to analyse changes in dry and wet conditions in Europe by the middle of the 21st century under the A1B emission scenario. They conclude that the study "adds confidence to the expectation that southern Europe is most probably facing an increased risk of longer, more frequent, severe, and widespread droughts, while northern Europe is facing increased risk of intensified wet events. These changes are expected to be particularly pronounced with regard to extreme events" (Heinrich and Gobiet, 2012).

Jacob et al. (2014) compared regional climate change patterns for Europe projected by the high-resolution regional climate change ensemble of EURO-CORDEX (RCP4.5 and 8.5 scenarios) with the A1B projections of the ENSEMBLES project. They found that the large-scale patterns of changes in precipitation are similar in all three scenarios. The projected seasonal mean changes in heavy precipitation for the three emission scenarios are also relatively similar, but some regional differences are noted. The largest differences are attributed to the increased regional detail in the CORDEX simulations, which is related to the higher horizontal resolution of ~12.5 km compared with 25 km for the A1B ENSEMBLES data, for which more homogeneous changes are calculated. The agreement between the ENSEMBLES and CORDEX results "strengthen the previous findings obtained from the ENSEMBLES data set" (Jacob et al., 2014).

In 2013, the Research Division at Met Éireann led a major study on the future of Ireland's climate. A subset of the ensemble of RCM simulations used in the current study was analysed and indicated that, while the average annual precipitation shows only a slight decrease by mid-century, there are substantial seasonal changes predicted with wetter winters and drier summers (Nolan et al., 2013). However, the projections of mean precipitation for winter exhibited great uncertainty as reflected in a large spread between the individual ensemble members. The frequencies of heavy precipitation events showed notable increases, particularly in winter.

3.1.6 Current study

The chaotic nature of weather and climate (natural variability), which is particularly noticeable in precipitation, requires an ensemble approach to support the statistical significance of climate modelling results. Not only are the models imperfect, as well as handling the physical processes in different ways, but there is also uncertainty in future concentrations of greenhouse gases and aerosols. The current study addresses this uncertainty, in part, by employing an MME approach. The ensemble approach used several different RCMs, driven by several GCMs, to simulate climate change. In addition, a number of possible future greenhouse gas scenarios are considered. Through the MME approach, the uncertainty in the projections can be partially quantified, providing a measure of confidence in the predictions. The models were run at high spatial resolution, up to 4 km, thus allowing sharper estimates of the regional variations in precipitation changes. Details of the different global climate datasets, the greenhouse gas emission scenarios and the downscaling models used to produce the ensemble of climate projections for Ireland are summarised in Chapter 1.

The current research consolidates and expands on the RCM rainfall projections of the Met Éireann report of 2013 (Nolan et al., 2013) by increasing the ensemble size. This allows likelihood levels to be assigned to the projections. In addition, the uncertainty of the projections can be more accurately quantified.

3.2 Regional climate model precipitation validations

Figure 3.1a presents the annual observed precipitation averaged over the 20-year period 1981–2000 (data from Walsh, 2012). Figure 3.1b presents the downscaled EC-Earth *mei1* data (see Table 1.2) as simulated by the CLM4 model at 4-km resolution (denoted CLM–EC-Earth). It is noted that the CLM–EC-Earth simulation accurately captures the magnitude and spatial characteristics of the historical precipitation climate. Figure 3.1c shows that the percentage errors range from approximately −20% to approximately +20%. The percentage error at each grid point (*i*, *j*) is given by:

$$per\_err_{(i,j)} = 100 \times \left(\frac{\overline{RCM}_{(i,j)} - \overline{OBS}_{(i,j)}}{\overline{OBS}_{(i,j)}} \right) \qquad (3.1)$$

where the $\overline{RCM}_{(i,j)}$ and $\overline{OBS}_{(i,j)}$ terms represent the RCM and observed values, respectively, at grid point (*i*, *j*), averaged over the period 1981–2000.

To quantify the overall bias evident in Figure 3.1c, the mean was calculated over all grid points covering Ireland, resulting in an *overall bias* of +2%. The bias

metric allows for the evaluation of the systematic errors of the RCMs but can hide large errors, as positive and negative values can cancel. For this reason, the percentage mean absolute error (MAE) metric was also used to evaluate the RCM precipitation errors. This metric is given by:

$$per\_MAE_{(i,j)} = 100 \times \left(\frac{\left| \overline{RCM}_{(i,j)} - \overline{OBS}_{(i,j)} \right|}{\overline{OBS}_{(i,j)}} \right) \quad (3.2)$$

Again, the mean was calculated over all grid points covering Ireland, resulting in an *overall MAE* of 9.4%.

The seasonal validations are presented in the rows of Figure 3.2. The first, second and third columns present the observed precipitation, the CLM–EC-Earth *mei1* precipitation and the percentage error, respectively. In general, the CLM–EC-Earth simulation data exhibit a positive bias for summer, a negative bias for autumn and a mixed signal for winter and spring. The largest errors were noted for summer, with *overall bias* and *overall MAE* values of 12% and 15%, respectively.

The above validations were repeated for each of the 10 past RCM ensemble members, as outlined in Table 1.2. The RCM *overall bias* values, separated by season, are presented in Figure 3.3a. The central line within each box is the median, the edges of the box are the 25th and 75th percentiles, the whiskers extend to the most extreme data points not considered outliers, and outliers are plotted individually. In general, the RCMs tend to overestimate precipitation for all seasons with median error values ranging from 8% (winter) to 17.6% (spring). Similarly, the RCM *overall MAE* values, separated by season, are presented in Figure 3.3b. The median MAE values range from 15.1% (autumn) to 22.9% (summer).

It was found that, while the accuracy generally decreased with lower model resolution, the output of the RCMs exhibits reasonable and realistic features as documented in the historical data record. It should be noted that the observed precipitation dataset has a margin of error of approximately ±10%, so the above validations should be considered within this context.

3.3 Precipitation projections for Ireland

3.3.1 Ensemble mean rainfall projections

Figure 3.4 presents the mean annual percentage change in precipitation for the medium- to low-emission and high-emission scenarios. The future period 2041–2060 is compared with the past period 1981–2000. There is an indication of a reduction in the overall annual precipitation of 0–10% for the medium- to low-emission ensemble and 1–8% for the high-emission ensemble.

Figure 3.5a presents the seasonal change (%) in precipitation for the medium- to low-emission scenario; the corresponding plots for high emissions are presented in Figure 3.5b. The strongest signals are a projected decrease for summer, with the largest impacts for the high-emission scenario. The summer reductions range from 2% to 17% for the medium- to low-emission scenario and from 9% to 24% for the high-emission scenario. The future spring months are also projected to be drier, with decreases ranging from 1% to 13% and from ~0% to 10% for the medium- to low-emission and high-emission scenarios, respectively. The spring and summer projected drying is analysed in more detail in section 3.3.2.

The drying signal for autumn is less robust. A projected increase in mean precipitation is noted for winter over most of Ireland for the high-emission scenario. However, the projections for autumn and winter exhibit great uncertainty, as reflected in a large spread between the individual ensemble members (not shown). The projections of mean precipitation for winter and autumn should therefore be viewed with a low level of confidence (however, projections of increases in heavy precipitation for autumn and winter are robust, as outlined in section 3.3.4).

The projected precipitation changes vary greatly between ensemble members, much more so than for the temperature projections. The regional details of Figures 3.4 and 3.5 are therefore not reliable. Furthermore, the disagreement between RCM projections can result in large individual outliners skewing the mean ensemble projection. For this reason, the “likelihood” projections are considered in the following sections. Recall from Chapter 1 that a “very likely” projection is defined as one in which over 90% of the ensemble members agree. Similarly, a “likely” projection is defined as one in which over 66% of the ensemble members agree. The likelihood values are calculated at each grid point using the full RCM ensemble of projections as outlined in Table 1.2.

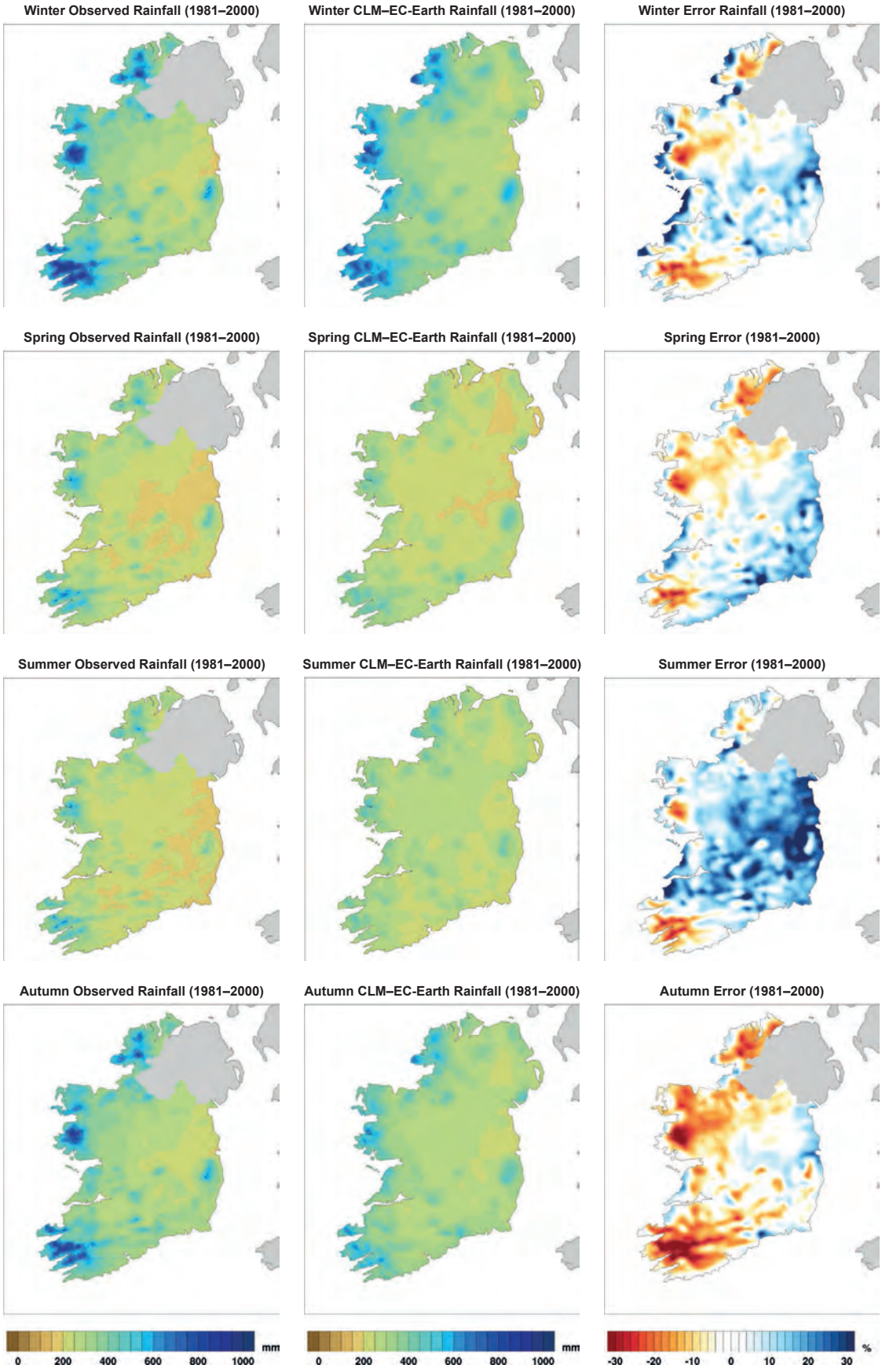

Figure 3.2. Seasonal precipitation for 1981–2000. The first, second and third columns contain observations, CLM–EC-Earth data and the error, respectively. The colour scale is kept fixed for each column and is included in the last row.

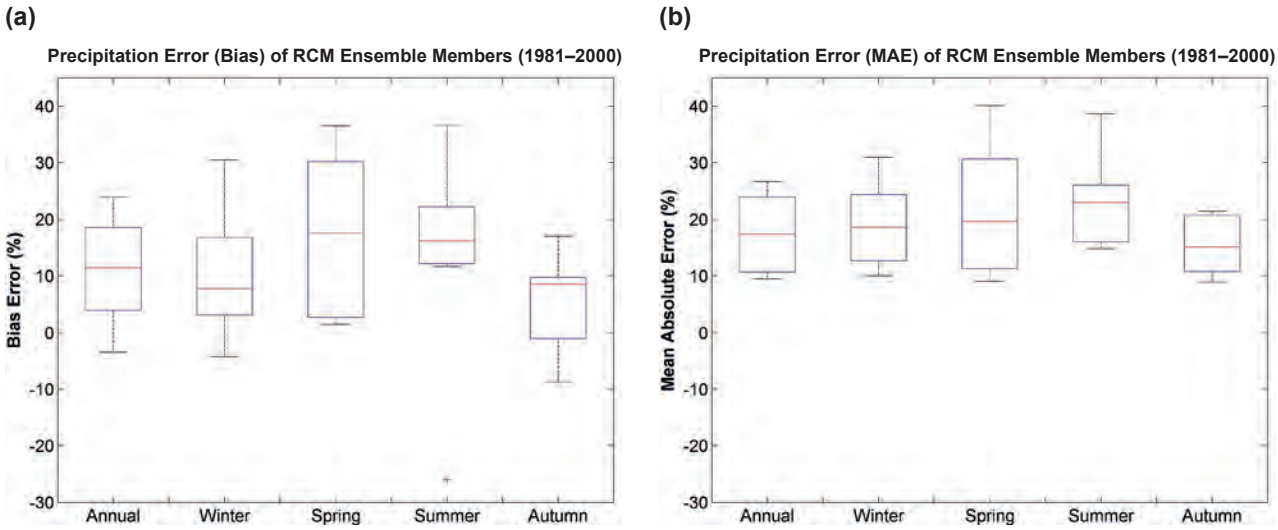

Figure 3.3. Annual and seasonal mean precipitation errors (%). (a) Overall bias; (b) overall MAE metrics. Each RCM past ensemble member is compared with observations for the 20-year period 1981–2000. The boxplots represent the spread of errors; the bottom and top whiskers represent the minimum and maximum, respectively, the bottom and top of the box represents the first and third quartiles, respectively, and the middle line represents the median error.

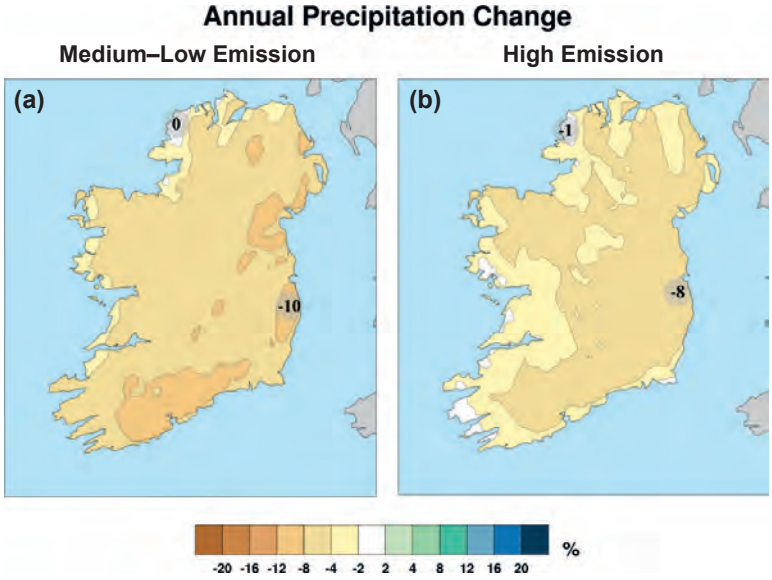

Figure 3.4. Projected change (%) in annual precipitation. (a) Medium- to low-emission scenario; (b) high-emission scenario. In each case, the future period 2041–2060 is compared with the past period 1981–2000. The numbers included on each plot are the minimum and maximum changes, displayed at their locations.

3.3.2 Robust mean rainfall projections (annual, spring and summer)

As the mean annual, spring and summer projections of section 3.3.1 are negative, the analysis of this section focuses on the likelihood of decreases. Furthermore, only robust projections are presented.

Figure 3.6, which presents the "likely" annual and spring projected decreases in rainfall, indicates a drying is "likely" to occur over most of the country by mid-century. The drying is more prominent for the medium- to low-emission scenario, with values ranging from ~0% to 8% (annual) and from 0% to 11% (spring). It follows it is "likely" that decreases in annual and spring precipitation

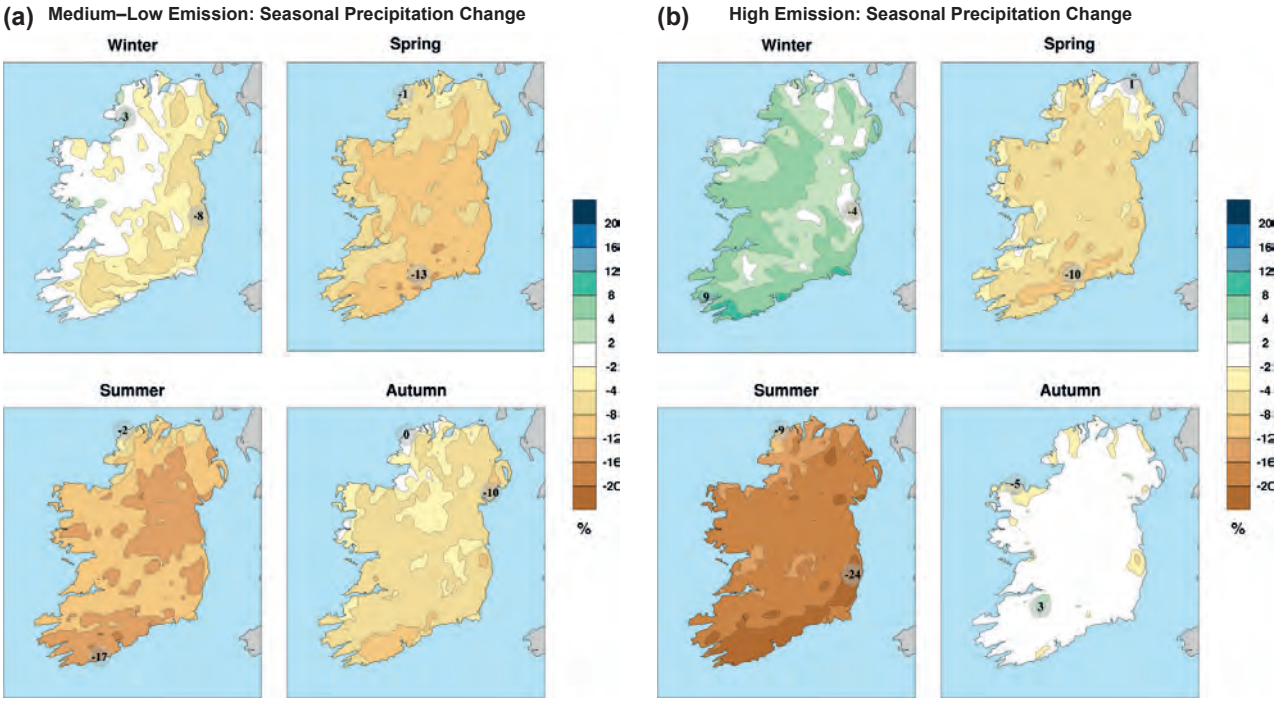

Figure 3.5. Projected changes (%) in seasonal precipitation. (a) Medium- to low-emission scenario; (b) high-emission scenario. In each case, the future period 2041–2060 is compared with the past period 1981–2000.

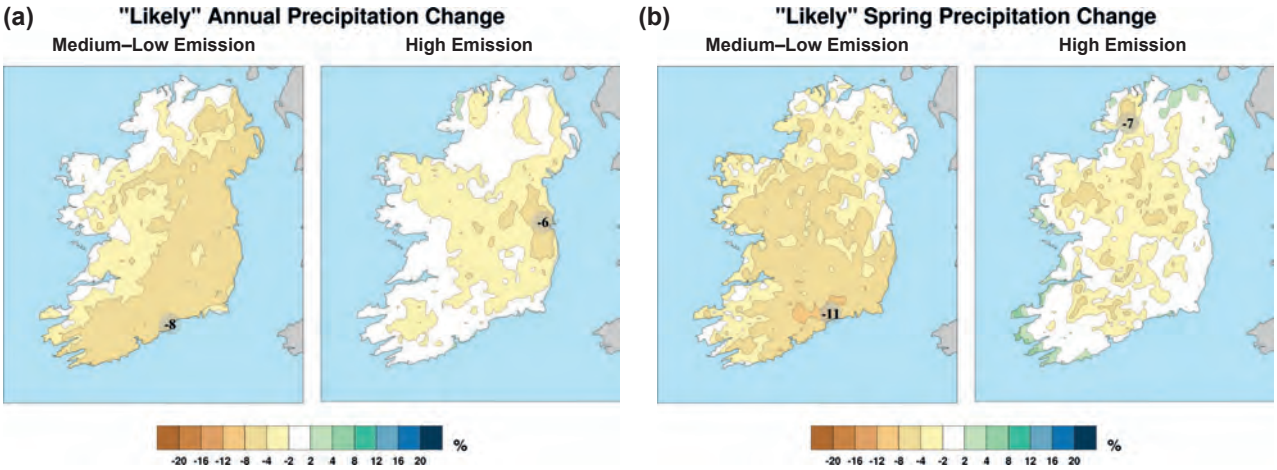

Figure 3.6. "Likely" change (%) in precipitation. (a) Annual; (b) spring. In each case, the future period 2041–2060 is compared with the past period 1981–2000.

will be greater than or equal to these values. A projected decrease is not evident at the *very likely* level (annual and spring), implying that at least 10% of the ensemble members are in disagreement (not shown).

Figure 3.7a shows that the projected summer drying signal is larger, with "likely" values ranging from 0% to 13% and from 3% to 20% for the medium- to low-emission and high-emission scenarios, respectively. It follows it is "likely" that reductions in summer precipitation will be greater than or equal to these values. The "very likely" summer projections, presented in Figure 3.7b, show that over 90% of the high-emission ensemble members project a decrease (or small change of ~0%) in precipitation over most of the country.

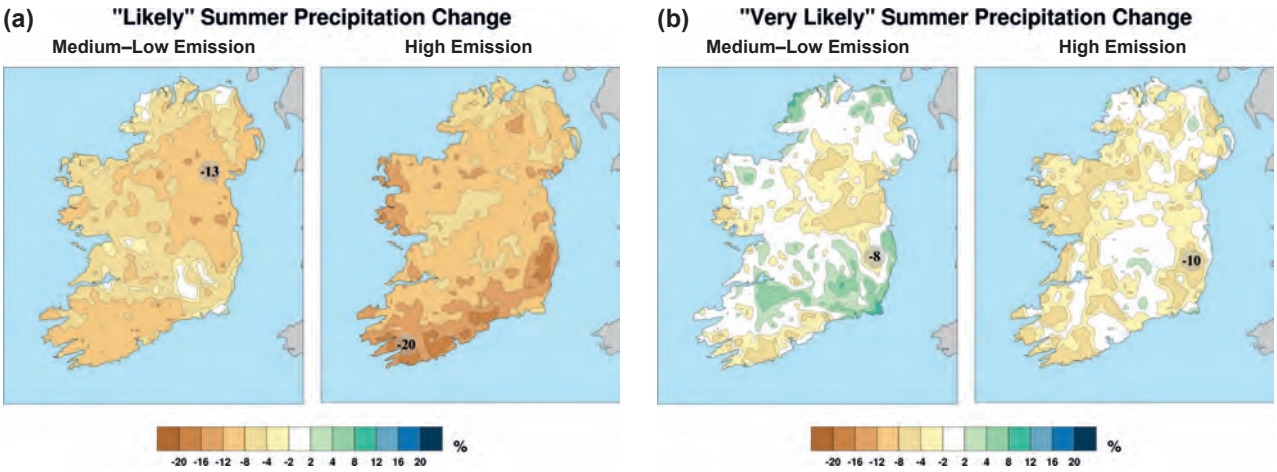

Figure 3.7. Projected change (%) in summer precipitation. (a) "Likely"; (b) "very likely". In each case, the future period 2041–2060 is compared with the past period 1981–2000.

Note that the accuracy of these statistical descriptions is based on the assumption that the ensemble members represent an unbiased sampling of the (unknown) future climate.

3.3.3 Robust increase in number of dry periods (annual, summer and autumn)

To quantify the potential impact of climate change on future drought events, the change in the number of dry periods was analysed. A dry period is defined as at least 5 consecutive days for which the daily precipitation is less than 1 mm. In this section, robust projections of future dry periods are presented.

Figure 3.8 presents the "likely" annual and autumn percentage changes in the number of dry periods. The figures indicate a "likely" increase in the number of annual and autumn dry periods over most of the country by mid-century. The increases are more prominent for the medium- to low-emission scenario, with values ranging from 7% to 28% (annual) and from 3% to 39% (autumn). It follows it is "likely" that increases in annual and autumn dry periods will be greater than or equal to these values (medium- to low-emission scenario).

Figure 3.9a shows that the projected increase in the number of dry periods for summer is larger, with "likely" values ranging from ~12% to 40% for both the medium- to low-emission and high-emission scenarios. It follows it is "likely" that the percentage increases in summer dry periods will be greater than or equal to these values. The "very likely" summer projections, presented in Figure 3.9b, show that over 90% of the ensemble members project an increase in dry periods over most of the country for the medium- to

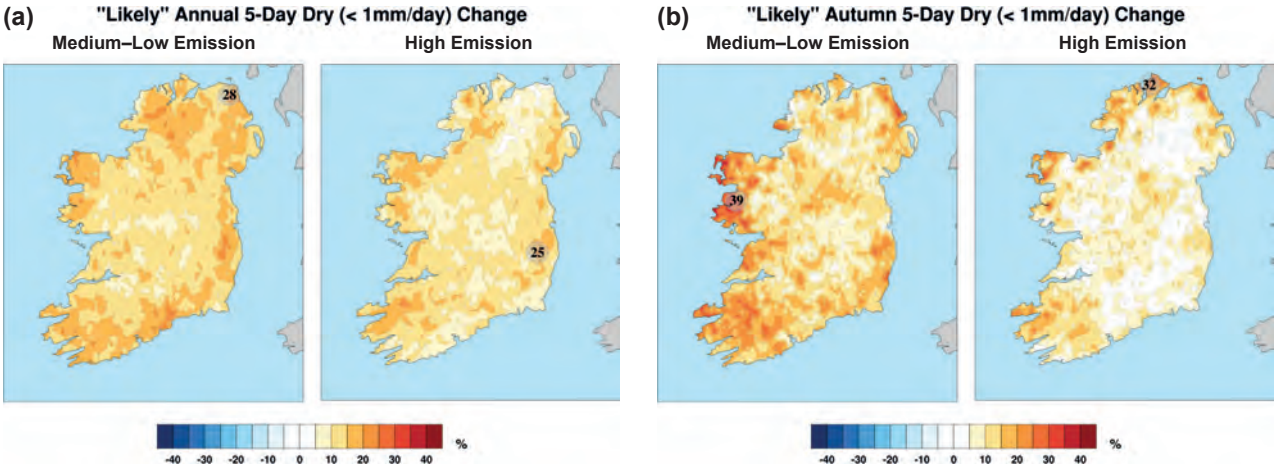

Figure 3.8. "Likely" change (%) in the number of dry periods. (a) Annual; (b) autumn. In each case, the future period 2041–2060 is compared with the past period 1981–2000.

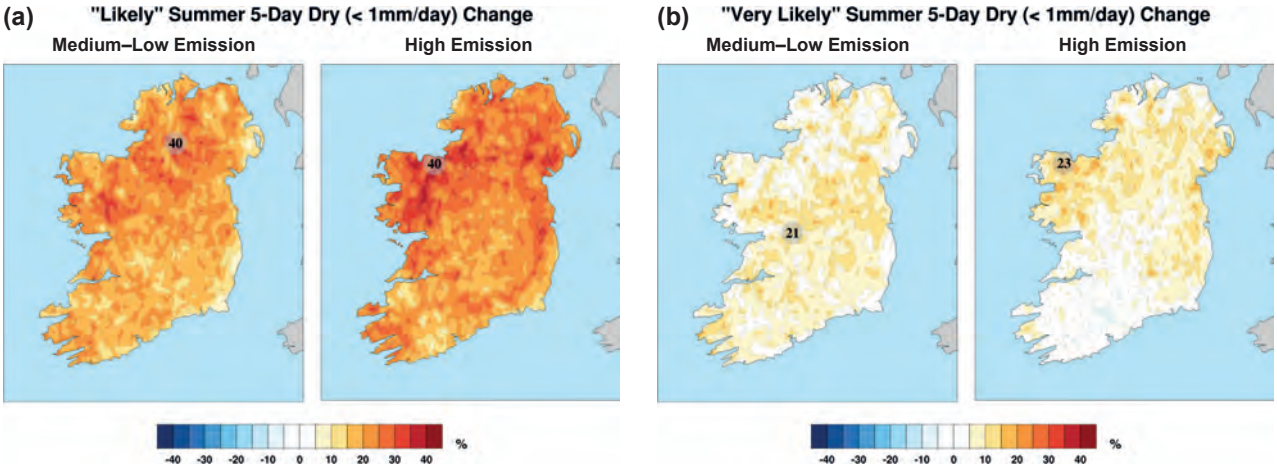

Figure 3.9. Projected change (%) in number of summer dry periods. (a) "Likely"; (b) "very likely". In each case, the future period 2041–2060 is compared with the past period 1981–2000.

low-emission scenario (values range from ~0% to 20%). The high-emission projections show a similar, but weaker, signal.

The projected percentage increase in the number of dry periods should be considered in the context of the observed number of dry periods. Figure 3.10 presents the annual, autumn and summer number of dry periods, averaged over the 20-year period 1981–2000.

3.3.4 Robust increases in number of wet days (annual, autumn and winter)

Changes in the occurrence of heavy rainfall events are of particular importance because of the link with flooding. In this section, robust mid-century projections of "wet days" and "very wet days" are presented. A "wet day" is defined as one on which the daily precipitation amount is greater than 20 mm. A "very wet day" is defined as one on which the daily precipitation is greater than 30 mm.

Figure 3.11 indicates a "likely" increase, under the high-emission scenario, in the number of wet days for the winter (mean value 24%) and autumn (mean value 18%) months. Figure 3.12 indicates a "likely" increase, under the high-emission scenario, in the number of annual (mean value 24%) and autumn (mean value 49%) very wet days. A "likely" increase in very wet days of ~30% was also noted over most of the country for the winter months under the high-emission scenario (not shown).

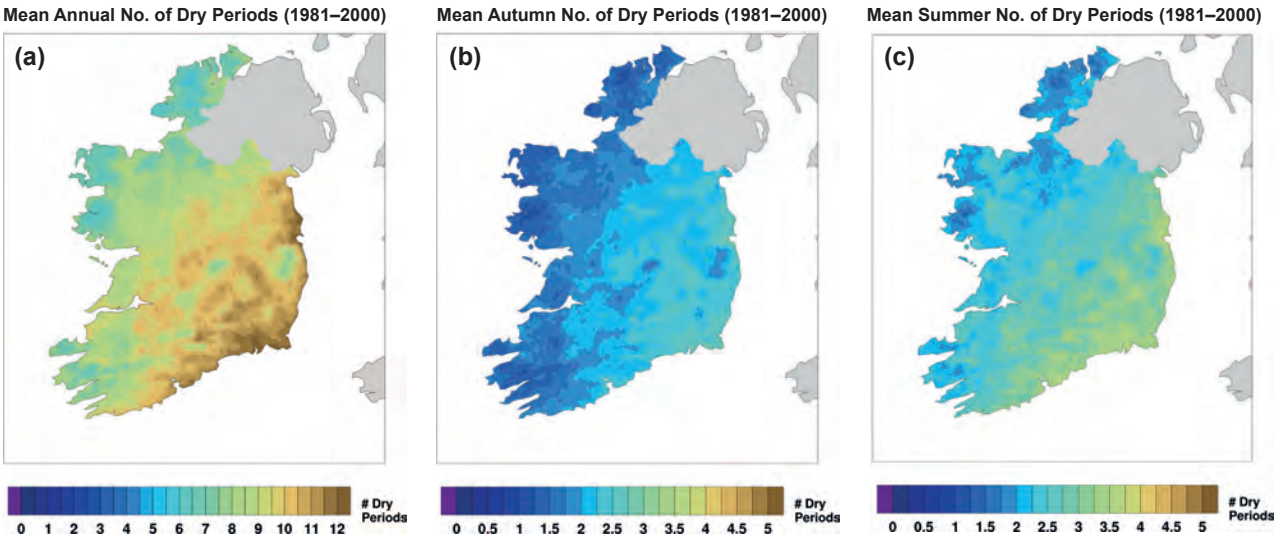

Figure 3.10. The observed number of dry periods averaged over the 20-year period 1981–2000. (a) Annual; (b) autumn; (c) summer. Note the different scale for the annual figure.

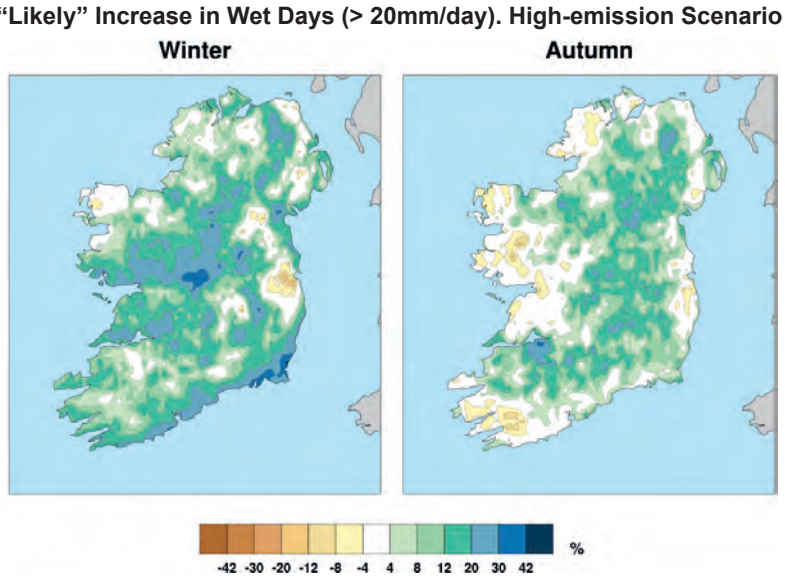

Figure 3.11. The "likely" increase in number of winter and autumn wet days (rainfall > 20 mm) for the high-emission scenario. In each case, the future period 2041–2060 is compared with the past period 1981–2000.

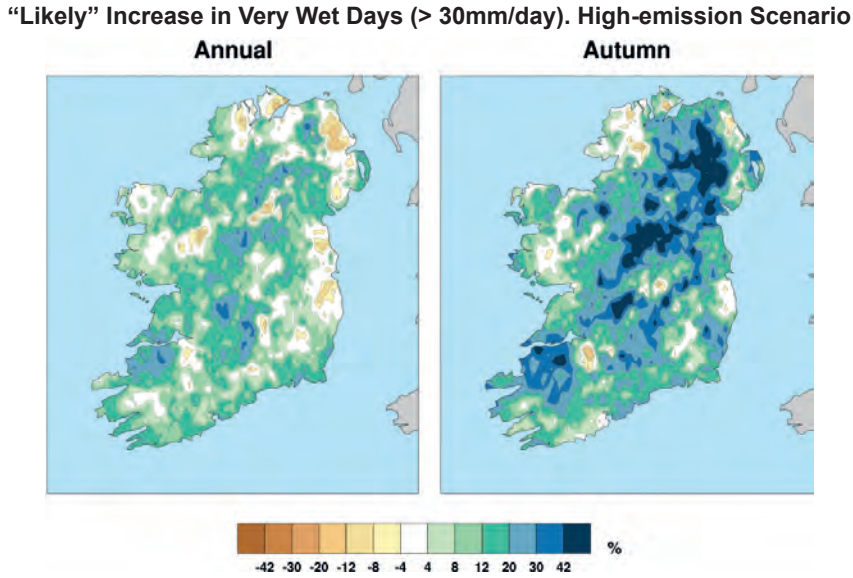

Figure 3.12. The "likely" increase in number of annual and autumn very wet days (rainfall > 30 mm) for the high-emission scenario. In each case, the future period 2041–2060 is compared with the past period 1981–2000.

The medium- to low-emission ensemble showed a similar, but weaker signal, in the projected number of wet and very wet days (not shown). The increased frequency of heavy precipitation is well marked in winter and autumn and over the full year, particularly for the high-emission scenario, but the regional details of Figures 3.11 and 3.12 are not reliable because of a large spread in the ensembles.

The projected increase in the number of wet days should be considered in the context of the observed number of wet days. Figure 3.13 presents the annual, winter and autumn numbers of wet days, averaged over the 20-year period 1981–2000. Similarly, the observed annual, winter and autumn numbers of very wet days are presented in Figure 3.14.

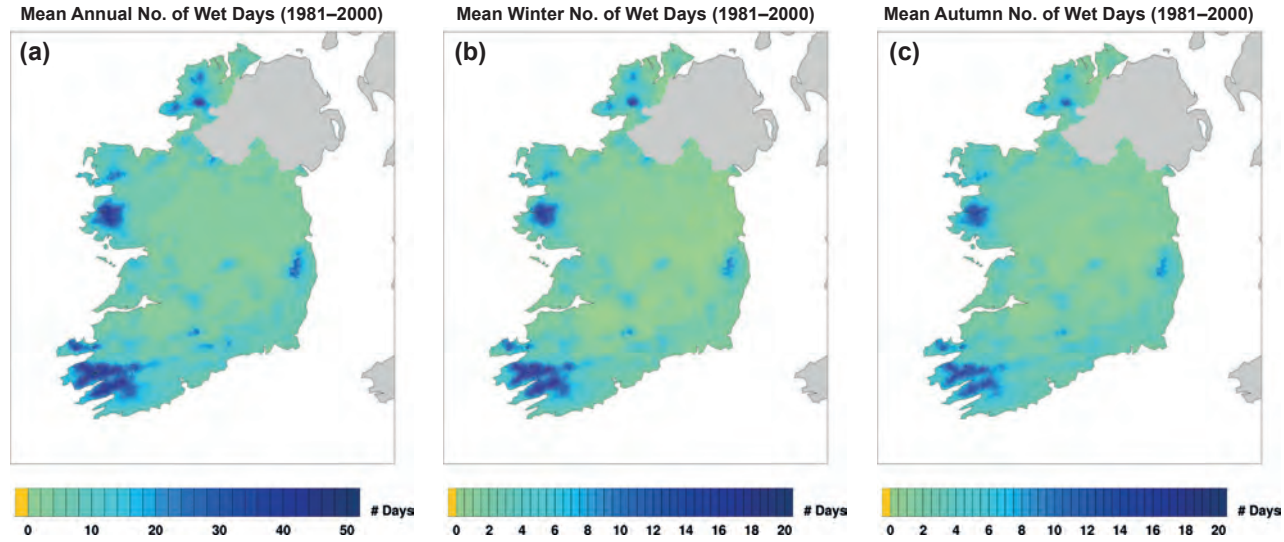

Figure 3.13. The observed number of wet days (rainfall > 20 mm) averaged over the 20-year period 1981–2000. (a) Annual; (b) winter; (c) autumn. Note the different scale for the annual figure.

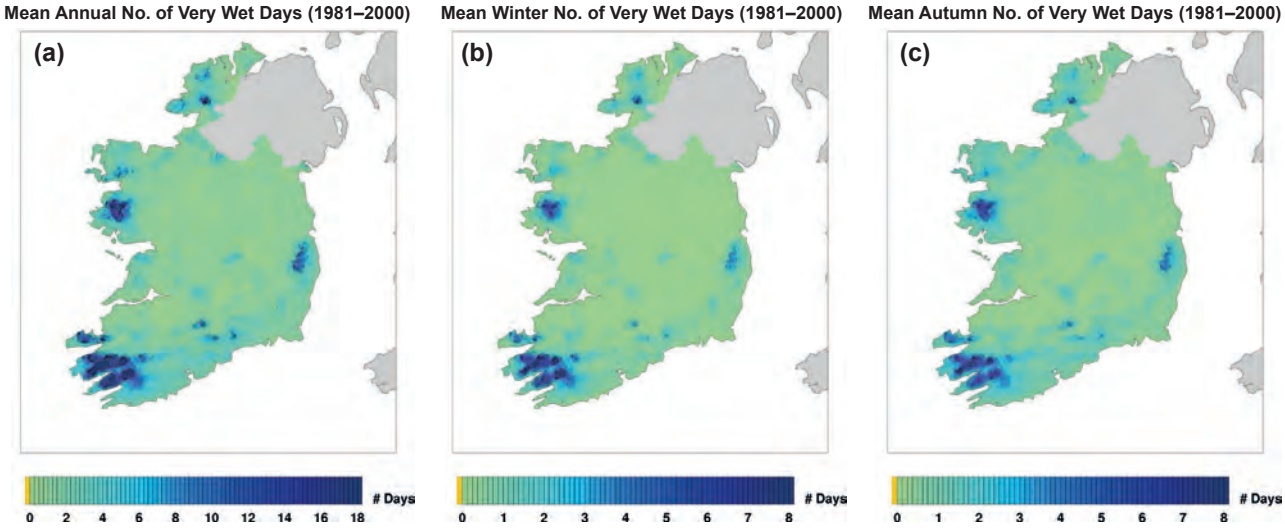

Figure 3.14. The observed number of very wet days (rainfall > 30 mm) averaged over the 20-year period 1981–2000. (a) Annual; (b) winter; (c) autumn. Note the different scale for the annual figure.

3.3.5 Changes in the shape of the future rainfall distribution

A more comprehensive step in moving from analysing mean values to the examination of extreme events is to consider the distribution function of a quantity. The distribution of a quantity involving discrete data (as here) can be represented by its empirical density function. Figure 3.15 presents the seasonal density functions (hereafter, density) of daily precipitation anomalies, at every grid point over Ireland. For each past simulation, the anomalies are calculated by subtracting the average daily precipitation total (calculated over the 20-year period 1981–2000) from the daily precipitation amounts.[4] Similarly, the future daily anomalies (2041–2060) are calculated by subtracting the historical average daily precipitation total (1981–2000) from each future ensemble member within the same group (see Table 1.2).

4 This results in two slightly different past densities (corresponding to the two future emission scenario groups). As differences were found to be very small, the medium- to low-emission past densities are excluded from Figures 3.15, 3.16 and 3.17.

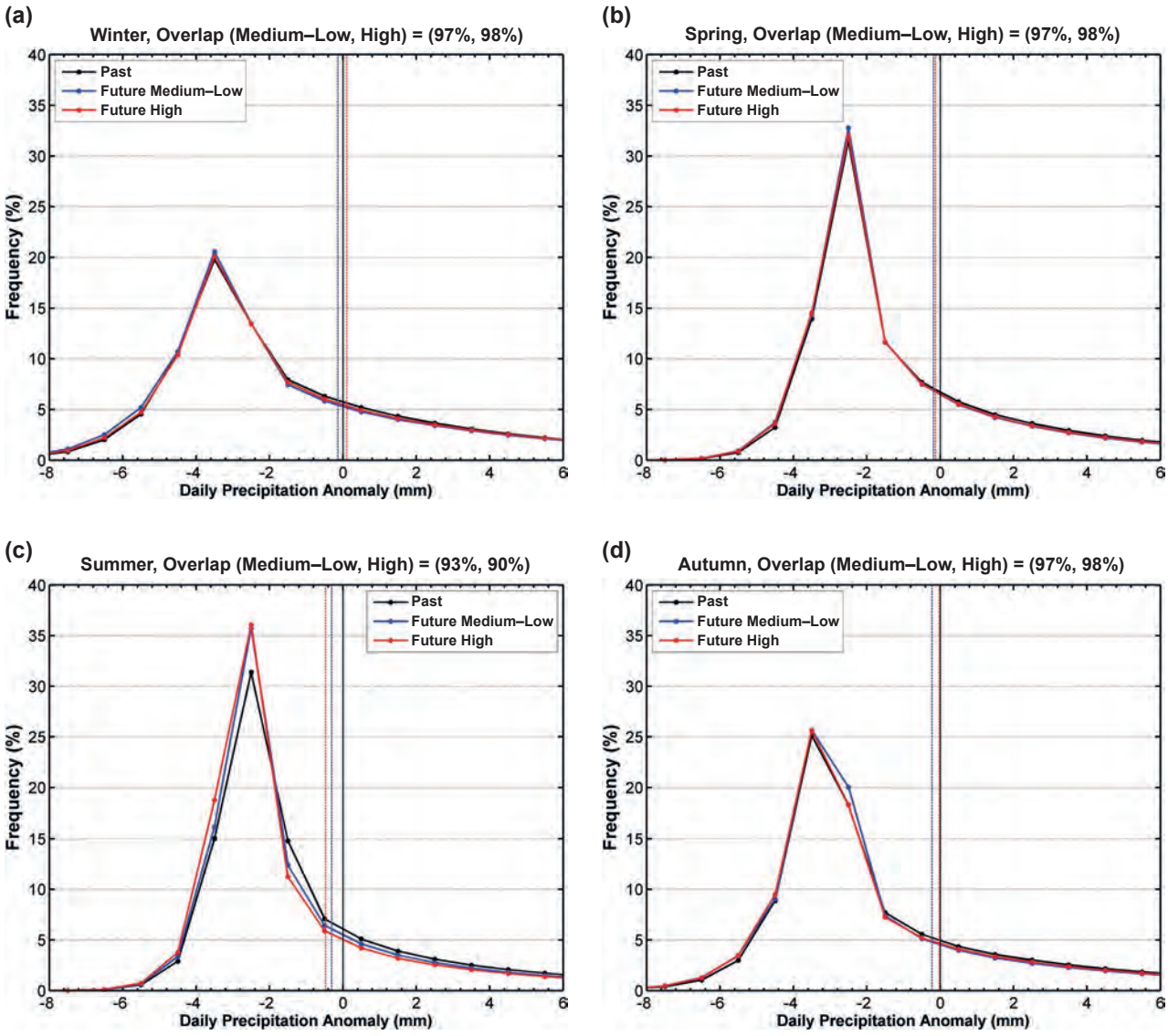

Figure 3.15. Empirical density functions illustrating the distribution of past (black), medium- to low-emission (blue) and high-emission (red) daily precipitation over Ireland. (a) Winter; (b) spring; (c) summer; (d) autumn. Each dataset has a size greater than 80 million. The distributions are created using histogram bins of size 1 mm. A measure of overlap indicates how much the future distributions have changed relative to the past (0% indicating no common area, 100% indicating complete agreement). Means are shown for historical (black vertical line), medium- to low-emission (blue vertical line) and high-emission (red vertical line) densities.

The density of the historical control period is shown in black, with the density of the medium- to low-emission scenario in blue and the high-emission scenario in red. An *overlap score* was calculated which assesses the similarity between the group's past and future (adapted from a process in Perkins et al., 2007; see section 2.3.3 of the present report for a mathematical description). This score is between 0% and 100%, with 100% indicating perfect agreement (climate completely unchanged) and 0% indicating no agreement (past and future climates have no values in common).

With the exception of summer, Figure 3.15 shows only small changes in the projected future precipitation distributions. The future summer distributions show a definite decrease in mean values (vertical lines) and a decrease in the right side of the distribution tail, strengthening the evidence from all the previous analysis of drying during summer. This result reinforces the projected mean changes shown in Figure 3.5, with large decreases projected for summer for both scenarios. The overlap scores range from 90% in summer (showing the largest changes across the distribution)

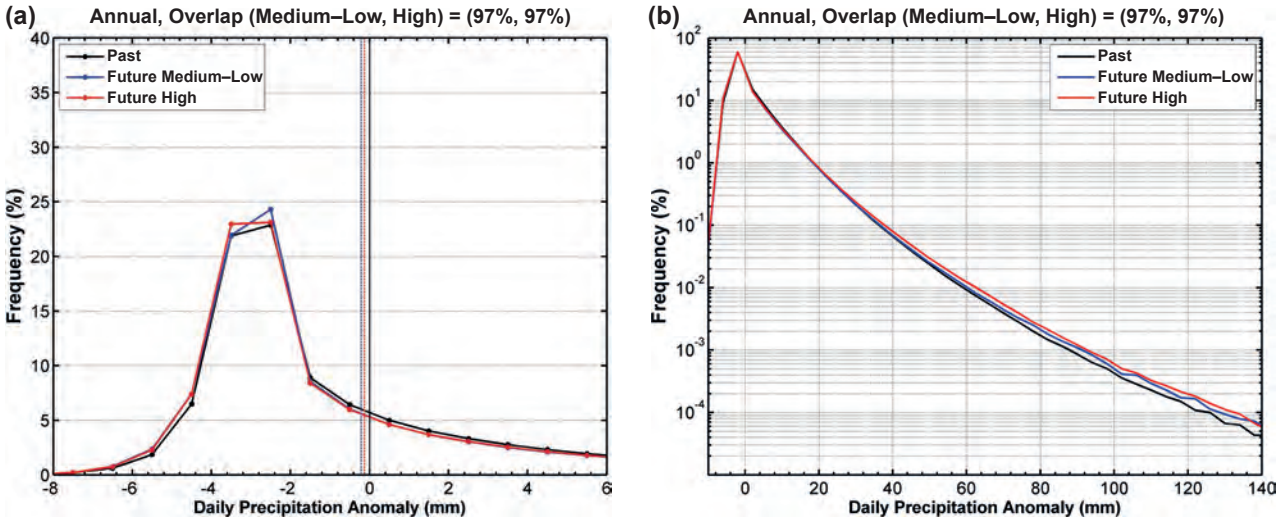

Figure 3.16. Empirical density functions illustrating the distribution of past (black), medium- to low-emission (blue) and high-emission (red) daily precipitation over Ireland. (a) Annual; (b) annual with the frequency displayed on a log scale. Each dataset has a size greater than 80 million. The distributions are created using histogram bins of size 1 mm (a) and 4 mm (b).

to 97–98% for all other seasons (showing the least change between historical and future densities). The annual density distributions, presented in Figure 3.16a, also show small changes with an overlap score of 97% for both the medium- to low-emission and high-emission scenarios. However, when the annual frequency is displayed on a log scale (Figure 3.16b), substantial increases in heavy precipitation events are evident. Similarly, the autumn and winter density distributions are presented on a log scale in Figure 3.17, with substantial increases in heavy precipitation evident for both seasons and both emission scenarios. Figures 3.16b and 3.17 reinforce the results of section 3.3.4, showing large projected increases in annual, winter and autumn wet days. It should be noted that, although large projected increases in heavy rainfall events are evident in Figures 3.16b and 3.17, the overlap scores are high (implying small changes between historical and future densities). This is because very heavy rainfall events are rare, as is evident from the frequency percentage values presented on the *y*-axis of the density function figures.

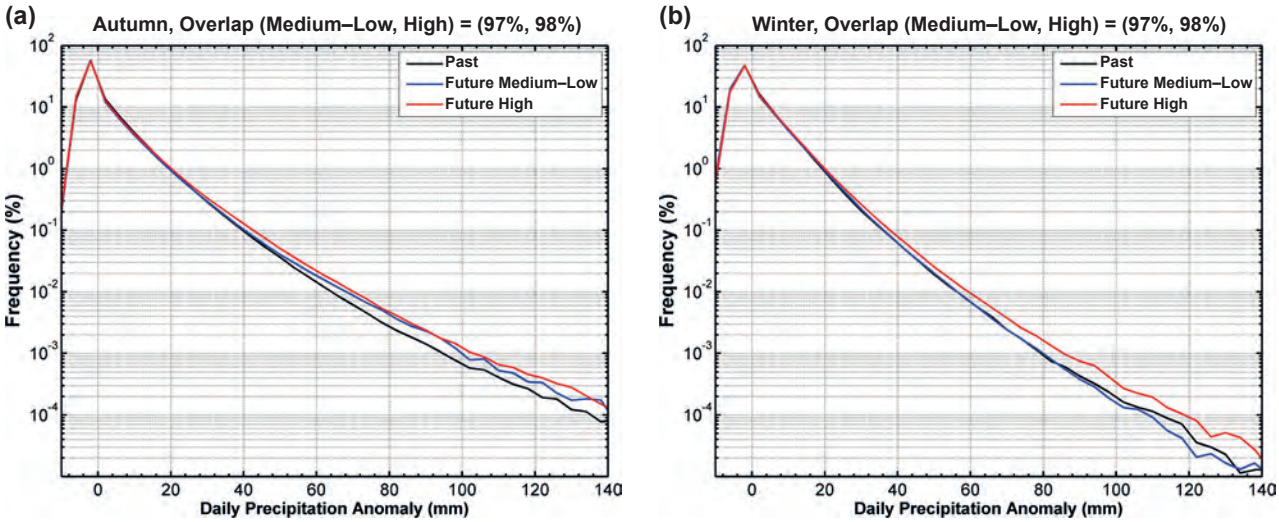

Figure 3.17. Empirical density functions illustrating the distribution of past (black), medium- to low-emission (blue) and high-emission (red) heavy precipitation over Ireland. (a) Autumn; (b) winter. The frequency is displayed on a log scale. Each dataset has a size greater than 80 million. The distributions are created using histogram bins of size 4 mm.

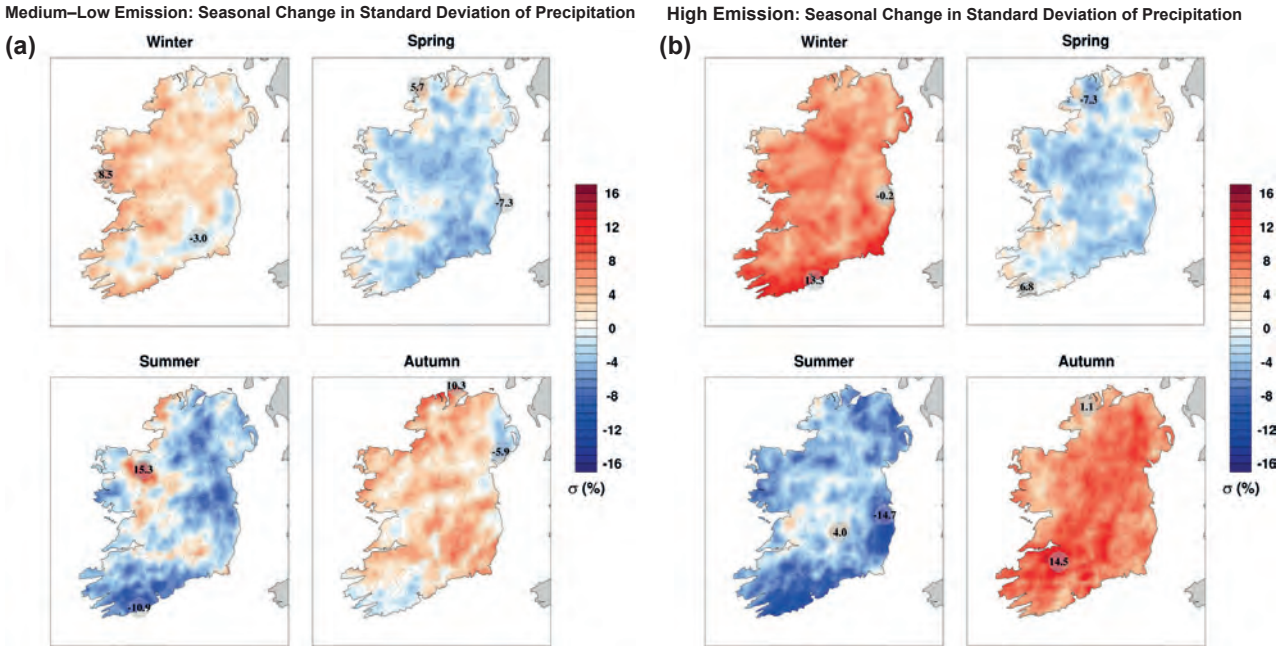

Figure 3.18. Seasonal projected changes (%) in the standard deviation of daily precipitation. (a) Medium- to low-emission ensemble; (b) high-emission ensemble. In each case, the future period 2041–2060 is compared with the past period 1981–2000. The numbers included on each plot are the minimum and maximum projected change, displayed at their location.

Figure 3.18 presents the seasonal projected changes in the standard deviation of daily rainfall amounts. The largest increases, of ~14%, are noted for autumn for the high-emission scenario. This is consistent with the results of the previous sections, showing a projected increase in both dry periods (Figure 3.8b) and wet days (Figures 3.11, 3.12 and 3.17a) for the autumn months. A large increase of ~10% is also projected for the high-emission winter standard deviation. This is consistent with previous results showing small changes in mean rainfall (Figure 3.5b) and large changes in heavy rainfall (Figures 3.11 and 3.17b). A general decrease in standard deviation is noted for summer, and is particularly evident for the high-emission scenario. This result, along with the large mean decreases projected in Figure 3.5, suggests the summer rainfall distribution of daily precipitation anomalies is shifted to the left (in the probability distribution) and has a smaller spread. This is consistent with the projected drying for summer (Figure 3.9) and the distributions and low overlap scores of Figure 3.15c. The smallest projected change in standard deviation is noted for spring. This is consistent with the projected decrease in mean precipitation (Figure 3.6b) and the similar past and future (slightly shifted to the left) distributions of Figure 3.15b. Figure 3.19 shows that the annual standard deviation of daily rainfall is projected to increase for the high-emission scenario. This is consistent with the projected annual increase in both dry (Figure 3.8a) and wet days (Figures 3.12 and 3.16b).

3.3.6 *Statistical significance of rainfall changes*

As precipitation is generally not normally distributed, the non-parametric Wilcoxon rank-sum and Kolmogorov–Smirnov tests were employed to assess the statistical significance of projected changes. The statistical significance of changes in the precipitation distributions of Figure 3.15 was tested against Ha_0 as outlined in section 1.8. Here, the alternative hypothesis states that the future distributions (Kolmogorov–Smirnov) or the future median values (Wilcoxon rank-sum) are different from the past. Both the Kolmogorov–Smirnov and Wilcoxon rank-sum tests show a high level of significance ($p \approx 0$) for the medium- to low-emission and high-emission scenarios across all seasons. We therefore conclude the projected changes in the future rainfall distributions and medians are statistically significant.

To determine the statistical significance of projected changes in a specific direction, the stronger Ha_1 and Ha_2 one-tail tests were employed. The Wilcoxon rank-sum Ha_1 test determined that the projected decreases for spring, summer and autumn are statistically significant

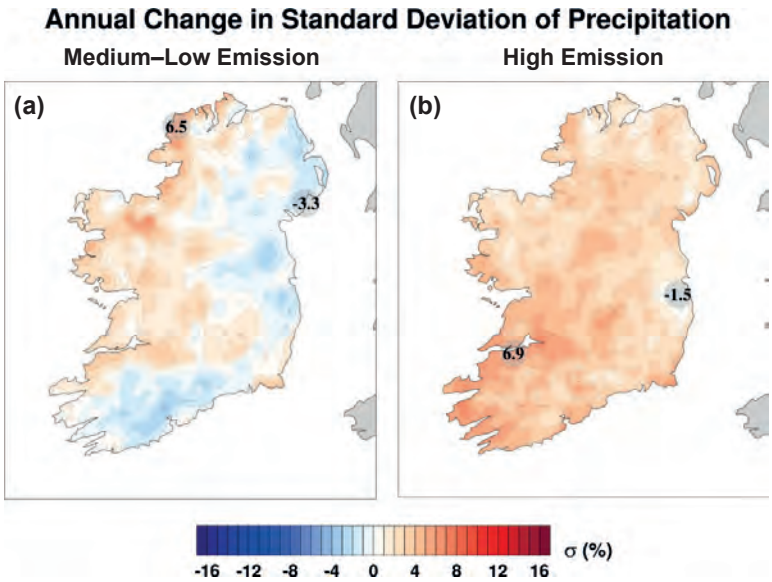

Figure 3.19. Annual projected changes (%) in the standard deviation of daily precipitation. (a) Medium- to low-emission ensemble; (b) high-emission ensemble. In each case, the future period 2041–2060 is compared with the past period 1981–2000. The numbers included on each plot are the minimum and maximum projected change, displayed at their locations.

($p < 0.001$) for both the medium- to low-emission and high-emission scenarios. The Ha_2 Wilcoxon rank-sum test determined that the projected increase during winter for the high-emission scenario (see Figures 3.5b and 3.15a) is not statistically significant at the 95% confidence level.

3.4 Conclusions

The impact of simulated global climate change on rainfall in Ireland was examined using the method of regional climate modelling. In view of unavoidable errors due to model (regional and global) imperfections, and the inherent limitation on predictability of the atmosphere arising from its chaotic nature, isolated projections of precipitation are of very limited value. To address this issue of uncertainty, an ensemble of RCMs was run.

The RCMs were validated using 20-year simulations of the past Irish climate (1981–2000), driven by the GCM datasets, and comparing the output against observational data. Extensive validations were carried out to test the ability of the RCMs to accurately model the precipitation climate of Ireland. Results confirm that the output of the RCMs exhibit reasonable and realistic features as documented in the historical data record.

The future climate was simulated using both medium- to low-emission and high-emission scenarios. The future period 2041–2060 was compared with the past period 1981–2000. Results show significant projected decreases in mean precipitation during spring and summer and over the entire year by mid-century. The projected decreases are largest for summer, with "likely" values ranging from 0% to 13% and from 3% to 20% for the medium- to low-emission and high-emission scenarios, respectively. The drying signal for autumn is less robust. A projected increase in mean precipitation for winter was noted over most of Ireland for the high-emission scenario. However, the projections of mean precipitation for autumn and winter exhibited great uncertainty, as reflected in a large spread between the individual ensemble members. The projections of mean precipitation for winter and autumn should therefore be viewed with a low level of confidence.

However, results show that heavy rainfall events are projected to increase substantially (by approximately 20%) during the winter and autumn months. The number of extended dry periods is also projected to increase substantially during autumn and summer and over the entire year by mid-century. The projected increases in dry periods are largest for summer, with "likely" values ranging from 12% to 40% for both emission scenarios.

Compared with the temperature projections of Chapter 2, there is less confidence in future projections of rainfall and this is reflected in a rather large spread, particularly at regional level, between the individual RCM ensemble members. Future work will attempt to address this issue

by increasing the RCM ensemble size and employing more up-to-date RCMs, GCMs and the RCP2.6 and RCP6.0 emission scenarios. Furthermore, the accuracy and usefulness of the rainfall predictions will be enhanced by running the RCMs at a higher spatial resolution.

The precipitation projections of this study could be attributed to many possible factors, such as a change in the NAO relative to the control period 1981–2000. A preliminary analysis of the RCM ensemble of the current report has shown that, while mean sea-level pressure (MSLP) is projected to increase by mid-century over Ireland, the number of intense storms is also projected to increase (see section 4.4). The projected increase in MSLP will probably lead to a decrease in precipitation during the summer, when intense storms are rare. Furthermore, the increase in very intense storms will probably lead to an increase in heavy precipitation events during autumn and winter. However, further investigation of these factors is necessary to attribute causation to the rainfall projections, and was beyond the scope of this study. Future work will attempt to address this issue.

The research consolidated and expanded on the RCM rainfall projections of a 2013 Met Éireann climate change report (Nolan et al., 2013) by increasing the ensemble size, allowing likelihood levels to be assigned to the projections. In addition, the uncertainty of the projections was more accurately quantified. The results from both studies are broadly consistent.

References

Chan, S., Kendon, E., Fowler, H., Blenkinsop, S. and Roberts, N., 2014. Projected increases in summer and winter UK sub-daily precipitation extremes from high-resolution regional climate models. Environmental Research Letters, 9, 084019.

Collins, M., Knutti, R., Arblaster, J., Dufresne, J.-L., Fichefet, T., Friedlingstein, P., Gao, X., Gutowski, W.J., Johns, T., Krinner, G., Shongwe, M., Tebaldi, C., Weaver, A.J. and Wehner, M., 2013. Long-term climate change: projections, commitments and irreversibility. In Stocker, T.F., Qin, D., Plattner, G.-K., Tignor, M., Allen, S.K., Boschung, J., Nauels, A., Xia, Y., Bex, V. and Midgley, P.M. (eds), Climate Change 2013: The Physical Science Basis. Contribution of Working Group I to the Fifth Assessment Report of the Intergovernmental Panel on Climate Change. Cambridge University Press, Cambridge.

Feser, F. and Barcikowska, M., 2012. The influence of spectral nudging on typhoon formation in regional climate models. Environmental Research Letters, 7, 014024.

Feser, F., Rockel, B., von Storch, H., Winterfeldt, J. and Zahn, M., 2011. Regional climate models add value to global model data: a review and selected examples. Bulletin of the American Meteorological Society, 92, 1181–1192.

Flato, G., Marotzke, J., Abiodun, B., Braconnot, P., Chou, S.C., Collins, W., Cox, P., Driouech, F., Emori, S., Eyring, V., Forest, C., Gleckler, P., Guilyardi, E., Jakob, C., Kattsov, V., Reason, C. and Rummukainen, M., 2013. Evaluation of Climate Models. In Stocker, T.F., Qin, D., Plattner, G.-K., Tignor, M., Allen, S.K., Boschung, J., Nauels, A., Xia, Y., Bex, V. and Midgley, P.M. (eds), Climate Change 2013: The Physical Science Basis. Contribution of Working Group I to the Fifth Assessment Report of the Intergovernmental Panel on Climate Change. Cambridge University Press, Cambridge.

Heinrich, G. and Gobiet, A., 2012. The future of dry and wet spells in Europe: a comprehensive study based on the ENSEMBLES regional climate models. International Journal of Climatology, 32, 1951–1970.

Jacob, D., Petersen, J., Eggert, B., Alias, A., Christensen, O.B., Bouwer, L.M., Braun, A., Colette, A., Déqué, M., Georgievski, G., Georgopoulou, E., Gobiet, A., Menut, L., Nikulin, G., Haensler, A., Hempelmann, N., Jones, C., Keuler, K., Kovats, S., Kröner, N., Kotlarski, S., Kriegsmann, A., Martin, E., van Meijgaard, E., Moseley, C., Pfeifer, S., Preuschmann, S., Radermacher, C., Radtke, K., Rechid, D., Rounsevell, M., Samuelsson, P., Somot, S., Soussana, J.-F., Teichmann, C., Valentini, R., Vautard, R., Weber, B. and Yiou, P., 2014. EURO-CORDEX: new high resolution climate change projections for European impact research. Regional Environmental Change, 14, 563–578.

Kanada, S., Nakano, M., Hayashi, S., Kato, T., Nakamura, M., Kurihara, K., and Kitoh, A., 2008: Reproducibility of maximum daily precipitation amount over Japan by a high-resolution non-hydrostatic model. Sola, 4, 105–108.

Kendon, E., Roberts, N., Senior, C. and Roberts, M., 2012. Realism of rainfall in a very high-resolution regional climate model. Journal of Climate, 25, 5791–5806.

Kendon, E.J., Roberts, N., Fowler, H., Roberts, M., Chan, S. and Senior, C., 2014. Heavier summer downpours with climate change revealed by weather forecast resolution model. Nature Climate Change, 4, 570–576.

Lenderink, G. and Van Meijgaard, E., 2008. Increase in hourly precipitation extremes beyond expectations from temperature changes. Nature Geoscience, 1, 1511–1514.

Lucas-Picher, P., Wulff-Nielsen, M., Christensen, J., Adalgeirsdottir, G., Mottram, R. and Simonsen, S., 2012. Very high resolution regional climate model simulations over Greenland: Identifying added value. Journal of Geophysical Research, 117, D02108.

Ma, H.-Y., Xie, S., Boyle, J.S., Klein, S.A. and Zhang, Y., 2013. Metrics and diagnostics for precipitation-related processes in climate model short-range hindcasts. Journal of Climate, 2, 1516–1534.

Met Éireann, n.d. Rainfall. Available online: www.met.ie/climate-ireland/rainfall.asp (accessed 13 July 2015).

Nolan P., McGrath, R., Gleeson, E. and Sweeney, C., 2013. Impacts of climate change on Irish precipitation. In Gleeson, E., McGrath, R. and Treanor, M. (eds), Ireland's Climate: The Road Ahead. Met Éireann, Dublin, pp. 57–61. Available online: www.met.ie/publications/IrelandsWeather-13092013.pdf (accessed 13 July 2015).

O'Gorman, P., Allan, R., Byrne, M. and Previdi, M., 2012. Energetic constraints on precipitation under climate change. Surveys in Geophysics, 33, 585–608.

Perkins, S.E., Pitman, A.J., Holbrook, N.J. and McAneney, J., 2007. Evaluation of the AR4 climate models' simulated daily maximum temperature, minimum temperature, and precipitation over Australia using probability density functions. Journal of Climate, 20, 4356–4376.

Prein, A.F., Gobiet, A., Suklitsch, M., Truhetz, H., Awan, N.K., Keuler, K. and Georgievski, G., 2013. Added value of convection permitting seasonal simulations. Climate Dynamics, 41, 2655–2677.

Rauscher, S.A., Coppola, E., Piani, C. and Giorgi, F., 2010. Resolution effects on regional climate model simulations of seasonal precipitation over Europe. Climate Dynamics, 35, 685–711.

Shkol'nik, I., Meleshko, V., Efimov, S. and Stafeeva E., 2012. Changes in climate extremes on the territory of Siberia by the middle of the 21st century: an ensemble forecast based on the MGO regional climate model. Russian Meteorology and Hydrology, 37, 71–84.

Trenberth, K.E., Dai, A., Rasmussen, R.M. and Parsons, D.B., 2003. The changing character of precipitation. Bulletin of the American Meteorological Society, 84, 1205–1217.

van der Linden, P. and Mitchell, J.F.B. (eds), 2009. ENSEMBLES: Climate Change and Its Impacts. Summary of Research and Results from the ENSEMBLES Project. Met Office Hadley Centre, Exeter.

Walsh, S., 2012. A Summary of Climate Averages for Ireland 1981–2010. Climatological Note No. 14. Met Éireann, Dublin. Available online: www.met.ie/climate-ireland/SummaryClimAvgs.pdf (accessed 13 July 2015).

Walsh, S. and Dwyer, N., 2012. Rainfall. In Dwyer, N. (ed.), The Status of Ireland's Climate, 2012. CCRP Report No. 26. EPA, Wexford.

Wild, O. and Leipert, B., 2010. The Earth radiation balance as driver of the global hydrological cycle. Environmental Research Letters, 5, 025203.

4 Impacts of climate change on Irish wind energy resource

Downscaled global simulation data from several RCMs were used to provide an assessment of the impacts of a warming climate on the wind energy resource of Ireland by mid-century. The future climate was simulated using both medium- to low-emission (B1, RCP4.5) and high-emission (A1B, A2, RCP8.5) scenarios. Results show significant projected decreases in the energy content of the wind for the spring, summer and autumn months. Projected increases for winter were found to be statistically insignificant. The projected decreases were largest for summer, with "likely" values ranging from 3% to 10% for the medium- to low-emission scenario and from 7% to 15% for the high-emission scenario.

To assess the potential impact of climate change on extreme cyclonic activity in the North Atlantic, an algorithm was developed to identify and track cyclones as simulated by the RCMs. Results indicate that the tracks of intense storms are projected to extend further south over Ireland relative to those in the reference simulation. An increase in extreme storm activity is expected to adversely affect the future wind energy supply.

4.1 Introduction

There is considerable interest among policymakers and the energy industry in renewable energy resources as a means of reducing carbon dioxide emissions to minimise climate change (Solomon et al., 2007). Within this context, it is desirable to increase the share of electricity generation from renewable sources such as wind and reduce the production from fossil sources. Under the EU Directive on the Promotion of the Use of Renewable Energy (2009/28/EC), Ireland is committed to ensuring that 16% of the total energy consumed in heating, electricity and transport is generated from renewable resources by 2020 (Department of Communications, Energy and Natural Resources, 2010). The Irish Government has also set a target of 40% electricity consumption from renewable sources by 2020. Wind energy is expected to provide approximately 90% of this target (Department of Communications, Energy and Natural Resources, 2010). In 2012, wind energy in Ireland accounted for 15.5% of our electricity needs (Sustainable Energy Authority of Ireland, 2014).

From a climate perspective, Ireland is ideally located to exploit the natural energy associated with the wind. Mean annual speeds are typically in the range 6–8.5 m/s at a 50-m level over land (Sustainable Energy Ireland, 2003): values that are sufficient to sustain commercial enterprises with current wind turbine technology. There is some evidence of a slight reduction in surface winds over past decades over both land and coastal areas around Ireland but the results are not robust (Vautard et al., 2010, see chapter 2, 'Other parameters'). A separate study of wind speed trends over northern Europe showed a decrease in wind speed for 1990–2005 (Atkinson et al., 2006).

The wind energy potential of the past Irish climate has been well documented (Troen and Petersen, 1989; Sustainable Energy Ireland, 2003; Standen et al., 2013). However, climate change may alter the wind patterns in the future; a reduction in speeds may reduce the commercial returns or pose problems for the continuity of supply; an increase in the frequency of severe winds (e.g. gale/storm gusts) may similarly impact on supply continuity. Conversely, an increase in the mean wind speed may have a positive effect on the available power supply.

4.1.1 European wind climatology projections

Hueging et al. (2013) investigated the impact of climate change on wind power generation potentials over Europe by considering ensemble projections from two RCMs driven by a GCM. They found that "over northern and central Europe, the wind energy potential is projected to increase, particularly in winter and autumn. In contrast, energy potential over southern Europe may experience a decrease in all seasons except for the Aegean Sea" (Hueging et al., 2013). Pryor et al. (2005) showed that for northern Europe there is evidence for increased wind energy density in the projected climate change simulations, particularly during the winter, whereas Pryor and Barthelmie (2010) suggest no detectable change in the wind resource or other external conditions that could jeopardise the continued exploitation of wind energy. Furthermore, Pryor et al. (2012) found a slight decline in interannual variability of wind energy potential under future climate conditions in northern Europe. Results

for the UK (Harrison et al., 2008; Cradden et al., 2012) indicate seasonal changes in potential wind production, with winter production generally increasing whereas summer production decreases.

4.1.2 Projections for Ireland

The C4I research group downscaled data from five GCMs over Ireland and the UK, using all SRES scenarios, achieving a finest horizontal resolution of 14 km. Looking at seasonal projections for 2021–2060, they found the energy content of the wind is projected to increase for winter and decrease for summer (McGrath and Lynch, 2008). These results were confirmed by Nolan et al. (2011, 2014). In 2013, the Research Division at Met Éireann led a major study on the future of Ireland's climate. A subset of the ensemble of RCM simulations used in the current study was analysed and projected an overall increase (~0–8%) in the energy content of the wind for the winter months and a decrease (4–14%) during the summer months (Nolan et al., 2013). Reductions were noted for spring, ranging from ~0% to 6%.

4.1.3 European extreme wind and storminess projections

Windstorms and associated high wind speeds are a major source of natural hazard risk for Ireland and many countries across Europe. Ireland and the UK were severely affected by an exceptional run of storms during the winter of 2013/2014, culminating in serious coastal damage and widespread, persistent flooding. Reports issued by the meteorological agencies of Ireland and the UK have confirmed that records for precipitation totals and extreme wind speeds were set during this period (Met Éireann, 2014, n.d.; Met Office, n.d.). A study by the Irish Climate and Research Unit at the National University of Ireland Maynooth, in collaboration with the Centre for Hydrological and Ecosystem Science at Loughborough University, found that the winter of 2013/2014 was the stormiest for at least 143 years, when storm frequency and intensity are considered together (Matthews et al., 2014). In addition to the potential widespread flooding and structural damage associated with storms, the wind energy supply can be negatively affected as wind turbines are shut down during periods of high wind speeds to prevent damage.

Feser et al. (2014) conducted a review of studies of storms over the North Atlantic and north-western Europe regarding the occurrence of potential long-term trends. Storm trends derived from re-analysis data and climate model data for the past were mostly limited to the last four to six decades. They found that "the majority of these studies find increasing storm activity north of about 55–60°N over the North Atlantic with a negative tendency southward". Furthermore, "future scenarios until about the year 2100 indicate mostly an increase in winter storm intensity over the North Atlantic and western Europe. However, future trends in total storm numbers are quite heterogeneous and depend on the model generation used." Zappa et al. (2013) analysed a Coupled Model Intercomparison Project phase 5 (CMIP5) ensemble of 19 GCMs and found a small, but significant, increase in the number and intensity of winter cyclones associated with strong wind speeds over the UK by the end of the century. A recent study with a very high-resolution version of the EC-Earth model (Haarsma et al., 2013) suggests an increase in the frequency of extreme wind storms affecting western Europe in future autumn seasons because of climate change.

4.1.4 Current study

The current study aims to assess the impacts of climate change on the future wind energy resource of Ireland. In addition, projected changes in the number and positions of extreme storms are analysed. The inherent uncertainty of climate predictions is partially addressed by employing an MME approach. The ensemble approach uses several different RCMs, driven by several GCMs, to simulate climate change. In addition, a number of possible future greenhouse gas scenarios are considered. Through the MME approach, the uncertainty in the projections can be partially quantified, proving a measure of confidence in the predictions.

As in the case of precipitation (see Chapter 3), near-surface winds are strongly influenced by local features, e.g. hills and valleys, and an accurate description of these effects requires high-resolution climate modelling. To address this issue, the RCMs were run at a spatial resolution of up to 4 km, thus allowing sharper estimates of the regional variations in the changes in wind speed and direction. Details of the different global climate datasets, the greenhouse gas emission scenarios and the downscaling models used to produce the ensemble of climate projections for Ireland are summarised in Chapter 1. Numerous studies have demonstrated the added value of high-resolution RCMs in the simulation

of near surface wind speeds (e.g. Kanamaru et al., 2007), particularly in coastal areas with complex topography (Feser et al., 2011; Winterfeldt et al., 2011).

The current research consolidates and expands on the RCM wind projections of the 2013 Met Éireann climate change report (Nolan et al., 2013) by increasing the ensemble size. This allows likelihood levels to be assigned to the projections. In addition, the uncertainty of the projections can be more accurately quantified.

4.2 Regional climate model wind validations

4.2.1 Validation of 10-m wind speed

The RCMs were validated using 20-year simulations of the past Irish climate (1981–2000), driven by both ECMWF ERA-40 global re-analysis and the GCM datasets, and comparing the output against Met Éireann observational data. Figure 4.1 compares observed 10-m wind speed data at nine synoptic stations spanning Ireland with the RCM ensemble members (12

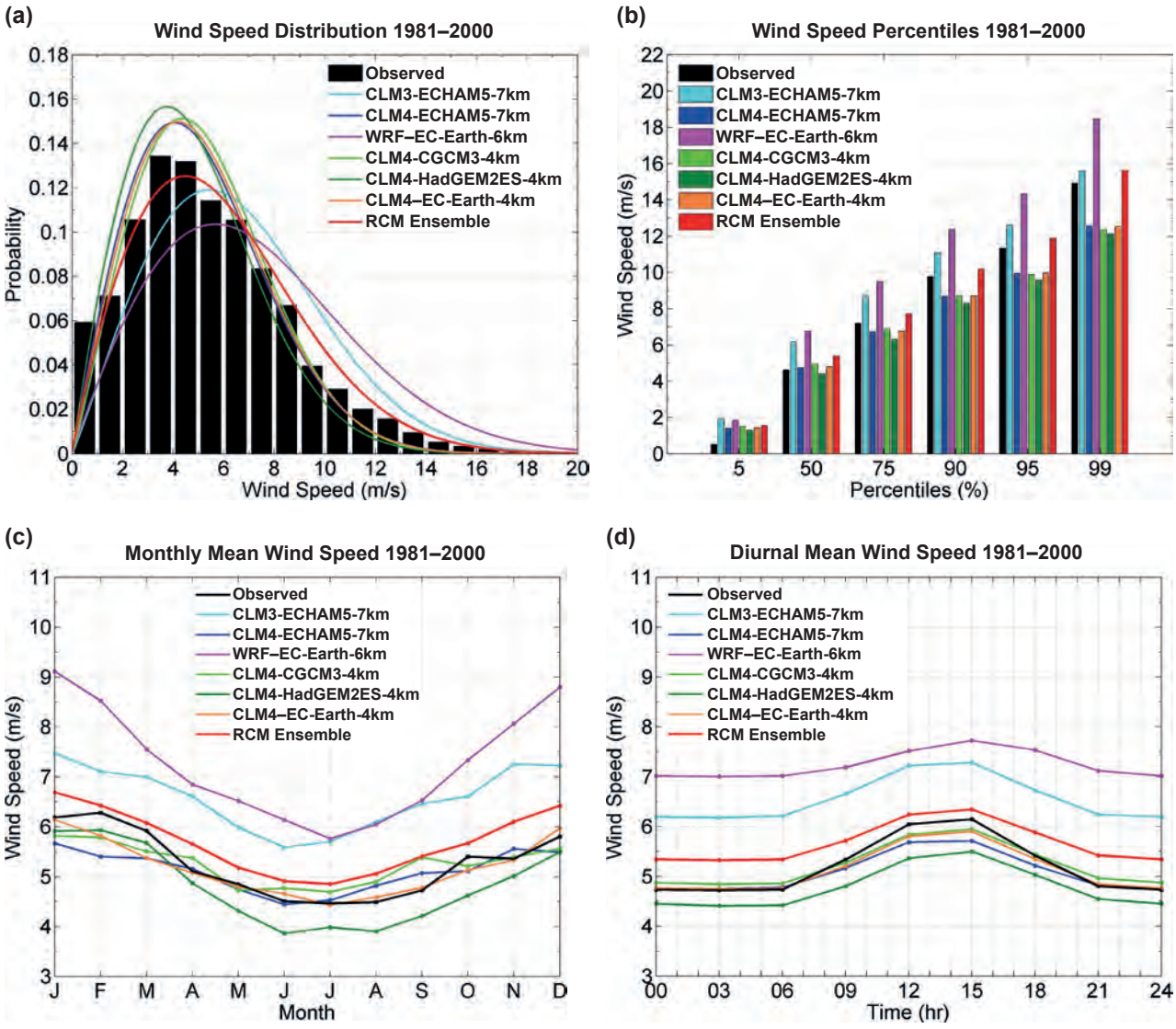

Figure 4.1. Comparing the observed 3-hourly 10-m winds at nine synoptic stations spanning Ireland with the RCM ensemble members for the period 1981–2000. (a) Wind speed distribution; (b) wind speed percentiles; (c) mean monthly wind speed; (d) mean diurnal cycle. The following RCM validation datasets are considered: CLM3-ECHAM5 7 km (two ensemble members), CLM4-ECHAM5 7 km (two ensemble members), WRF–EC-Earth 6 km (three ensemble members), CLM4-CGCM3.1 4 km (one ensemble member), CLM4-HadGEM2-ES 4 km (one ensemble member), CLM4–EC-Earth 4 km (three ensemble members) and the total RCM ensemble (12 members). For (c) and (d), the RCM dataset means are considered.

in total; see Table 1.2), for 1981–2000. The stations are Belmullet, Casement Aerodrome, Cork Airport, Claremorris, Dublin Airport, Mullingar, Rosslare, Shannon Airport and Valentia Observatory. The observed wind data for Rosslare station were limited to the 16-year period 1981–1996. The observed wind speeds are calculated each hour using the mean value in the preceding 10 minutes. The locations of the stations (excluding Casement Aerodrome) can be seen in the wind rose plot of Figure 4.2. Figure 4.1a presents the observed and model wind speed distributions. The CLM3-ECHAM5 7-km and WRF–EC-Earth 6-km distributions show a positive bias in the probability of obtaining higher wind speeds, whereas the remaining simulations show a small negative bias. This is reflected in Figure 4.1b, the wind speed percentiles, 4.1c, the mean monthly wind speed, and 4.1d, the diurnal cycle, where, although we have relatively good agreement, the CLM3-ECHAM5 7-km and WRF–EC-Earth 6-km data overestimate the wind speeds by approximately 18% and 30%, respectively. A wind speed percentile P is defined as a wind speed, such that P% of all wind speeds of the dataset are less than this value.

The WRF model is known to overestimate the wind speed (Jimenez and Dudhia, 2012). Future work will attempt to correct for this bias by adapting the *topo_wind* parameterising scheme: a topographic correction for surface winds to represent extra drag from subgrid topography and enhanced flow at hill tops (Jimenez and Dudhia, 2012).

Figure 4.1a shows that the full 12-member ensemble dataset (plotted in red) provides the best fit with observations for the probability distributions of low to mid-range wind speeds. In addition, Figure 4.1b shows that the ensemble dataset shows improvements over the individual ensemble members for wind speed percentiles at the higher scale ($P \geq 75$).

4.2.2 *Validation of the energy content of the wind*

To investigate the ability of the RCMs to simulate the energy content of the wind, the cube of the 10-m wind speed is analysed. Figure 4.3 shows a contour plot of the diurnal cycle of mean cube 10-m wind speed per month averaged over the nine synoptic station locations. As expected, the energy content of the wind is at a maximum during the middle of the day in winter and at a minimum during the night in summer. Again, the CLM3-ECHAM5 7-km and WRF–EC-Earth 6-km simulations show a positive bias, whereas the remaining RCMs show a negative bias because of their inability to estimate wind speeds at the higher scale. The most accurate representation of the energy content of the wind is provided by the RCM ensemble mean as presented in Figure 4.3h. Figure 4.3i shows that the RCM ensemble percentage errors range from −10% to +40%.

4.2.3 *Validation of wind direction*

Near-surface winds are strongly influenced by local features and an accurate description of these effects requires high-resolution climate modelling. The impacts of resolution are evident in Figure 4.4, which shows the 10-m wind roses at Casement Aerodrome,

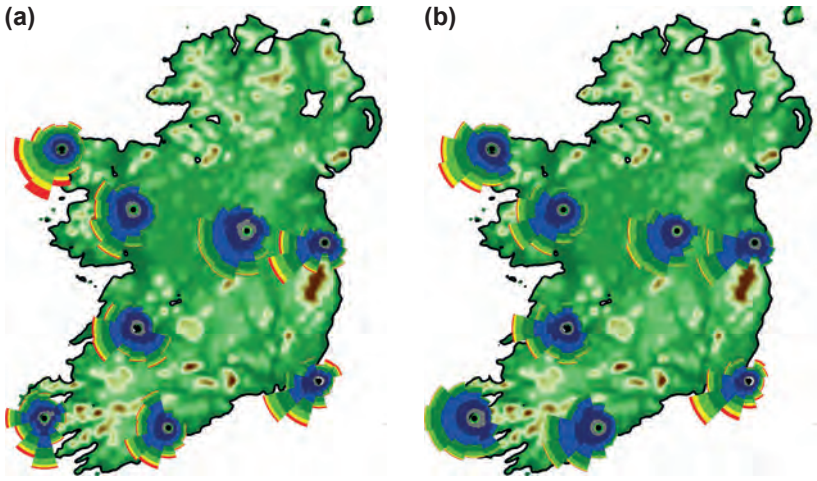

Figure 4.2. Annual 10-m wind roses at eight Met Éireann synoptic stations spanning Ireland. (a) Observed data; (b) CLM4–EC-Earth 4-km data.

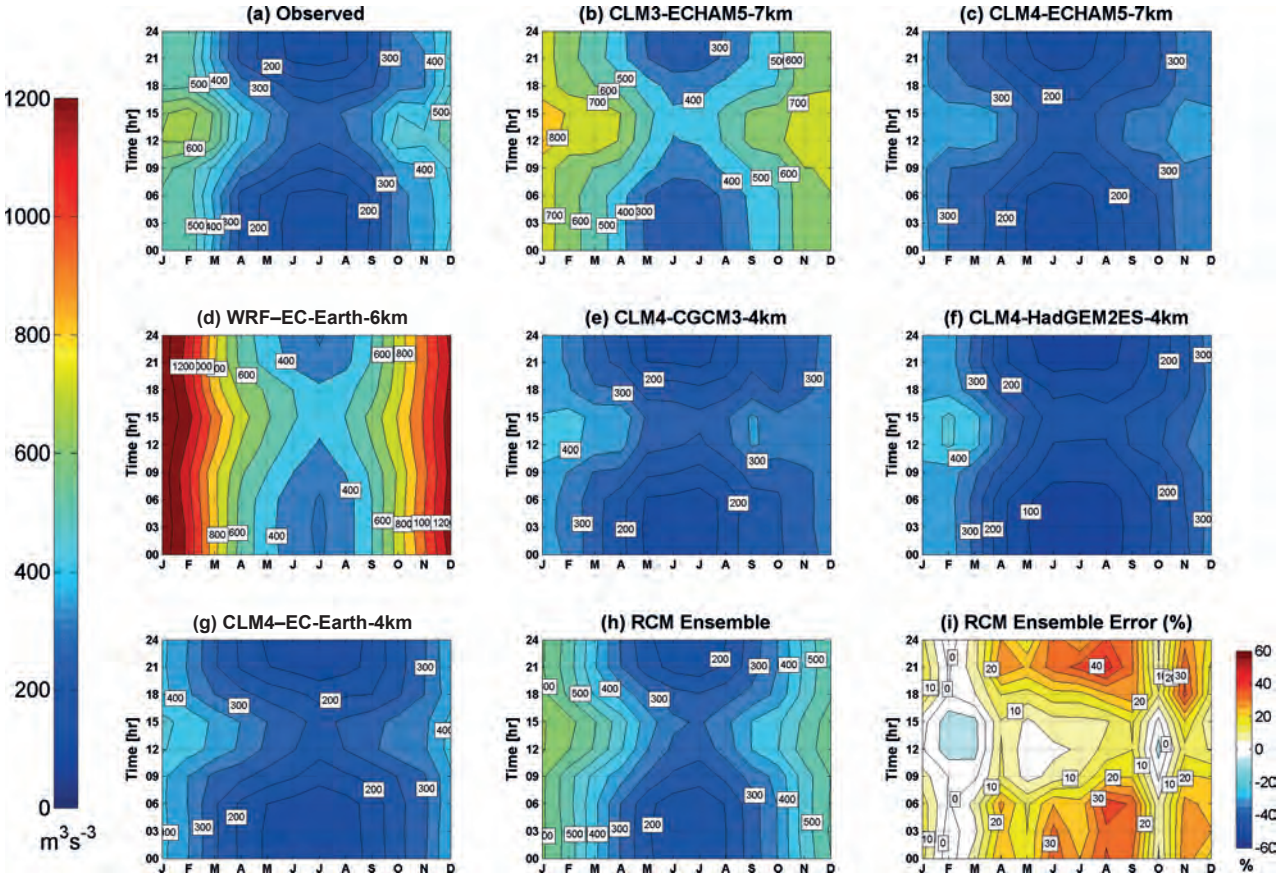

Figure 4.3. Annual diurnal 10-m mean cubed wind speed, averaged over nine station locations for 1981–2000. (a) Observation; (b) CLM3-ECHAM5 7 km (two ensemble members); (c) CLM4-ECHAM5 7 km (two ensemble members); (d) WRF–EC-Earth 6 km (three ensemble members); (e) CLM4-CGCM3.1 4 km (one ensemble member); (f) CLM4-HadGEM2-ES 4 km (one ensemble member); (g) CLM4–EC-Earth 4 km (three ensemble members); (h) RCM ensemble mean (12 members); (i) RCM ensemble percentage error.

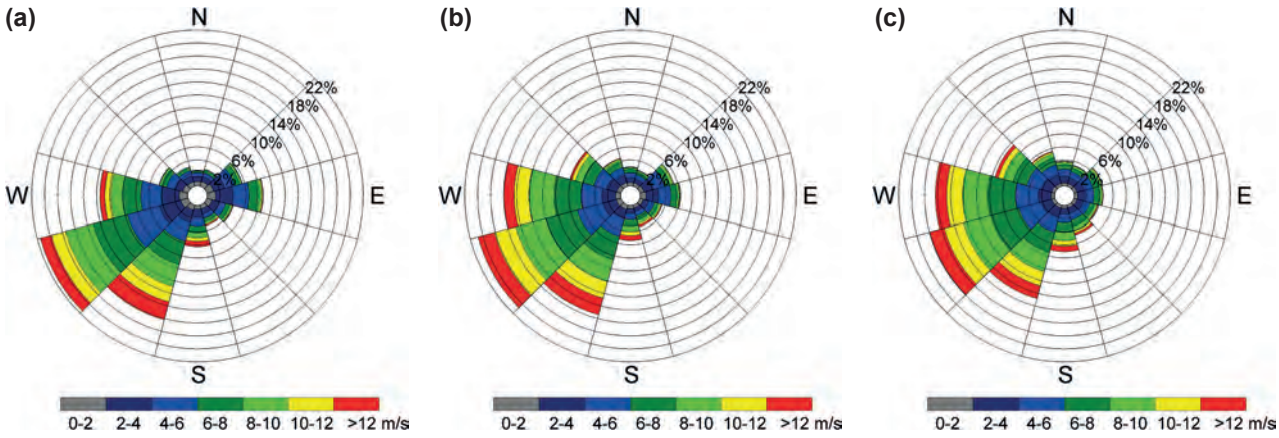

Figure 4.4. The 10-m wind roses at Casement Aerodrome for 1981–2000. (a) Observed; (b) WRF–EC-Earth ensemble (three members) 6-km resolution; (c) WRF–EC-Earth ensemble (three members) 18-km resolution. Each sector shows the percentage breakdown of the wind speed in intervals of 2 m/s.

located north of the Wicklow Mountains. The observed wind rose, presented in Figure 4.4a, demonstrates that the mountains act as a barrier, preventing south and south-easterly winds. This is represented by the high-resolution WRF–EC-Earth 6-km simulations (Figure 4.4b), whereas the WRF–EC-Earth 18-km simulations (Figure 4.4c) underestimate the south-westerly and easterly winds.

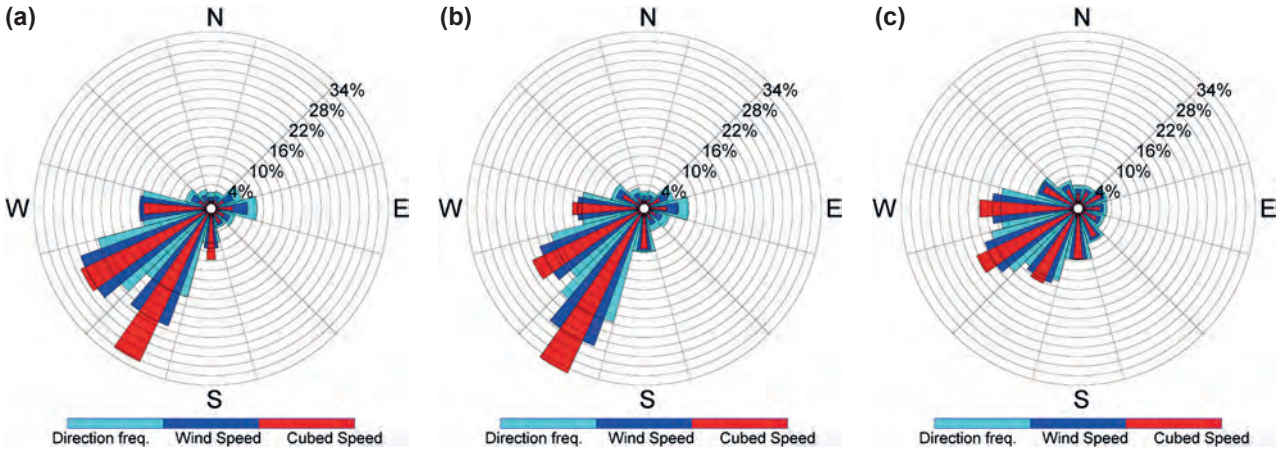

Figure 4.5. The 10-m wind power roses at Casement Aerodrome for 1981–2000. (a) Observed; (b) CLM4–EC-Earth ensemble (three members) 4-km resolution; (c) CLM4–EC-Earth ensemble (three members) 18-km resolution. The wind power rose shows the directional frequency (light blue segments), the contribution of each sector to the total mean wind speed (blue segments) and the contribution of each sector to the total mean cube of the wind speed (red segments).

The importance of high-resolution wind modelling is confirmed by Figure 4.5, which shows the 10-m wind power roses at Casement Aerodrome. The wind power rose shows the directional frequency (outer light blue segments), the contribution of each sector to the total mean wind speed (middle blue segments) and the contribution of each sector to the total mean cube of the wind speed (inner red segments). The CLM4–EC-Earth 4-km simulations (Figure 4.5b) are in good agreement with observations (Figure 4.5a); the wind direction, speed and power segments mostly have a south-south-west to south-west contribution. The lower resolution CLM4–EC-Earth 18-km simulations (Figure 4.5c) do not capture these local features.

The observed and CLM4–EC-Earth 4-km annual 10-m wind roses at eight synoptic stations for 1981–2000 are presented in Figure 4.2a and 4.2b, respectively. The stations are Belmullet, Cork Airport, Claremorris, Dublin Airport, Mullingar, Rosslare, Shannon Airport and Valentia Observatory. Similarly, the wind roses for winter, spring, summer and autumn are presented in Figures 4.6 to 4.9. With the exception of Valentia Observatory (located in the south-west), the model data provide an accurate representation of the wind directions. The relatively poor accuracy noted at Valentia is probably because of the local heterogeneity of the topography; the station is located in a coastal/mountainous region. The observed and CLM4–EC-Earth 4-km 10-m wind

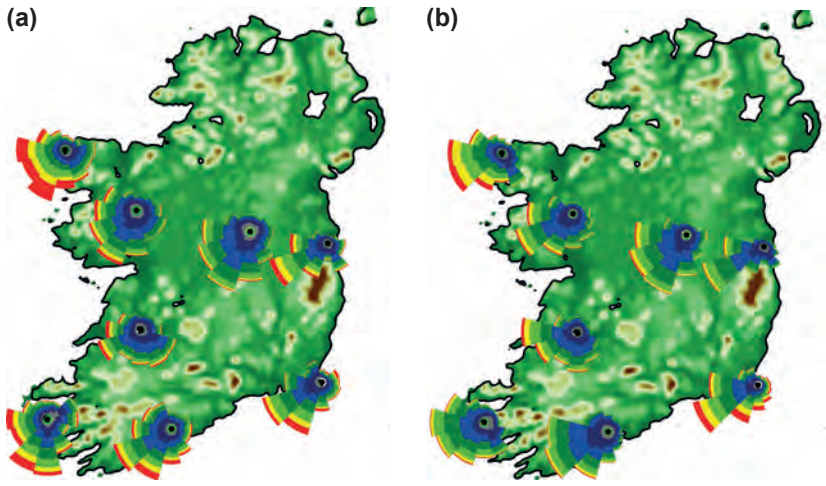

Figure 4.6. Winter 10-m wind roses at eight Met Éireann synoptic stations spanning Ireland. (a) Observed data; (b) CLM4–EC-Earth 4-km data.

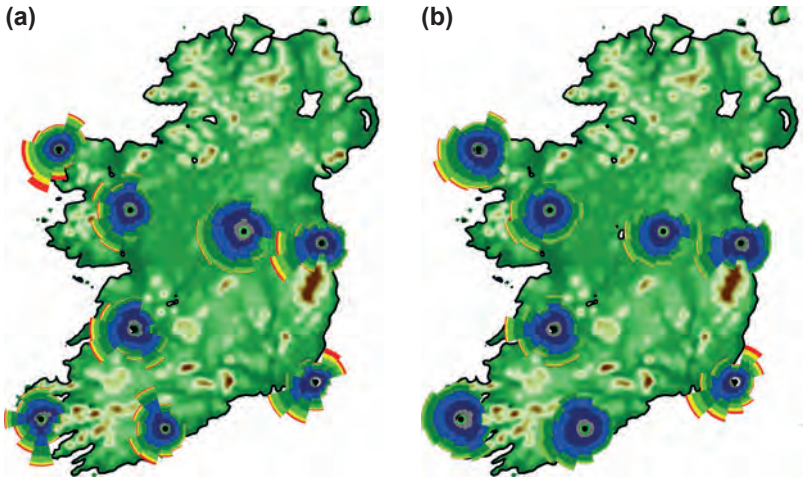

Figure 4.7. Spring 10-m wind roses at eight Met Éireann synoptic stations spanning Ireland. (a) Observed data; (b) CLM4–EC-Earth 4-km data.

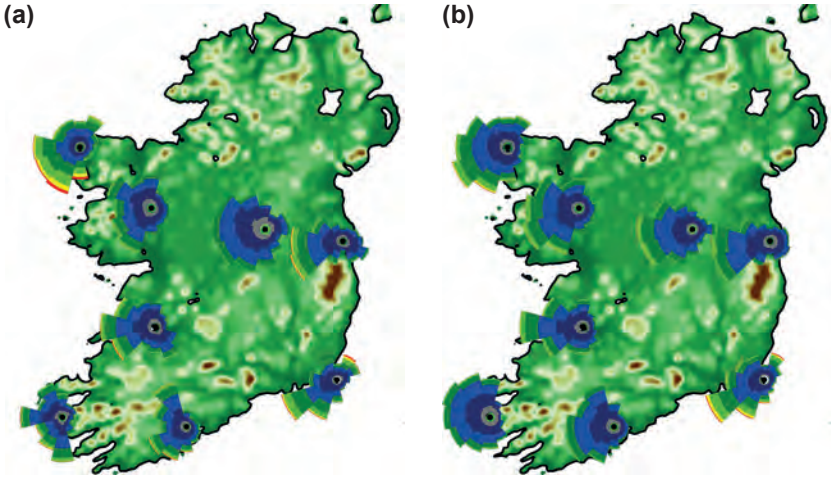

Figure 4.8. Summer 10-m wind roses at eight Met Éireann synoptic stations spanning Ireland. (a) Observed data; (b) CLM4–EC-Earth 4-km data.

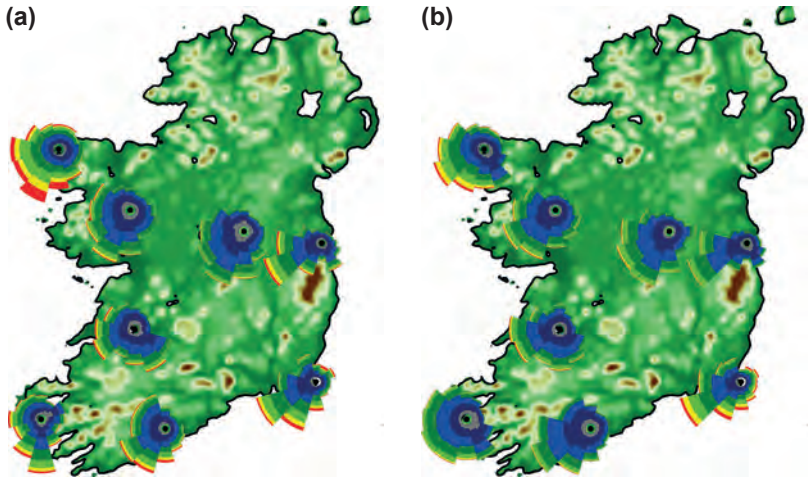

Figure 4.9. Autumn 10-m wind roses at eight Met Éireann synoptic stations spanning Ireland. (a) Observed data; (b) CLM4–EC-Earth 4-km data.

power roses, presented in Figures 4.10 to 4.14, confirm the ability of the RCM to accurately simulate wind direction with respect to mean wind speed and power.

The wind rose validations were repeated for all members of the RCM ensemble. It was found that, while the wind direction skill decreased with lower model resolution, the output of the RCMs provided a good fit to observed wind direction.

While the primary purpose of the wind rose figures (4.2 and 4.6 to 4.14) is to validate the RCMs, they also provide a useful source of information on the current wind energy resource of Ireland.

4.3 Wind projections for Ireland

4.3.1 Ensemble mean 60-m wind power projections

Since the typical height of wind turbines is approximately 60 m, we focus on wind projections at this height. To investigate the effects of climate change on the energy content of the wind, the projected changes in the 60-m mean cube wind speed are analysed.

Figure 4.15 shows the annual percentage change in the 60-m mean cube wind speed for the medium- to low-emission and high-emission scenarios. The future period 2041–2060 is compared with the past period 1981–2000. The models project an annual reduction in the energy content of the wind of 3–7% for the

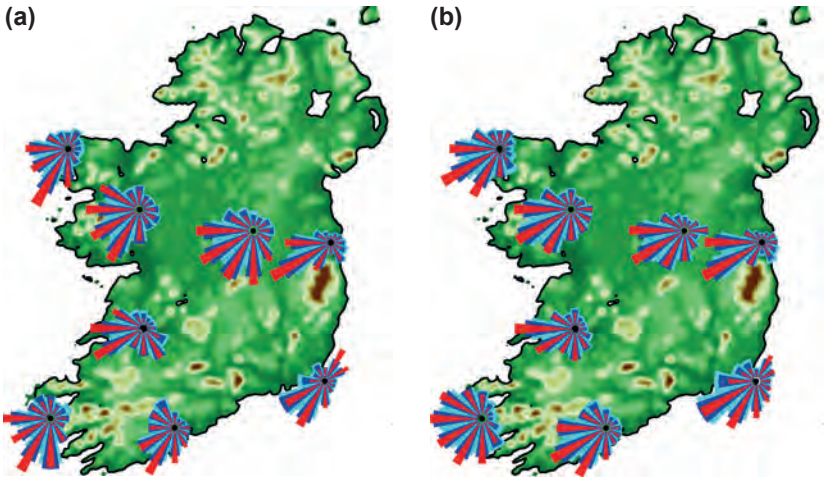

Figure 4.10. Annual 10-m wind power roses at eight Met Éireann synoptic stations spanning Ireland. (a) Observed data; (b) CLM4–EC-Earth 4-km data.

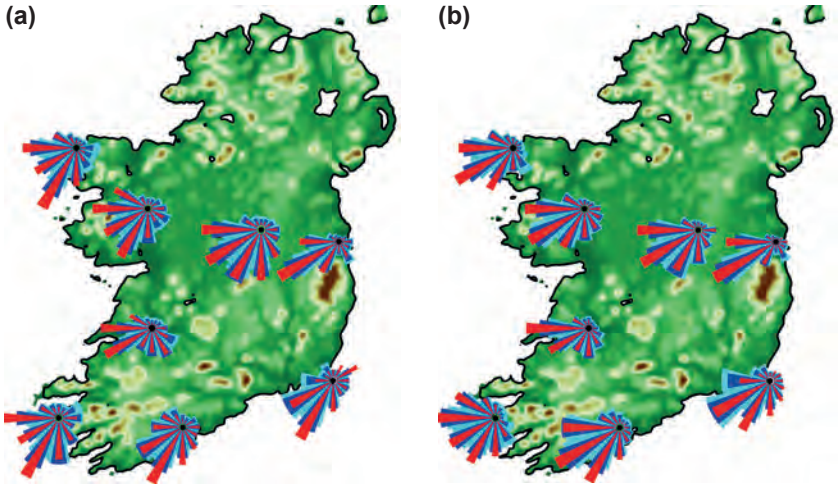

Figure 4.11. Winter 10-m wind power roses at eight Met Éireann synoptic stations spanning Ireland. (a) Observed data; (b) CLM4–EC-Earth 4-km data.

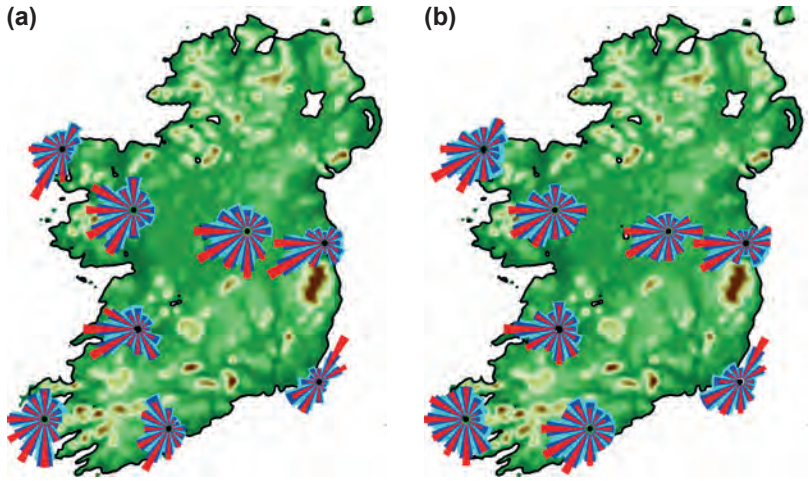

Figure 4.12. Spring 10-m wind power roses at eight Met Éireann synoptic stations spanning Ireland. (a) Observed data; (b) CLM4–EC-Earth 4-km data.

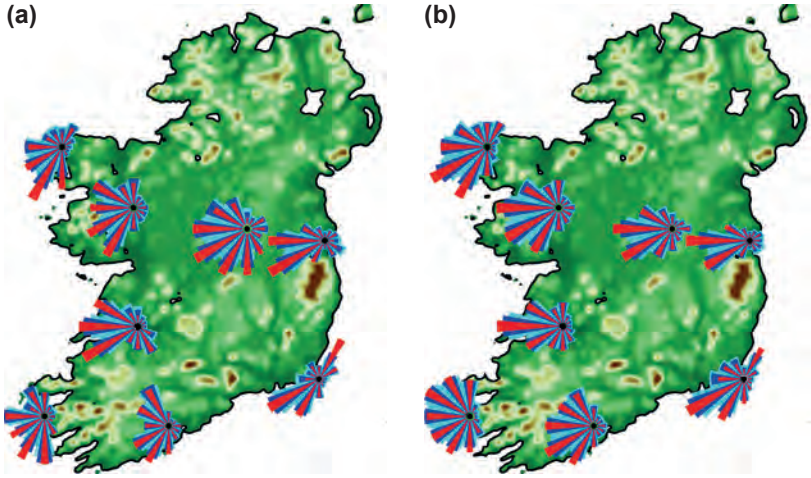

Figure 4.13. Summer 10-m wind power roses at eight Met Éireann synoptic stations spanning Ireland. (a) Observed data; (b) CLM4–EC-Earth 4-km data.

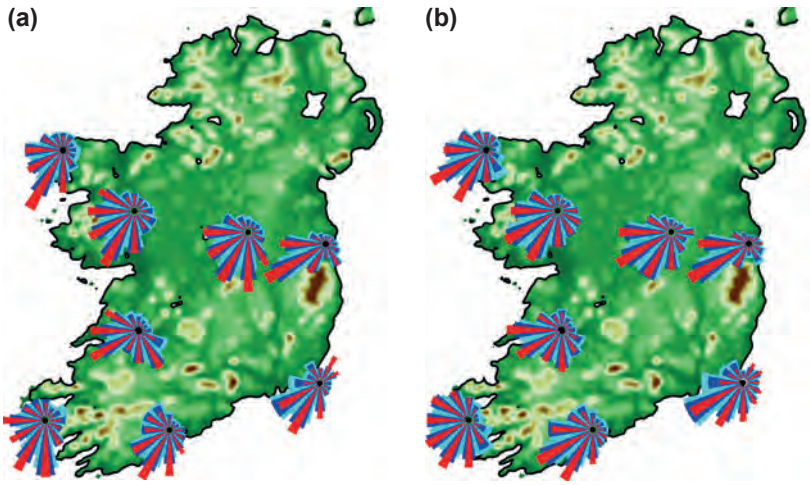

Figure 4.14. Autumn 10-m wind power roses at eight Met Éireann synoptic stations spanning Ireland. (a) Observed data; (b) CLM4–EC-Earth 4-km data.

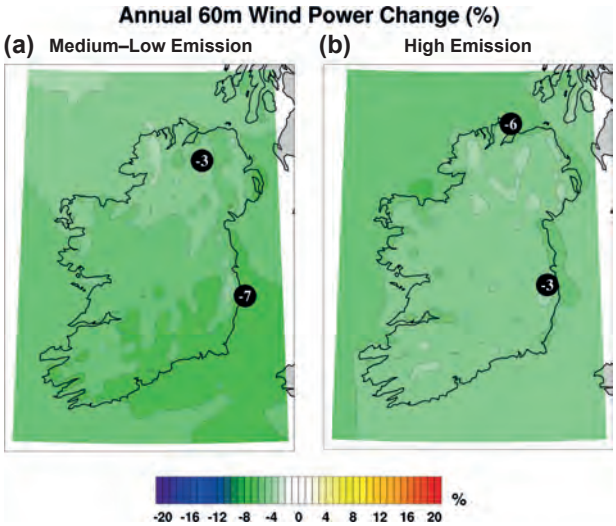

Figure 4.15. Ensemble projected change (%) in annual 60-m mean wind power. (a) Medium- to low-emission scenario; (b) high-emission scenario. In each case, the future period 2041–2060 is compared with the past period 1981–2000. The numbers included on each plot are the minimum and maximum changes, displayed at their locations.

medium- to low-emission ensemble and 3–6% for the high-emission ensemble.

Figure 4.16a presents the seasonal change (%) in the energy content of the 60-m wind under the medium- to low-emission scenario, with the corresponding plots for high emissions presented in Figure 4.16b. The strongest signals are a projected decrease for summer, with the largest impacts for the high-emission scenario. The summer reductions range from 4% to 12% for the

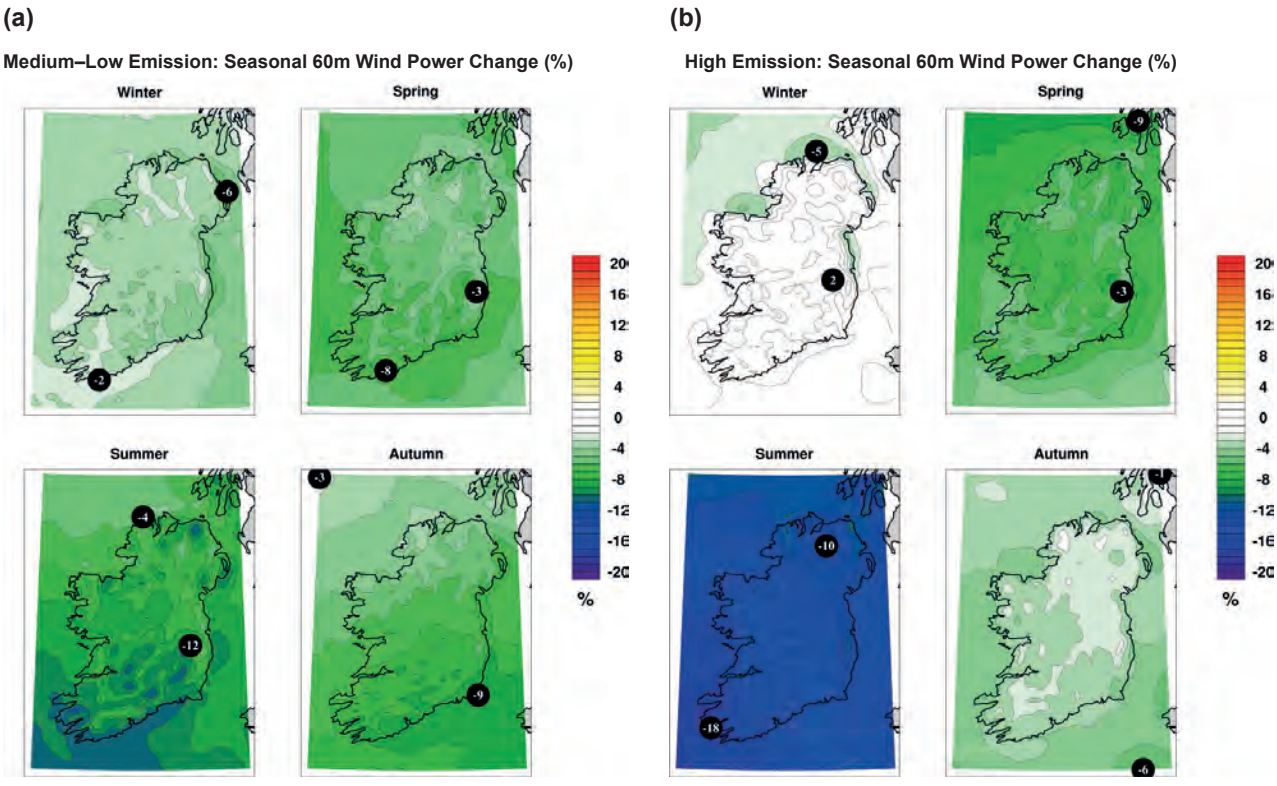

Figure 4.16. Projected changes (%) in seasonal 60-m mean wind power. (a) Medium- to low-emission scenario; (b) high-emission scenario. In each case, the future period 2041–2060 is compared with the past period 1981–2000.

medium- to low-emission scenario and from 10% to 18% for the high-emission scenario. The spring months are also projected to have less available wind power, with decreases ranging from 3% to 8% and from 3% to 9% for the medium- to low-emission and high-emission scenarios, respectively. For autumn, a projected decrease of 3–9% is noted for the medium- to low-emission scenario, while the signal for the high-emission ensemble is small. The annual, spring, summer and autumn projected decreases are analysed in more detail in section 4.3.2.

The signals for winter (both emission scenarios) and autumn (high-emission scenario) are less robust. A small projected increase in the 60-m mean cube wind speed is noted for winter over most of Ireland for the high-emission scenario. Small reductions are noted for autumn (high emission) and winter (medium to low emission). However, the projections for autumn and winter exhibit great uncertainty, as reflected in a large spread between the individual ensemble members (not shown here). The projections of the 60-m energy content of the wind for winter (both emission scenarios) and autumn (high emission) should therefore be viewed with a low level of confidence.

The wind projections vary greatly between ensemble members, much more so than for the temperature projections. This can result in large individual outliners skewing the mean ensemble projection. For this reason, we consider the "likelihood" projections below. Recall from Chapter 1 that a "very likely" projection is defined as one in which over 90% of the ensemble members agree. Similarly, a "likely" projection is defined as one in which over 66% of the ensemble members agree.

4.3.2 Robust 60-m wind power projections (annual, spring, summer and autumn)

Figure 4.17 presents the "likely" annual and spring mean 60-m wind power projections. The figures indicate reductions are "likely" to occur over most of the country for the future spring months and over the full year by mid-century. The reductions are small for the high-emission annual data but are more prominent for the other simulations, with values ranging from to 0% to 5% (annual, medium to low emission) and from 0% to 6% (spring, both scenarios). It follows it is "likely" that decreases in annual and spring 60-m wind power will be greater than or equal to these values. Robust projections were also noted for autumn for the medium- to low-emission ensemble, with "likely" reductions ranging from 1% to 9% (not shown). Figure 4.18a shows that the projected summer reductions are larger, with "likely" values ranging from 3% to 10% and from 7% to 15% for the medium- to low-emission and high-emission scenarios, respectively. It follows it is "likely" that decreases in summer 60-m mean wind power will be greater than or equal to these values. The "very likely" summer projections, presented in Figure 4.18b, show that over 90% of the ensemble members project a reduction over most of the country, with values ranging from ~0% to 6% and from 3% to 9% for the medium- to low-emission and high-emission scenarios, respectively. Note that the accuracy of these statistical descriptions is based on

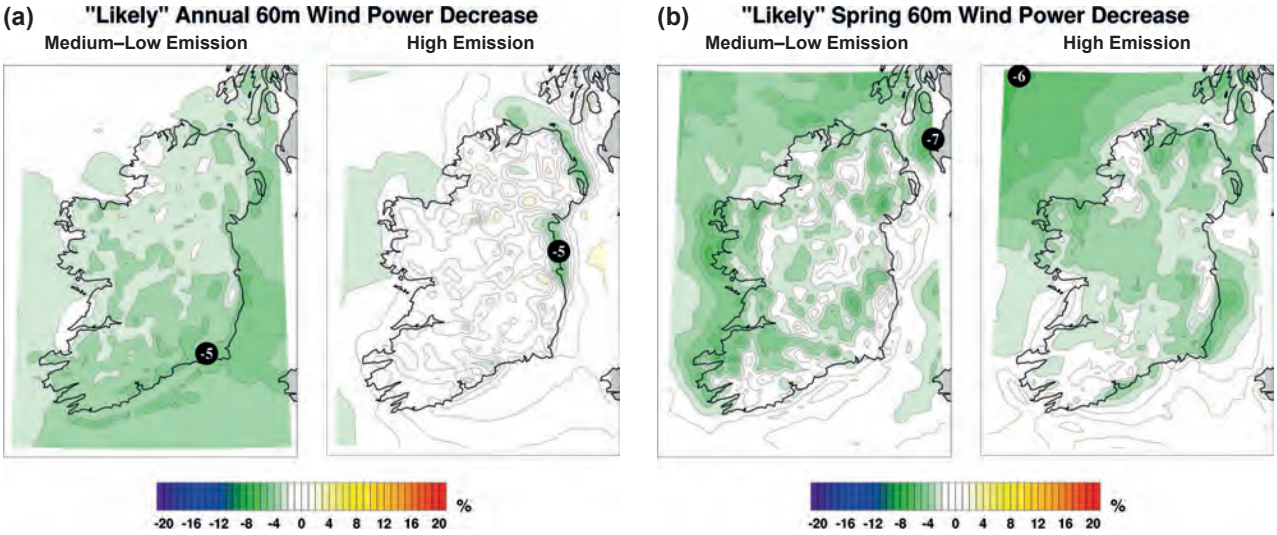

Figure 4.17. "Likely" decrease in 60-m mean wind power. (a) Annual; (b) spring. In each case, the future period 2041–2060 is compared with the past period 1981–2000.

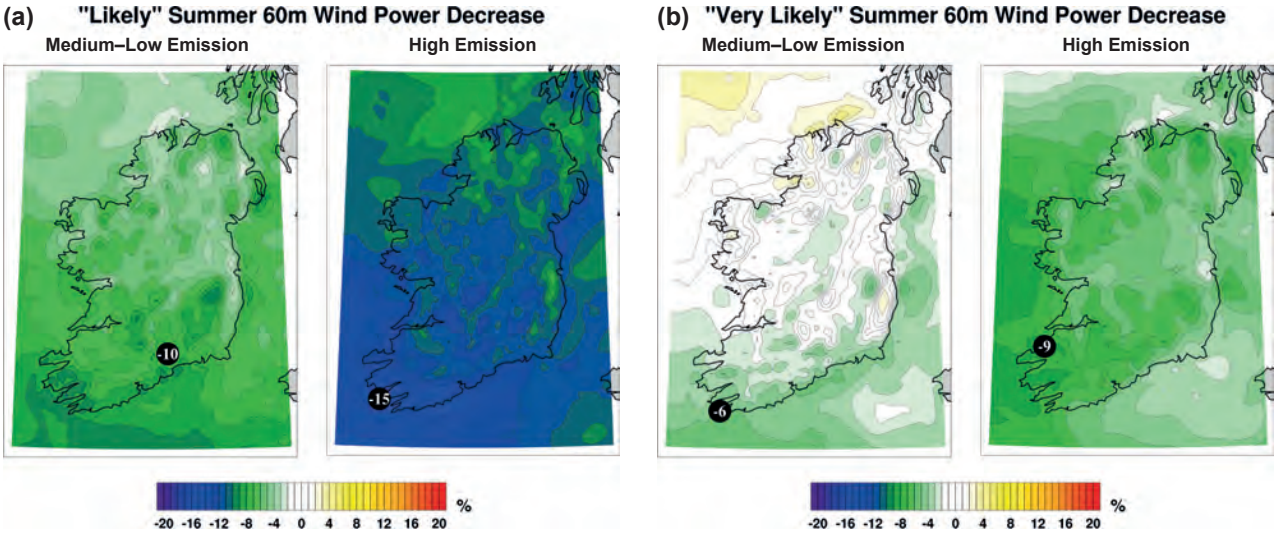

Figure 4.18. Projected decrease in summer 60-m mean wind power. (a) "Likely"; (b) "very likely". In each case, the future period 2041–2060 is compared with the past period 1981–2000.

the assumption that the ensemble members represent an unbiased sampling of the (unknown) future climate.

4.3.3 Projected changes in monthly/diurnal 60-m wind power

Figure 4.19 presents a contour plot of the diurnal cycle of mean cube 60-m wind speed per month, over all grid points covering Ireland and, for the purpose of offshore wind farm research, a small portion of the surrounding sea. The ensembles of past and future high-emission simulations are presented in Figure 4.19a and 4.19b, respectively. The 60-m energy content of the wind is at a maximum during the middle of the day in winter and minimum during the night in summer. The percentage difference is presented in Figure 4.19c. Small increases are noted during October, December and February, with no obvious diurnal trend. However, as noted in section 4.3.1, there is low confidence in the projections for winter (both scenarios) and autumn (high-emission scenario). The largest projected decreases are noted during July and August, particularly during the afternoon. There is high confidence in the summer and spring projections, as outlined in section 4.3.2. The medium- to low-emission projections were found to have a similar, but weaker, signal.

4.3.4 Projected changes in 60-m wind direction

Since wind farms are designed and constructed to make optimal use of the prevailing wind direction, it is important to assess the potential effects of climate change on future wind directions over Ireland. Figure 4.20 presents 60-m wind roses at Arklow wind farm and various locations spanning Ireland for (a) the past winter ensemble of control runs (1981–2000), (b) the winter ensemble of high-emission future simulations, (c) the past summer ensemble of control runs and (d) the summer ensemble of high-emission future simulations. Although changes in wind speed are projected, the general wind directions do not change substantially. For the winter months, a small increase in south-westerly winds is noted. For the summer months, the wind directions show only minor changes. Given that near-surface wind speeds are strongly influenced by the local topography, it is not surprising that the projected change in wind directions is small.

Figure 4.21 shows 60-m wind power roses at Arklow wind farm and various locations spanning Ireland for (a) the past winter ensemble of control runs (1981–2000), (b) the winter ensemble of high-emission future simulations, (c) the past summer ensemble of control runs and (d) the summer ensemble of high-emission future simulations. Again, small changes in the 60-m wind power roses are projected.

The wind rose analysis was repeated for the medium- to low-emission simulations and results were found to be similar. In addition, projections for spring and autumn showed small changes for both scenarios (not shown).

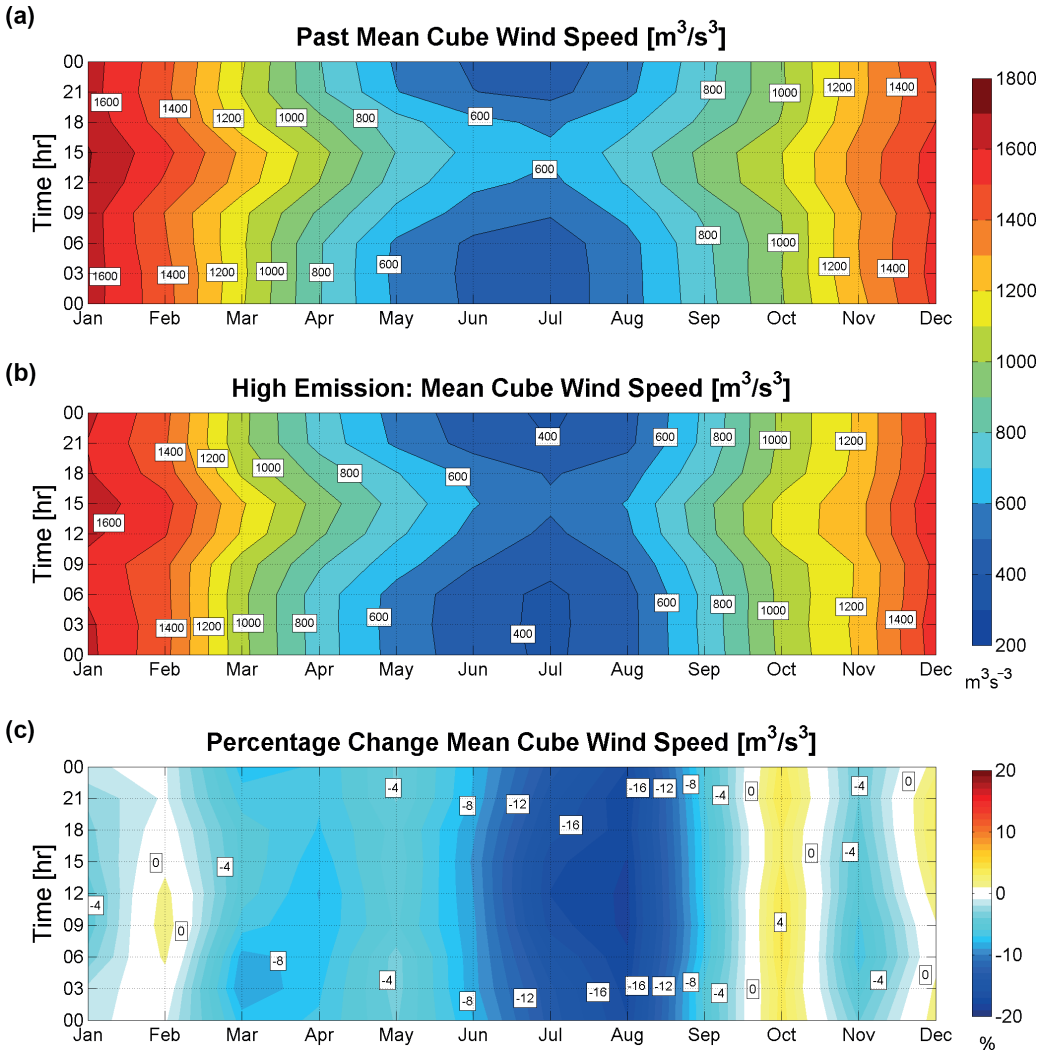

Figure 4.19. Annual diurnal 60-m mean cubed wind speed over Ireland and a small portion of the surrounding sea. (a) Ensemble of past simulations, 1981–2000; (b) ensemble of high-emission future simulations, 2041–2060; (c) projected percentage change.

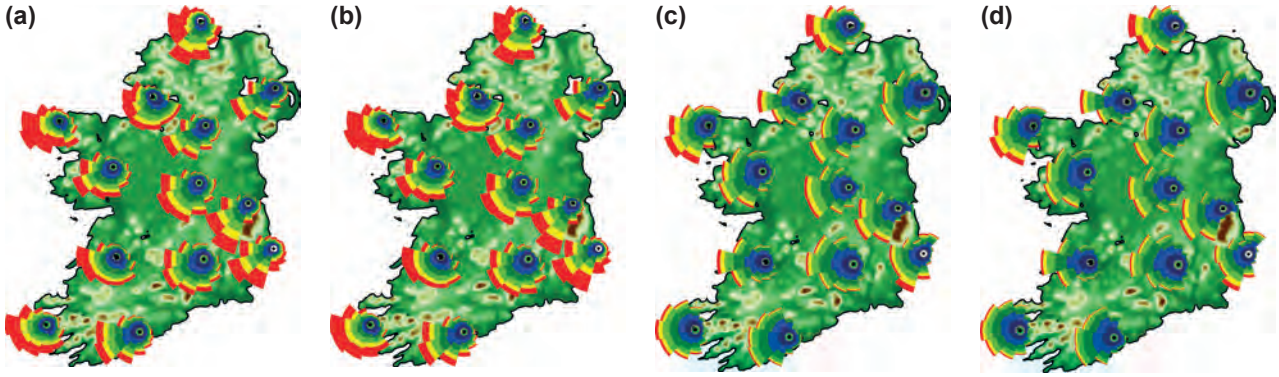

Figure 4.20. Wind roses at 60-m at various locations spanning Ireland. (a) Winter ensemble of past simulations, 1981–2000; (b) winter ensemble of high-emission future simulations, 2041–2060; (c) summer ensemble of past simulations, 1981–2000; (d) summer ensemble of high-emission future simulations, 2041–2060.

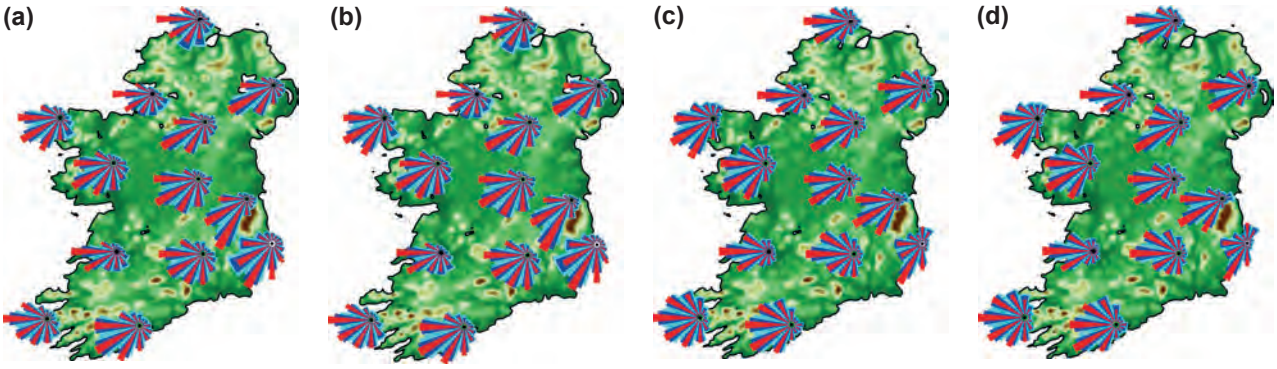

Figure 4.21. Wind power roses at 60-m at various locations spanning Ireland. (a) Winter ensemble of past simulations, 1981–2000; (b) winter ensemble of high-emission future simulations, 2041–2060; (c) summer ensemble of past simulations, 1981–2000; (d) summer ensemble of high-emission future simulations, 2041–2060.

4.3.5 Changes in the shape of the future 60-m wind speed distribution

In addition to projected changes in the mean wind speed and power, changes in the variability of the wind speed and the shape of the wind speed distribution are important for energy applications. The distribution of a quantity involving discrete data (as here) can be represented by its empirical density function. Figure 4.22 presents the seasonal density functions (hereafter, density) of daily mean 60-m wind speed anomalies, at every grid point over Ireland. For each past simulation, the anomalies are calculated by subtracting the mean wind speed over the 20-year period 1981–2000 from the mean daily wind speed values.[5] Similarly, the future daily anomalies (2041–2060) are calculated by subtracting the historical mean wind speed (1981–2000) from each future ensemble member within the same group (see Table 1.2).

The density of the past period is shown in black, with the densities of the medium- to low-emission and high-emission scenarios in blue and red, respectively. An *overlap score* was calculated which assesses the similarity between the group's past and future (adapted from a process in Perkins et al., 2007; see section 2.3.3 of the present report for a mathematical description). This score is between 0% and 100%, with 100% indicating perfect agreement (climate completely unchanged) and 0% indicating no agreement (past and future climates have no values in common).

5 This results in two slightly different past densities (corresponding to the two future emission scenario groups). As differences were found to be very small, the medium- to low-emission past densities are excluded from Figures 4.22 and 4.25.

With the exception of summer, Figure 4.22 shows only small changes in the projected 60-m daily mean wind speed distributions. The annual distributions also show small projected changes (not shown). The future summer distributions show a definite decrease in mean values (vertical lines) and a decrease in the right side of the distribution tail, strengthening the evidence from all previous analyses of large projected deductions in wind power during summer. The overlap scores range from 95% in summer (showing the largest changes across the distribution) to 97–99% for all other seasons (showing the least change between historical and future densities). Although the projected annual, spring and autumn wind speed distributions show small changes, this can translate to relatively large changes in wind power, as is evident from Figures 4.15 and 4.16.

Figures 4.23 and 4.24 show small projected changes in the standard deviation of daily mean 60-m wind speed for all seasons and the full year, respectively. The largest decreases are projected for summer, with values ranging from ~1% to 5% for the high-emission scenario. This is consistent with the relatively large projected changes in the summer wind speed distributions (Figure 4.22c).

4.3.6 Potential changes in extreme wind speeds

Figure 4.23 shows projected increases in the standard deviation (spread) of daily mean 60-m wind speed over most of Ireland during winter by mid-century. In addition, the winter 60-m mean wind speed shows small projected changes (~1%, not shown). This projected small change in the mean, coupled with an increase in the spread of wind speed, suggests an increase in high (and low) wind speeds during future

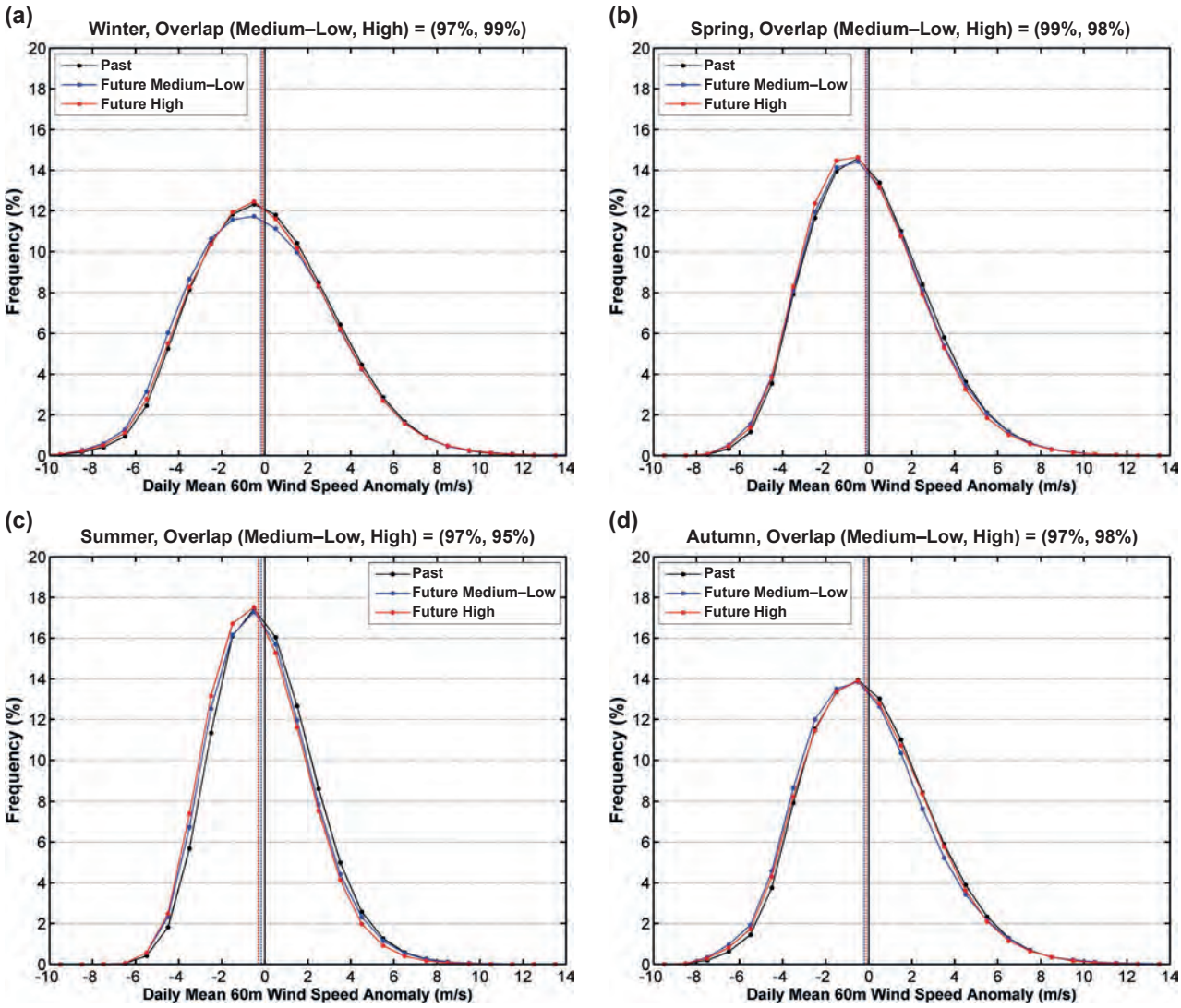

Figure 4.22. Empirical density functions illustrating the distribution of past (black), medium- to low-emission (blue) and high-emission (red) 60-m daily mean wind speed over Ireland. (a) Winter; (b) spring; (c) summer; (d) autumn. Each dataset has a size greater than 80 million. The distributions are created using histogram bins of size 1 m/s. A measure of overlap indicates how much the future distributions have changed relative to the past (0% indicating no common area, 100% indicating complete agreement). Means are shown for historical (black vertical line), medium- to low-emission (blue vertical line) and high-emission (red vertical line) densities.

winters. This is confirmed by Figure 4.25a, the winter daily maximum 60-m wind speed anomaly distribution, which shows increases in extreme wind speeds for both ensemble scenarios. A similar signal is evident for the annual maximum daily wind speed distribution (Figure 4.25b).

To further quantify the projected change in extreme wind speeds, the percentage change in the top 1% of 60-m winds was calculated for the medium- to low-emission and high-emission scenarios. Results show small projected increases in extreme wind speeds over Ireland by mid-century. The signal is strongest for the high-emission ensemble, with the majority of the simulations showing an increase of 3–4% in extreme wind speeds over the south and east of Ireland by mid-century (not shown).

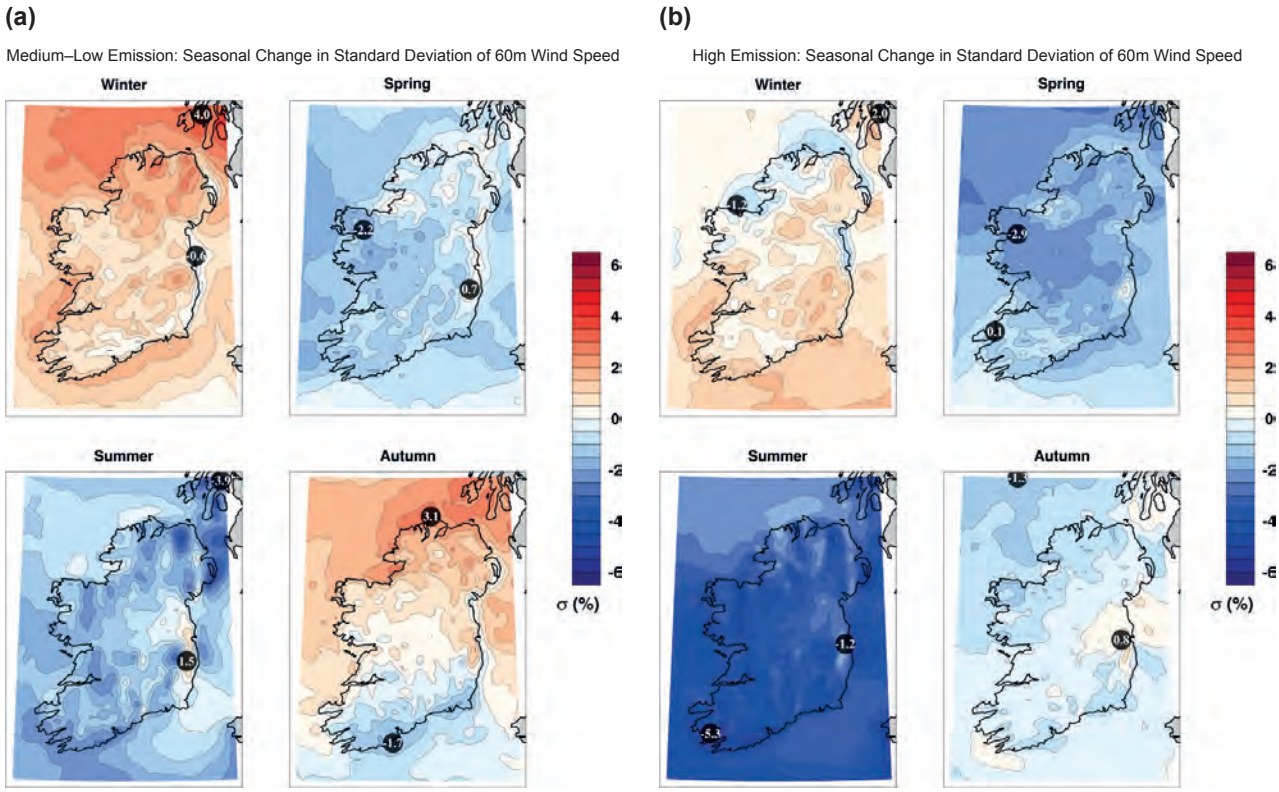

Figure 4.23. Seasonal projected changes (%) in the standard deviation of daily mean 60-m wind speed. (a) Medium- to low-emission ensemble; (b) high-emission ensemble. In each case, the future period 2041–2060 is compared with the past period 1981–2000. The numbers included on each plot are the minimum and maximum projected change, displayed at their locations.

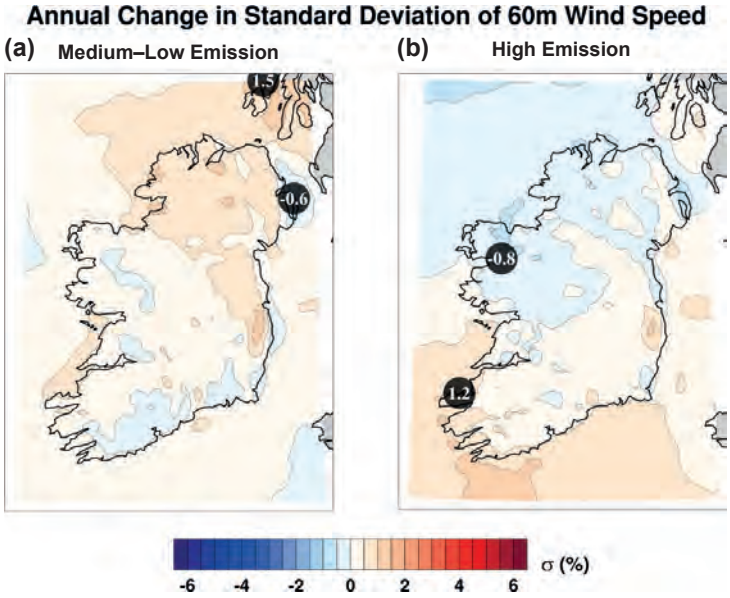

Figure 4.24. Annual projected changes (%) in the standard deviation of daily mean 60m wind speed. (a) Medium- to low-emission ensemble; (b) high-emission ensemble. In each case, the future period 2041–2060 is compared with the past period 1981–2000. The numbers included on each plot are the minimum and maximum projected change, displayed at their locations.

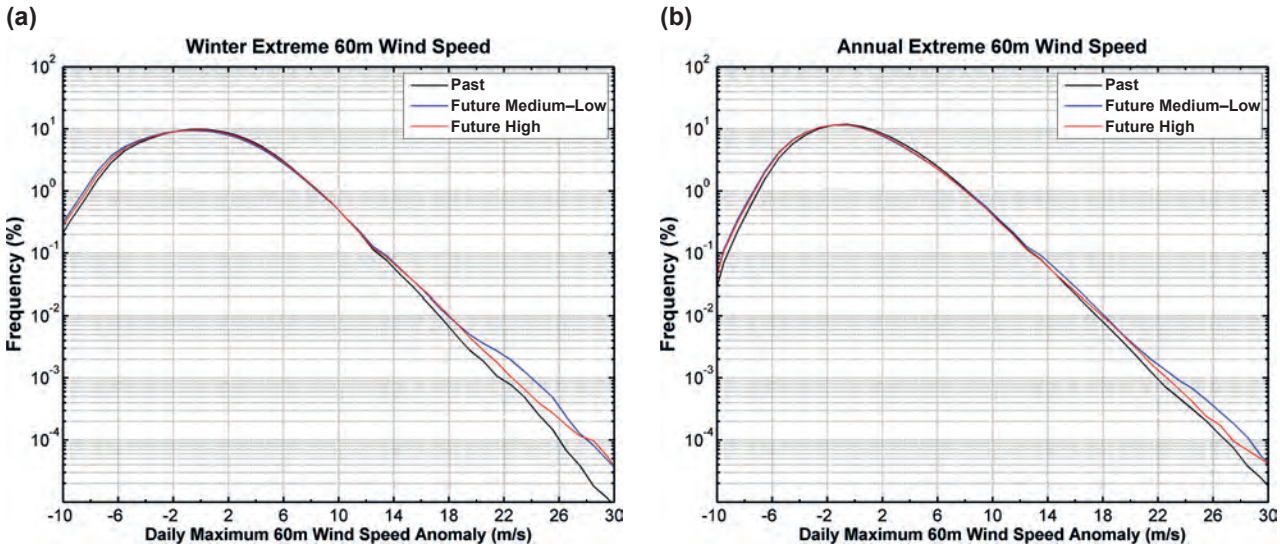

Figure 4.25. Empirical density functions illustrating the distribution of past (black), medium- to low-emission (blue) and high-emission (red) 60-m daily maximum wind speeds over Ireland. (a) Winter; (b) annual. The frequency is displayed on a log scale. Each dataset has a size greater than 80 million. The distributions are created using histogram bins of size 1 m/s.

4.3.7 Statistical significance of wind speed and wind power changes

The statistical significance of changes in the daily mean 60-m wind speed distributions of Figure 4.22 was tested against Ha_0 as outlined in Chapter 1. Here, the alternative hypothesis states that the future distributions (Kolmogorov–Smirnov) or the future median values (Wilcoxon rank-sum) are different from the past. Both the Kolmogorov–Smirnov and Wilcoxon rank-sum tests show high level of significance ($p \approx 0$) for the medium- to low-emission and high-emission scenarios across all seasons. We therefore conclude the projected changes in the future 60-m wind speed distributions and medians are statistically significant.

The statistical significance of changes in the cube wind speed was also analysed. The Wilcoxon rank-sum Ha_1 test determined that the projected decreases for spring, summer and autumn (see sections 4.3.1 and 4.3.2) are statistically significant ($p < 0.001$) for both the medium- to low-emission and high-emission scenarios. The Ha_2 Wilcoxon rank-sum test determined that the projected increase during winter for the high-emission scenario (see Figure 4.16b) is not statistically significant at the 95% confidence level.

4.4 Projected changes in extreme storm tracks and mean sea-level pressure

Given the large societal impacts of extreme storms, there is considerable interest in the potential impact of climate change on extreme cyclonic activity in the North Atlantic. In addition to the potential widespread flooding and structural damage associated with intense storms, the wind energy supply can be negatively affected, as wind turbines are shut down during periods of high wind speeds to prevent damage. An algorithm was developed to identify and track cyclones as simulated by the RCMs.

4.4.1 Storm-tracking algorithm

The simulated MSLP values of the RCMs are output onto a horizontal grid of size $N_x \times N_y$. For example, the WRF 18-km domain size is 189 × 204 (see Figure 1.1). A surface grid point (i, j) is identified as a low-pressure centre if the following criteria are met:

- The MSLP value, $p(i, j)$, is less than a given threshold, τ, e.g. 940 hPa.
- The point is a local minimum of MSLP.

A point (i, j) is defined as a local minimum if $p(i, j)$ is less than the MSLP values of all 80 surrounding grid points (Figure 4.26). Since for each point we examine the 80

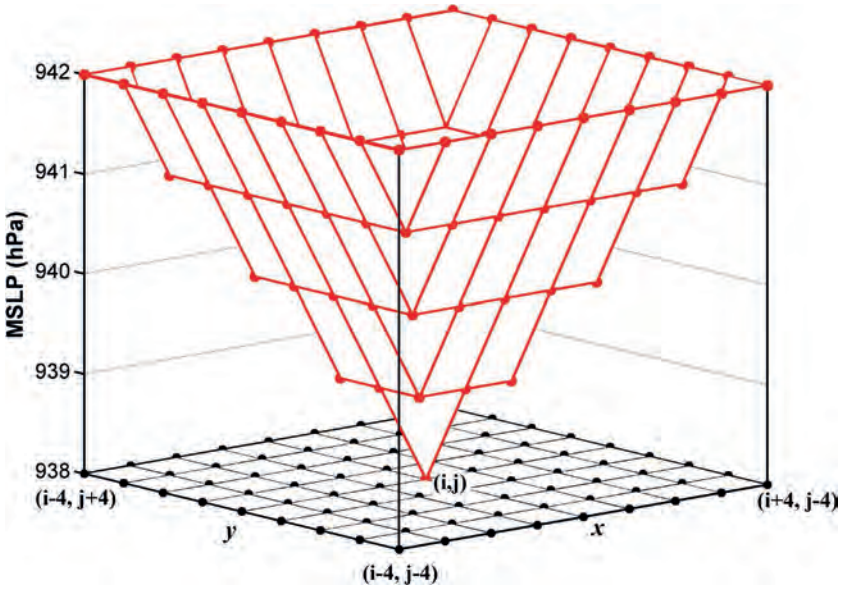

Figure 4.26. Location of a local MSLP minimum. Here the point (*i*, *j*) is defined as a low-pressure centre, since all MSLP values of the surrounding 80 grid points are greater than $p(i, j) = 938$ hPa.

surrounding grid points, the model domain boundaries ($i = 1$ or N_x, $j = 1$ or N_y) and the three nearest points to the boundaries are not considered for the storm-tracking analysis.

For example, a grid point is defined as a cyclone centre if $p(i, j) < \tau$ and

$p(i, j) < p(i+k, j+l)$, $\forall k, l \in \{-4, \ldots +4\}$ (k and l not both 0)

where $4 < i < N_x - 3$ and $4 < j < N_y - 3$.

To track the movement of the cyclones, the centres are located at output times t and $t+3$ hours. A cyclone at time t is considered to be the same cyclone identified at time $t+3$ hours if the estimated speed of movement, based on the great circle distance between the positions, is less than 120 km/hour.

The storm-tracking analysis focuses on the AR5 RCP scenario simulations as outlined in Table 4.1. To examine the potential impact of climate change on intense storms, only cyclones with core MSLP less than 940 hPa are considered. In addition, only cyclones that exist for at least 12 hours are considered.

4.4.2 Extreme storm track projections

The past (1981–2000) and future (2041–2060) RCP8.5 ensemble storm tracks, as simulated by the RCM 18-km resolution simulations, are presented in Figure 4.27. The simulations show that the tracks of intense storms are projected to extend further south than those in the reference simulation. This is confirmed by the RCM 50-km simulation data, as presented in Figure 4.28. The analysis was repeated for the RCP4.5 emission simulations, and projections of future intense storm tracks were found to have a similar, but weaker, signal. The majority of the extreme storm events were found to occur during the winter months for both the past and future simulations.

Table 4.1. The RCM simulations used for the storm tracking and MSLP analysis

Period/scenario	Ensemble members
Past 1981–2000	CLM4–EC-Earth, mei1, mei2, mei3 WRF–EC-Earth, mei1, mei2, mei3 CLM4-HadGEM2-ES
Future RCP4.5 2041–2060	CLM4–EC-Earth, me41, me42, me43 WRF–EC-Earth, me41, me42, me43 CLM4-HadGEM2-ES, RCP4.5
Future RCP8.5 2041–2060	CLM4–EC-Earth, me81, me82, me83 WRF–EC-Earth, me81, me82, me83 CLM4-HadGEM2-ES, RCP8.5

(a) Past storm tracks, 1981–2000, MSLP < 940 hPa, RCM 18-km resolution

(b) RCP8.5 storm tracks, 2041–2060, MSLP < 940 hPa, RCM 18-km resolution

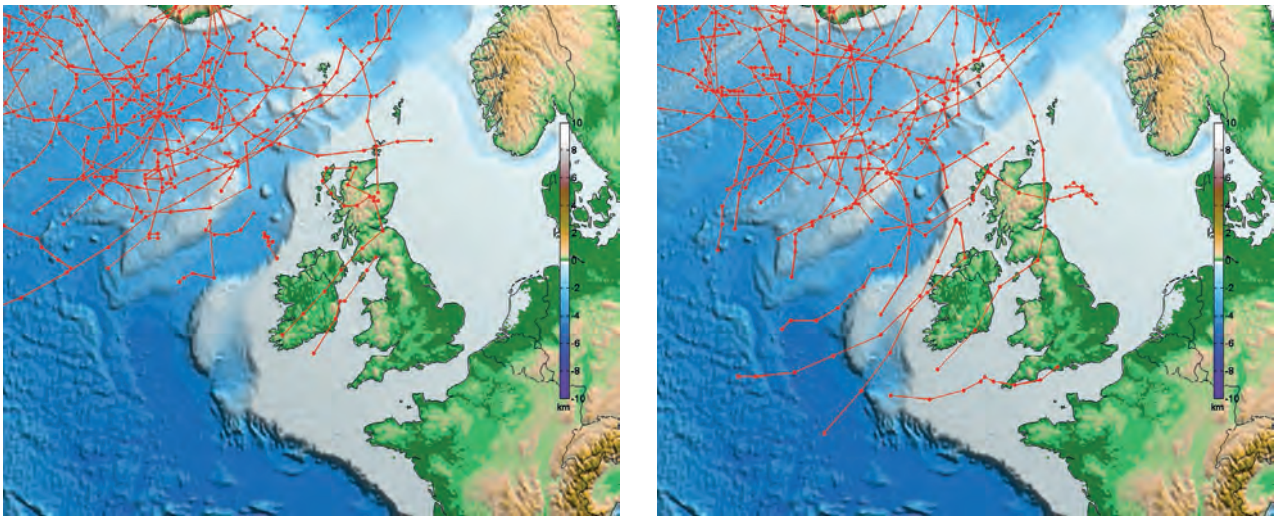

Figure 4.27. Tracks of storms with a core MSLP of less than 940 hPa and with a lifetime of at least 12 hours. (a) Past RCM 18-km simulations (1981–2000); (b) RCP8.5 RCM 18-km simulations (2041–2060).

(a) Past storm tracks, 1981–2000, MSLP < 940 hPa, RCM 50-km resolution

(b) RCP8.5 storm tracks, 2041–2060, MSLP < 940 hPa, RCM 50-km resolution

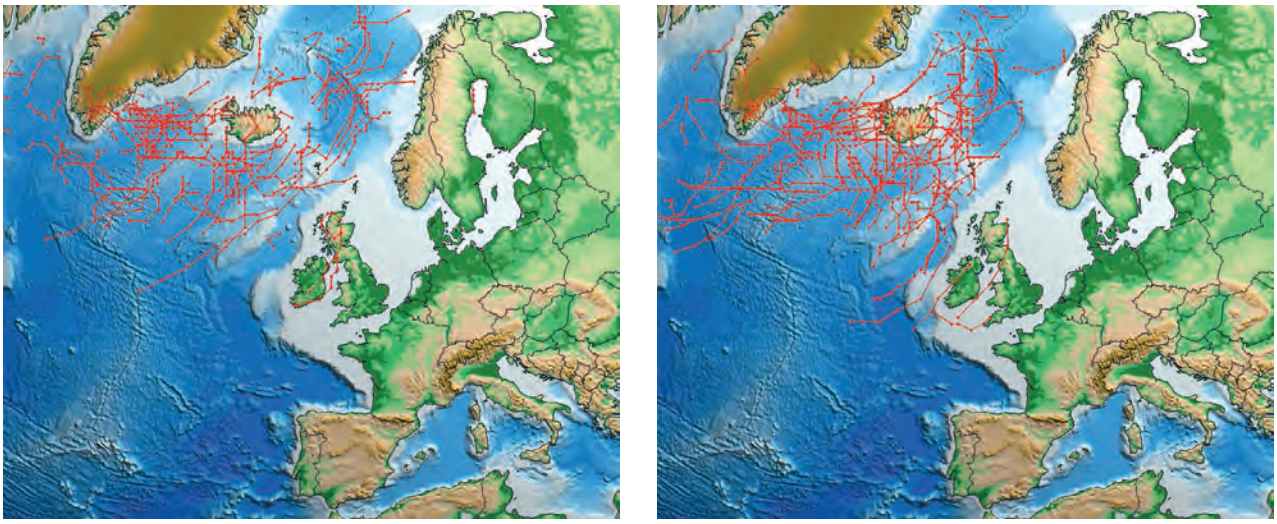

Figure 4.28. Tracks of storms with a core MSLP of less than 940 hPa and with a lifetime of at least 12 hours. (a) Past RCM 50-km simulations (1981–2000); (b) RCP8.5 RCM 50-km simulations (2041–2060).[1]

1 Topographical mapping software from Bezdek and Sebera (2013).

It should be noted that extreme storms, as presented in Figures 4.27 and 4.28, are rare events. Therefore, the storm projections should be considered with a level of caution. Future work will focus on analysing a larger ensemble, thus allowing a robust statistical analysis of extreme storm track projections.

4.4.3 Projections of mean sea-level pressure

While the results of section 4.4.2 show a projected increase in intense storms affecting Ireland by mid-century, the overall number of cyclones is projected to decrease. For example, the number of cyclones with

core MSLP of 980 hPa is projected to decrease by approximately 10% for both emission scenarios (not shown). This result is consistent with Figure 4.29, which presents the average MSLP calculated over the 20-year past (1981–2000) and future (2041–2060) periods. Again, the MSLP analysis focuses on the AR5 RCP scenario simulations as outlined in Table 4.1.

It is noted that the future simulations project an increase in MSLP of approximately 2 hPa over Ireland by mid-century. The increase is slightly more pronounced for the RCP8.5 projections. This result is robust, as is evident from the "likely" projections of Figure 4.30. The figures indicate that over 66% of the ensemble members project an increase of at least ~1.2 hPa (RCP4.5) and ~1.6 hPa (RCP8.5) over Ireland by mid-century. Similarly, the "likely" MSLP projections for winter, spring, summer and autumn are presented in Figures 4.31, 4.32, 4.33 and 4.34, respectively. The "likely" projected increases in average MSLP range from ~0.6 hPa (winter, RCP4.5) to ~2.2 hPa (summer, RCP8.5).

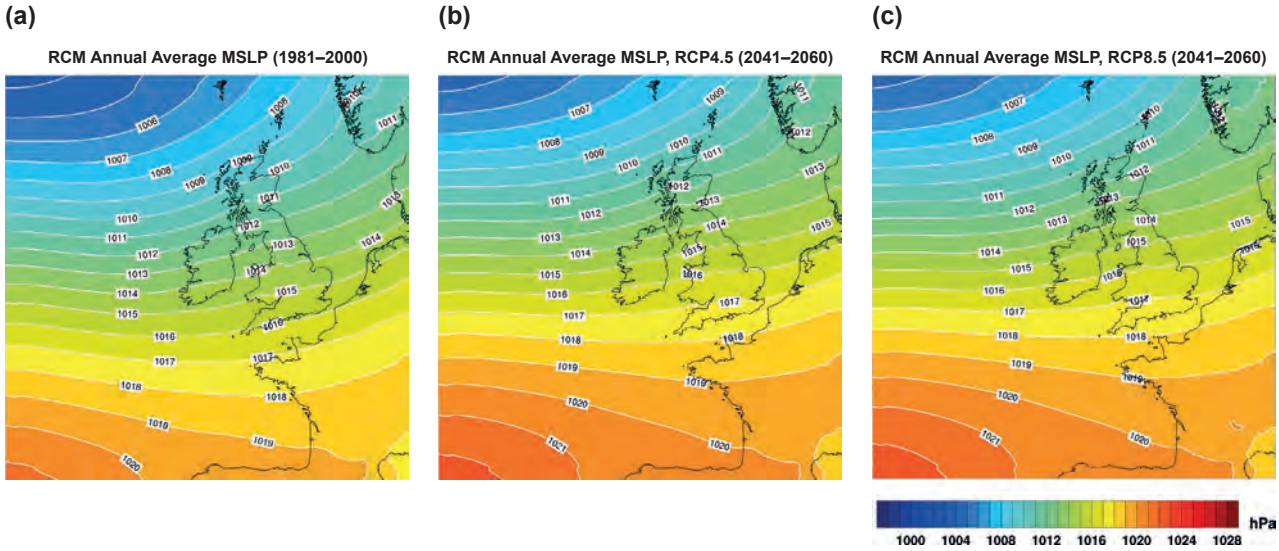

Figure 4.29. RCM average MSLP. (a) Past simulations (1981–2000); (b) RCP4.5 simulations (2041–2060); (c) RCP8.5 simulations (2041–2060).

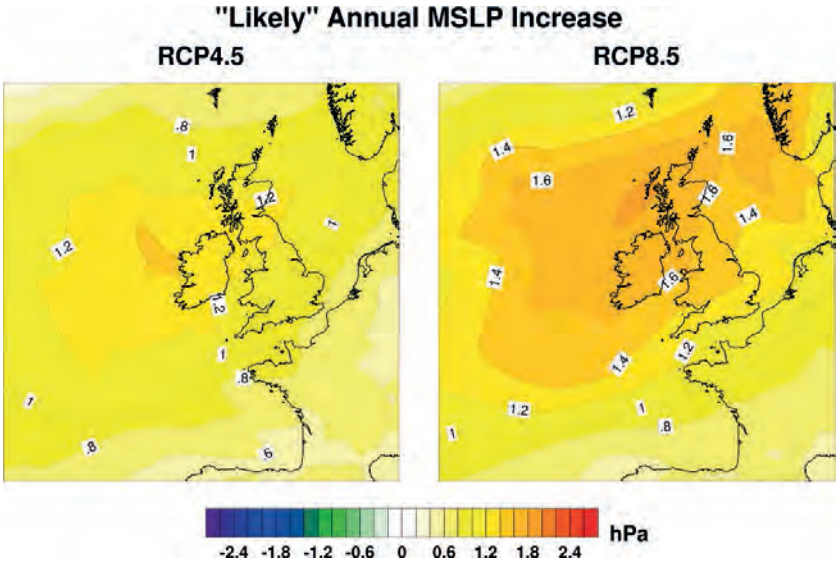

Figure 4.30. The "likely" increase in annual average MSLP for the RCP4.5 and RCP8.5 simulations. In each case, the future period 2041–2060 is compared with the past period 1981–2000.

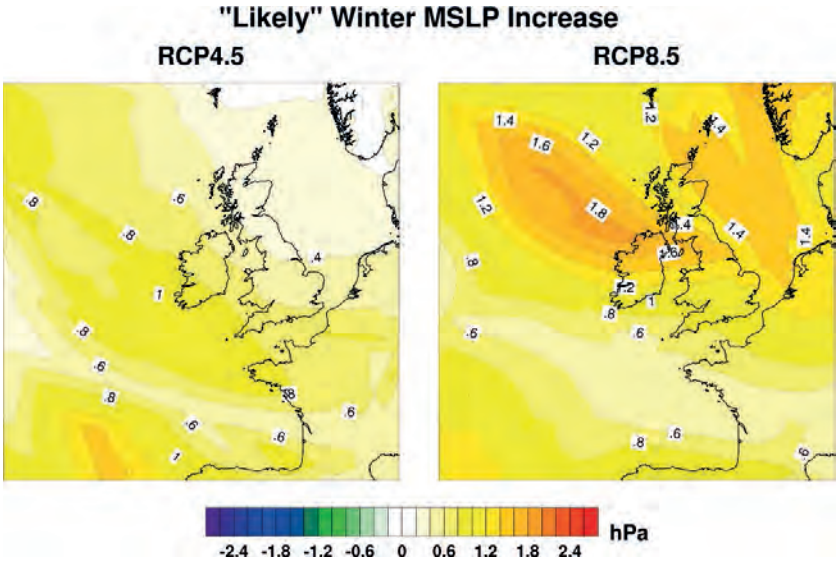

Figure 4.31. The "likely" increase in winter average MSLP for the RCP4.5 and RCP8.5 simulations. In each case, the future period 2041–2060 is compared with the past period 1981–2000.

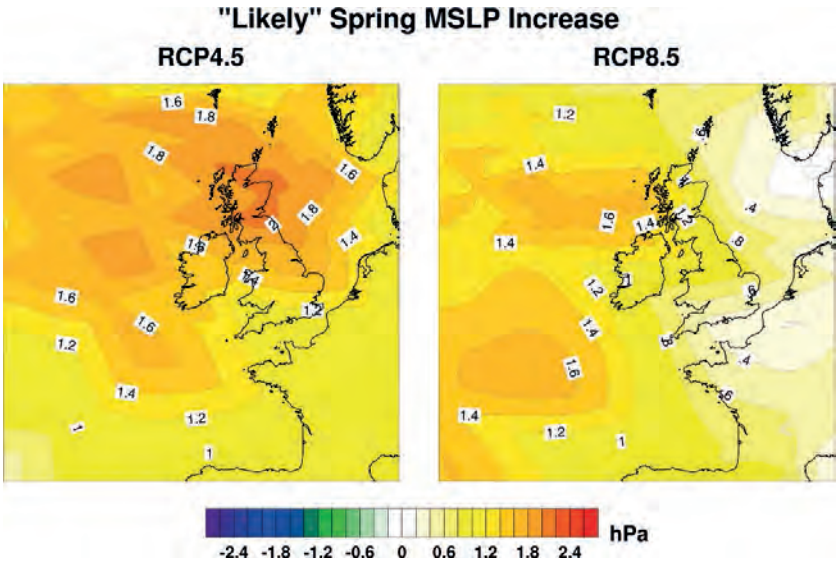

Figure 4.32. The "likely" increase in spring average MSLP for the RCP4.5 and RCP8.5 simulations. In each case, the future period 2041–2060 is compared with the past period 1981–2000.

4.5 Conclusions

The impact of simulated global climate change on the wind energy resource of Ireland was assessed using the method of regional climate modelling. In view of unavoidable errors due to model (regional and global) imperfections, and the inherent limitation on predictability of the atmosphere arising from its chaotic nature, isolated predictions are of very limited value. To address this issue of model uncertainty, an ensemble of RCMs was run. The RCMs were run at high spatial resolution, up to 4 km, thus allowing a better assessment of the local effects of climate change on the wind energy resource of Ireland.

The RCMs were validated using 20-year simulations of the past Irish climate (1981–2000), driven by both ECMWF ERA-40 global re-analysis and the GCM datasets and comparing the output against observational data. Extensive validations were carried out to test the ability of the RCMs to accurately model the wind climate of Ireland. Results confirm that the outputs of the RCMs exhibit reasonable and realistic features as documented in the historical data record.

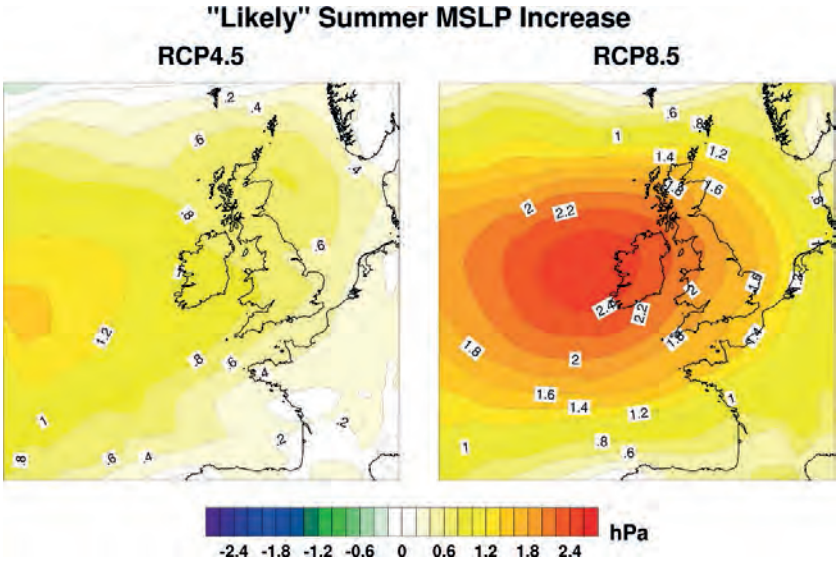

Figure 4.33. The "likely" increase in summer average MSLP for the RCP4.5 and RCP8.5 simulations. In each case, the future period 2041–2060 is compared with the past period 1981–2000.

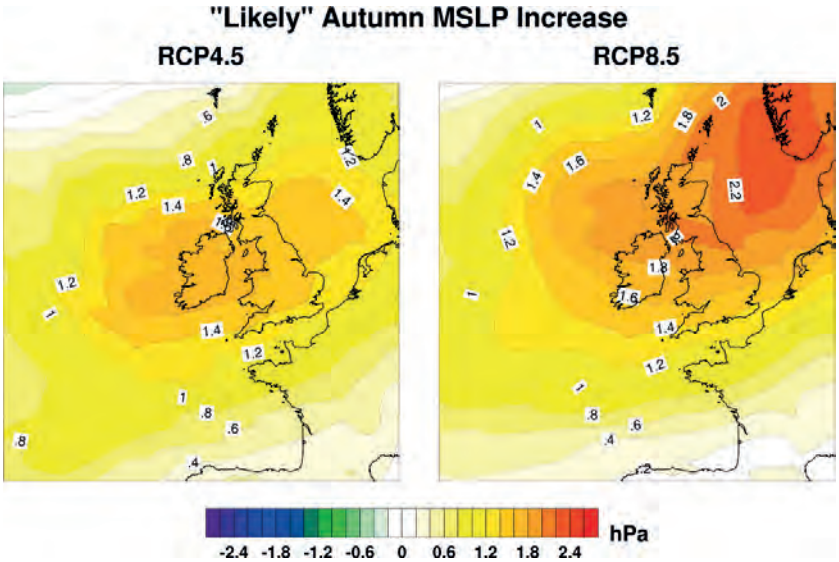

Figure 4.34. The "likely" increase in autumn average MSLP for the RCP4.5 and RCP8.5 simulations. In each case, the future period 2041–2060 is compared with the past period 1981–2000.

The future climate was simulated using both medium- to low-emission and high-emission scenarios. The future period 2041–2060 was compared with the past period 1981–2000. Results for both scenarios show significant projected decreases in the energy content of the wind over the entire year and during the spring and summer months, by mid-century. The medium- to low-emission simulations show a significant projected decrease during autumn. The projected decreases are largest for summer, with "likely" values ranging from 3% to 10% for the medium- to low-emission scenario and from 7% to 15% for the high-emission scenario. The projected decreases are robust, as the majority of the ensemble members are in agreement for both the medium- to low-emission and high-emission scenarios, thus increasing the confidence in the projections. Projected increases for winter were found to be statistically insignificant. Small increases in extreme wind speeds are projected over Ireland by mid-century. Projections of wind direction show no substantial change.

The research consolidates and expands on the RCM projections of previous studies (McGrath and Lynch, 2008; Nolan et al., 2011, 2013, 2014) by increasing the ensemble size. This allows likelihood levels to be assigned to the projections. In addition, the uncertainties of the projections are more accurately quantified. The current study has shown that projected increases in the energy content of the wind during winter, as also noted by McGrath and Lynch (2008) and Nolan et al. (2011, 2013, 2014), exhibit great uncertainty, as reflected in a large spread between the individual ensemble members. The projections outlined in the current study agree with these previous studies in that they all show substantial decreases in the future wind energy resource during summer by mid-century.

To assess the potential impact of climate change on extreme cyclonic activity in the North Atlantic, an algorithm was developed to identify and track cyclones as simulated by the RCMs. Results indicate that, by mid-century, the tracks of intense storms are projected to extend further south over Ireland than those in the reference simulations. In contrast, the overall number of North Atlantic cyclones is projected to decrease by approximately 10%. The projected decrease in overall cyclone activity is consistent with the projected increase in average MSLP for all seasons by mid-century. A plausible explanation put forward for similar projections of cyclone activity (Semmier et al., 2008) is that a decreased meridional temperature gradient and the associated reduced baroclinicity in the future climate could be responsible for the decrease of the total number of cyclones (Geng and Sugi, 2003). Furthermore, the higher moisture supply due to a generally higher sea surface temperature and the related increase in latent heat fluxes could trigger strong-intensity cyclones (Hall et al., 1994). Future storm-tracking work will focus on analysing a larger ensemble, thus allowing a robust statistical analysis of extreme storm track projections.

The MSLP and storm-tracking results are among many possible factors that could be attributed to the wind projections of this study. The projected increase in MSLP will probably lead to a decrease in mean wind speed (and wind power) during summer, spring and autumn, when intense storms are rare. Furthermore, the projected increase in very intense storms is likely to be partially responsible for the projected increase in extreme wind speeds during winter. The mixed signal for projections of winter mean wind power may be attributed to an overall increase in MSLP, coupled with an increase in intense storm activity. However, further investigation of these factors is necessary to attribute causation to the wind projections of the current study. Future work will attempt to address this issue.

References

Atkinson, N., Harman, K., Lynn, M., Schwarz, A. and Tindal, A., 2006. Long-Term Wind Speed Trends in Northwestern Europe. Technical report. Garrad Hassan.

Bezdek, A. and Sebera, J., 2013. MATLAB script for 3D visualizing geodata on a rotating globe. Computers & Geosciences, 56, 127–130. Available online: http://dx.doi.org/10.1016/j.cageo.2013.03.007 (accessed 13 July 2015).

Cradden, L., Harrison, G. and Chick, J., 2012. Will climate change impact on wind power development in the UK? Climatic Change, 115, 837–852.

Department of Communications, Energy and Natural Resources, 2010. National Renewable Energy Action Plan, Ireland, 2010. Department of Communications, Energy and Natural Resources, Dublin. Available online: www.dcenr.gov.ie/NR/rdonlyres/C71495BB-DB3C-4FE9-A725–0C094FE19BCA/0/2010NREAP.pdf (accessed 13 July 2015).

Feser, F., Rockel, B., von Storch, H., Winterfeldt, J. and Zahn, M., 2011. Regional climate models add value to global model data: a review and selected examples. Bulletin of the American Meteorological Society, 92, 1181–1192.

Feser, F., Barcikowska, M., Krueger, O., Schenk, F., Weisse, R. and Xia, L., 2014. Storminess over the North Atlantic and northwestern Europe: a review. Quarterly Journal of the Royal Meteorology Society, 141, 350–382.

Geng, Q. and Sugi, M., 2003. Possible change of extratropical cyclone activity due to enhanced greenhouse gases and sulphate aerosols: study with a high-resolution AGCM. Journal of Climate, 16, 2262–2274.

Haarsma, R.J., Hazeleger, W., Severijns, C., de Vries, H., Sterl, A., Bintanja, B., van Oldenborgh, B.J. and van den Brink, H.W., 2013. More hurricanes to hit western Europe due to global warming. Geophysical Research Letters, 40, 1783–1788.

Hall, N.M.J., Hoskins, B.J., Valdes, P.J. and Senior, C.A., 1994. Storm tracks in a high resolution GCM with doubled carbon dioxide. Quarterly Journal of the Royal Meteorological Society, 120, 1209–1230.

Harrison, G.P., Cradden, L.C. and Chick, J.P., 2008. Preliminary assessment of climate change impacts on the UK onshore wind energy resource. Energy Sources, 30, 1286–1299.

Hueging, H., Haas, R., Born, K., Jacob, D. and Pinto, JG., 2013. Regional changes in wind energy potential over Europe using regional climate model ensemble projections. Journal of Applied Meteorology and Climatology, 52, 903–917.

Jimenez, P. and Dudhia, J., 2012. Improving the representation of resolved and unresolved topographic effects on surface wind in the WRF Model. Journal of Applied Meteorology and Climatology, 51, 300–316.

Kanamaru, H. and Kanamitsu, M., 2007. Fifty-seven-year California reanalysis downscaling at 10 km (CaRD10). Part II: Comparison with North American regional reanalysis. Journal of Climate, 20, 5572–5592.

McGrath, R. and Lynch, P. (eds), 2008. Ireland in a Warmer World: Scientific Predictions of the Irish Climate in the Twenty First Century. Met Éireann, Dublin.

Matthews, T., Murphy, C., Wilby, R.L. and Harrigan, S., 2014. Stormiest winter on record for Ireland and UK. Nature Climate Change, 4, 738–740.

Met Éireann, 2014. Winter Review 2013/2014. Available online: www.met.ie/climate/MonthlyWeather/clim-2014-win.pdf (accessed 13 July 2015).

Met Éireann, n.d. Winter 2013/2014. Available online: www.met.ie/climate-ireland/weather-events/WinterStorms13_14.pdf (accessed 13 July 2015).

Met Office, n.d. Winter 2013/2014. Available online: www.metoffice.gov.uk/climate/uk/summaries/2014/winter (accessed 13 July 2015).

Nolan, P., Gleeson, E. and McGrath, R, 2013. Impact of climate change on surface winds over Ireland. In Gleeson, E., McGrath, R. and Treanor, M. (eds), Ireland's Climate: The Road Ahead. Met Éireann, Dublin, pp. 71–76. Available online: www.met.ie/publications/IrelandsWeather-13092013.pdf (accessed 13 July 2015).

Nolan, P., Lynch, P. and Sweeney, C., 2014. Simulating the future wind energy resource of Ireland using the COSMO-CLM model. Wind Energy, 17, 19–37.

Nolan, P., Lynch, P., McGrath, R., Semmler, T. and Wang, S., 2011. Simulating climate change and its effects on the wind energy resource of Ireland. Wind Energy, 15, 593–608.

Perkins, S.E., Pitman, A.J., Holbrook, N.J. and McAneney, J., 2007. Evaluation of the AR4 climate models' simulated daily maximum temperature, minimum temperature, and precipitation over Australia using probability density functions. Journal of Climate, 20, 4356–4376.

Pryor, S.C. and Barthelmie, R.J., 2010. Climate change impacts on wind energy: a review. Renewable and Sustainable Energy Reviews, 14, 430–437.

Pryor, S.C., Barthelmie, R.J. and Kjellstrom, E., 2005. Analyses of the potential climate change impact on wind energy resources in northern Europe using output from a regional climate model. Climate Dynamics, 25, 815–835.

Pryor, S.C., Barthelmie, R.J., Clausen, N.E., Drews, M., MacKeller, N. and Kjellström, E., 2012. Analyses of possible changes in intense and extreme wind speeds over northern Europe under climate change scenarios. Climate Dynamics, 38, 189–208.

Semmler, T., Varghese, S., McGrath, R., Nolan, P., Wang, S., Lynch, P. and O'Dowd, C., 2008. Regional model simulation of North Atlantic cyclones: present climate and idealized response to increased sea surface temperature. Journal of Geophysical Research, 113, D02107.

Solomon, S., Qin, D., Manning, M., Chen, Z., Marquis, M., Averyt, K., Tignor, M.M.B. and Miller, H.L. Jr (eds), 2007. Climate Change 2007: The Physical Science Basis. Cambridge University Press, Cambridge.

Standen, J., Wilson, C. and Vosper, S., 2013. Remodelling the Irish national onshore and offshore wind atlas, Version 2.0. Technical Report, Met Office. Available online: www.seai.ie/Renewables/Wind_Energy/Wind_Maps/2013-Wind-Atlas-Project-Reports/CombinedReport_SEAI_part1.pdf (accessed 8 September 2015).

Sustainable Energy Authority of Ireland, 2014. Renewable Energy in Ireland 2012 www.seai.ie/Publications/Statistics_Publications/Renewable_Energy_in_Ireland/Renewable-Energy-in-Ireland-2012.pdf (accessed 13 July 2015).

Sustainable Energy Ireland, 2003. Wind Atlas 2003. Report No. 4Y103A-1-R1. Sustainable Energy Authority, Dublin. Available online: www.sei.ie/uploadedfiles/RenewableEnergy/IrelandWindAtlas2003.pdf (accessed 13 July 2015).

Troen, I. and Petersen, E.L., 1989. European Wind Atlas. Risø National Laboratory for the Commission of the European Communities, Roskilde.

Vautard, R., Cattiaux, J., Yiou, P., Thépaut, J.N. and Ciais, P., 2010. Northern Hemisphere atmospheric stilling partly attributed to an increase in surface roughness. Nature Geoscience, 3, 756–761.

Winterfeldt, J., Geyer, B. and Weisse, R., 2011. Using QuikSCAT in the added value assessment of dynamically downscaled wind speed. International Journal of Climatology, 31, 1028–1039.

Zappa, G., Shaffrey, L.C., Hodges, K.I., Sansom, P.G. and Stephenson, D.B., 2013. A multimodel assessment of future projections of North Atlantic and European extratropical cyclones in the CMIP5 climate models. Journal of Climate, 26, 5846–5862.

Abbreviations

AR	Assessment Report
ARW	Advanced Research Weather Research and Forecasting
C4I	Community Climate Change Consortium for Ireland
cdf	Cumulative distribution function
CGCM	Coupled Global Climate Model
CLM	Climate Limited-area Modelling
CORDEX	Coordinated Regional climate Downscaling Experiment
COSMO	Consortium for Small Scale Modeling
ECMWF	European Centre for Medium-Range Weather Forecasts
GCM	Global climate model
HadGEM2-ES	Hadley Centre Global Environment Model version 2 Earth System configuration
IPCC	Intergovernmental Panel on Climate Change
MAE	Mean absolute error
MME	Multi-model ensemble
MSLP	Mean sea-level pressure
NAO	North Atlantic Oscillation
NCAR	National Center for Atmospheric Research
pdf	Probability distribution function
RCM	Regional climate model
RCP	Representative Concentration Pathway
SRES	Special Report on Emissions Scenarios
WRF	Weather Research and Forecasting

AN GHNÍOMHAIREACHT UM CHAOMHNÚ COMHSHAOIL

Tá an Ghníomhaireacht um Chaomhnú Comhshaoil (GCC) freagrach as an gcomhshaol a chaomhnú agus a fheabhsú mar shócmhainn luachmhar do mhuintir na hÉireann. Táimid tiomanta do dhaoine agus don chomhshaol a chosaint ó éifeachtaí díobhálacha na radaíochta agus an truaillithe.

Is féidir obair na Gníomhaireachta a roinnt ina trí phríomhréimse:

Rialú: *Déanaimid córais éifeachtacha rialaithe agus comhlíonta comhshaoil a chur i bhfeidhm chun torthaí maithe comhshaoil a sholáthar agus chun díriú orthu siúd nach gcloíonn leis na córais sin.*

Eolas: *Soláthraímid sonraí, faisnéis agus measúnú comhshaoil atá ar ardchaighdeán, spriocdhírithe agus tráthúil chun bonn eolais a chur faoin gcinnteoireacht ar gach leibhéal.*

Tacaíocht: *Bímid ag saothrú i gcomhar le grúpaí eile chun tacú le comhshaol atá glan, táirgiúil agus cosanta go maith, agus le hiompar a chuirfidh le comhshaol inbhuanaithe.*

Ár bhFreagrachtaí

Ceadúnú

- Déanaimid na gníomhaíochtaí seo a leanas a rialú ionas nach ndéanann siad dochar do shláinte an phobail ná don chomhshaol:
- saoráidí dramhaíola (m.sh. láithreáin líonta talún, loisceoirí, stáisiúin aistrithe dramhaíola);
- gníomhaíochtaí tionsclaíocha ar scála mór (m.sh. déantúsaíocht cógaisíochta, déantúsaíocht stroighne, stáisiúin chumhachta);
- an diantalmhaíocht (m.sh. muca, éanlaith);
- úsáid shrianta agus scaoileadh rialaithe Orgánach Géinmhodhnaithe (OGM);
- foinsí radaíochta ianúcháin (m.sh. trealamh x-gha agus radaiteiripe, foinsí tionsclaíocha);
- áiseanna móra stórála peitril;
- scardadh dramhuisce;
- gníomhaíochtaí dumpála ar farraige.

Forfheidhmiú Náisiúnta i leith Cúrsaí Comhshaoil

- Clár náisiúnta iniúchtaí agus cigireachtaí a dhéanamh gach bliain ar shaoráidí a bhfuil ceadúnas ón nGníomhaireacht acu.
- Maoirseacht a dhéanamh ar fhreagrachtaí cosanta comhshaoil na n-údarás áitiúil.
- Caighdeán an uisce óil, arna sholáthar ag soláthraithe uisce phoiblí, a mhaoirsiú.
- Obair le húdaráis áitiúla agus le gníomhaireachtaí eile chun dul i ngleic le coireanna comhshaoil trí chomhordú a dhéanamh ar líonra forfheidhmiúcháin náisiúnta, trí dhíriú ar chiontóirí, agus trí mhaoirsiú a dhéanamh ar leasúchán.
- Cur i bhfeidhm rialachán ar nós na Rialachán um Dhramhthrealamh Leictreach agus Leictreonach (DTLL), um Shrian ar Shubstaintí Guaiseacha agus na Rialachán um rialú ar shubstaintí a ídíonn an ciseal ózóin.
- An dlí a chur orthu siúd a bhriseann dlí an chomhshaoil agus a dhéanann dochar don chomhshaol.

Bainistíocht Uisce

- Monatóireacht agus tuairisciú a dhéanamh ar cháilíocht aibhneacha, lochanna, uiscí idirchriosacha agus cósta na hÉireann, agus screamhuiscí; leibhéil uisce agus sruthanna aibhneacha a thomhas.
- Comhordú náisiúnta agus maoirsiú a dhéanamh ar an gCreat-Treoir Uisce.
- Monatóireacht agus tuairisciú a dhéanamh ar Cháilíocht an Uisce Snámha.

Monatóireacht, Anailís agus Tuairisciú ar an gComhshaol

- Monatóireacht a dhéanamh ar cháilíocht an aeir agus Treoir an AE maidir le hAer Glan don Eoraip (CAFÉ) a chur chun feidhme.
- Tuairisciú neamhspleách le cabhrú le cinnteoireacht an rialtais náisiúnta agus na n-údarás áitiúil (m.sh. tuairisciú tréimhsiúil ar staid Chomhshaol na hÉireann agus Tuarascálacha ar Tháscairí).

Rialú Astaíochtaí na nGás Ceaptha Teasa in Éirinn

- Fardail agus réamh-mheastacháin na hÉireann maidir le gáis cheaptha teasa a ullmhú.
- An Treoir maidir le Trádáil Astaíochtaí a chur chun feidhme i gcomhair breis agus 100 de na táirgeoirí dé-ocsaíde carbóin is mó in Éirinn

Taighde agus Forbairt Comhshaoil

- Taighde comhshaoil a chistiú chun brúnna a shainaithint, bonn eolais a chur faoi bheartais, agus réitigh a sholáthar i réimsí na haeráide, an uisce agus na hinbhuanaitheachta.

Measúnacht Straitéiseach Timpeallachta

- Measúnacht a dhéanamh ar thionchar pleananna agus clár beartaithe ar an gcomhshaol in Éirinn (m.sh. mórphleananna forbartha).

Cosaint Raideolaíoch

- Monatóireacht a dhéanamh ar leibhéil radaíochta, measúnacht a dhéanamh ar nochtadh mhuintir na hÉireann don radaíocht ianúcháin.
- Cabhrú le pleananna náisiúnta a fhorbairt le haghaidh éigeandálaí ag eascairt as taismí núicléacha.
- Monatóireacht a dhéanamh ar fhorbairtí thar lear a bhaineann le saoráidí núicléacha agus leis an tsábháilteacht raideolaíochta.
- Sainseirbhísí cosanta ar an radaíocht a sholáthar, nó maoirsiú a dhéanamh ar sholáthar na seirbhísí sin.

Treoir, Faisnéis Inrochtana agus Oideachas

- Comhairle agus treoir a chur ar fáil d'earnáil na tionsclaíochta agus don phobal maidir le hábhair a bhaineann le caomhnú an chomhshaoil agus leis an gcosaint raideolaíoch.
- Faisnéis thráthúil ar an gcomhshaol ar a bhfuil fáil éasca a chur ar fáil chun rannpháirtíocht an phobail a spreagadh sa chinnteoireacht i ndáil leis an gcomhshaol (m.sh. Timpeall an Tí, léarscáileanna radóin).
- Comhairle a chur ar fáil don Rialtas maidir le hábhair a bhaineann leis an tsábháilteacht raideolaíoch agus le cúrsaí práinnfhreagartha.
- Plean Náisiúnta Bainistíochta Dramhaíola Guaisí a fhorbairt chun dramhaíl ghuaiseach a chosc agus a bhainistiú.

Múscailt Feasachta agus Athrú Iompraíochta

- Feasacht chomhshaoil níos fearr a ghiniúint agus dul i bhfeidhm ar athrú iompraíochta dearfach trí thacú le gnóthais, le pobail agus le teaghlaigh a bheith níos éifeachtúla ar acmhainní.
- Tástáil le haghaidh radóin a chur chun cinn i dtithe agus in ionaid oibre, agus gníomhartha leasúcháin a spreagadh nuair is gá.

Bainistíocht agus struchtúr na Gníomhaireachta um Chaomhnú Comhshaoil

Tá an ghníomhaíocht á bainistiú ag Bord lánaimseartha, ar a bhfuil Ard-Stiúrthóir agus cúigear Stiúrthóirí. Déantar an obair ar fud cúig cinn d'Oifigí:

- An Oifig Aeráide, Ceadúnaithe agus Úsáide Acmhainní
- An Oifig Forfheidhmithe i leith cúrsaí Comhshaoil
- An Oifig um Measúnú Comhshaoil
- An Oifig um Cosaint Raideolaíoch
- An Oifig Cumarsáide agus Seirbhísí Corparáideacha

Tá Coiste Comhairleach ag an nGníomhaireacht le cabhrú léi. Tá dáréag comhaltaí air agus tagann siad le chéile go rialta le plé a dhéanamh ar ábhair imní agus le comhairle a chur ar an mBord.

EPA Research Report 159

Ensemble of regional climate model projections for Ireland

Author: Paul Nolan, Irish Centre for High-End Computing and Meteorology and Climate Centre, School of Mathematical Sciences, University College Dublin

epaResearch
Climate - Water - Sustainability
Identifying pressures • Informing policy • Developing solutions

Background

Climate Change is the major challenge of our time. At a global scale, there is robust understanding of the observed changes in various elements of the climate system, and from this there is compelling analysis of the potential changes in climate in store for the planet over the next several decades. Analysis of climate change at a regional or national scale is more challenging, and therefore the projections of future climate change more uncertain. Nevertheless, using the global models as the starting point, it is possible to initiate regional climate models, operating at much higher spatial resolution, to generate insights at the scale of interest to decision makers on the ground, looking to respond and adapt in the best way possible to the impacts of climate change.

Identifying Pressures

Ireland's north Atlantic location leaves us open to disparate factors which will influence our potential future climate. That our climate is changing is beyond doubt. The challenge is to provide researchers, decision makers and the general public with the detailed, high quality information required to make informed decisions on policy development and investments which will be resilient to the impact of climate change.

This report provides an outline of the regional climate modelling undertaken to determine the potential impacts of climate change in Ireland, based on a number of possible future scenarios, and to highlight the key findings. The project has also provided a large database, which can be interrogated for various meteorological parameters, essential for detailed analysis across a diverse range of sectoral concerns.

Informing Policy

Findings from this study indicate that by the middle of this century:

- Mean annual temperatures will increase by 1–1.6°C, with the largest increases seen in the east of the country.
- Hot days will get warmer by 0.7–2.6°C compared with the baseline period.
- Cold nights will get warmer by 1.1–3.1°C.
- Averaged over the whole country, the number of frost days is projected to decrease by over 50%.
- The average length of the growing season will increase by over 35 days per year.
- Significant decreases in rainfall during the spring and summer months are likely.
- Heavy rainfall events will increase in winter and autumn.
- The energy content of the wind is projected to decrease during spring, summer and autumn. The projected decreases are largest for summer, with values ranging from 3% to 15%.
- Storms affecting Ireland will decrease in frequency, but increase in intensity, with increased risk of damage.

Developing Solutions

The research provides Ireland with a data resource to explore Ireland's future climate and enables the assessment of the scale of impacts across sectors, at regional and local scales.

Comhshaol, Pobal agus Rialtas Áitiúil
Environment, Community and Local Government

EPA Research: McCumiskey House, Richiew, Clonskeagh, Dublin 14.

Phone: 01 268 0100
Twitter: @EPAResearchNews
Email: research@epa.ie

www.epa.ie

EPA Research Webpages
www.epa.ie/researchandeducation/research/